

UNCLASSIFIED

AD 276 867

*Reproduced
by the*

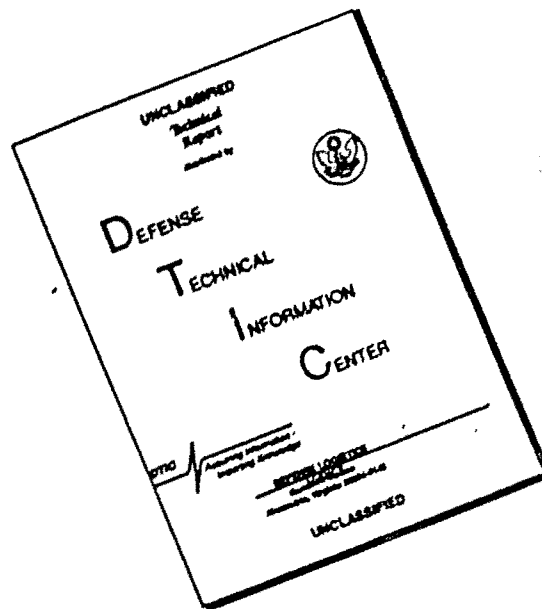
ARMED SERVICES TECHNICAL INFORMATION AGENCY
ARLINGTON HALL STATION
ARLINGTON 12, VIRGINIA



UNCLASSIFIED

NOTICE: When government or other drawings, specifications or other data are used for any purpose other than in connection with a definitely related government procurement operation, the U. S. Government thereby incurs no responsibility, nor any obligation whatsoever; and the fact that the Government may have formulated, furnished, or in any way supplied the said drawings, specifications, or other data is not to be regarded by implication or otherwise as in any manner licensing the holder or any other person or corporation, or conveying any rights or permission to manufacture, use or sell any patented invention that may in any way be related thereto.

DISCLAIMER NOTICE



THIS DOCUMENT IS BEST QUALITY AVAILABLE. THE COPY FURNISHED TO DTIC CONTAINED A SIGNIFICANT NUMBER OF PAGES WHICH DO NOT REPRODUCE LEGIBLY.

**BLANK PAGES
IN THIS
DOCUMENT
WERE NOT
FILMED**

Report No. 3

62-3-6
Contract DA-36-039-SC-78321
DA Project Nr. 3A-99-15-001

276867

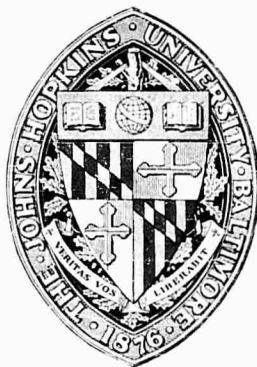
276 867

CATALOGED BY ASTIA
AS AD NO.

Sponsored by
U. S. Army Signal Research and Development Laboratory
Ft. Monmouth, New Jersey

DIELECTRICS FOR SATELLITES AND SPACE VEHICLES

Final Report for the period
March 1, 1959 to February 28, 1962



DIELECTRICS LABORATORY
The Johns Hopkins University
Baltimore, Maryland

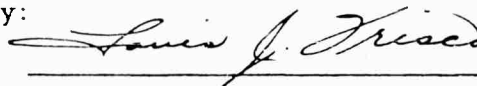
Report No. 3
March 30, 1962

Contract DA-36-039-SC-78321
DA Project Nr. 3A-99-15-001

DIELECTRICS FOR SATELLITES
AND SPACE VEHICLES

Final Report
for the period
March 1, 1959 to February 28, 1962

Prepared by:



Louis J. Frisco
Research Contract Director

THE JOHNS HOPKINS UNIVERSITY
DIELECTRICS LABORATORY
BALTIMORE 2, MARYLAND

CONTENTS

I.	Purpose	1
	A. Objective	1
	B. Materials	1
	C. Electrical Properties	3
	D. Environmental Conditions	3
II.	Abstract	5
III.	Factual Data	6
	A. Environmental Factors	6
	1. Vacuum	6
	2. Ultraviolet Radiation	8
	3. X-rays	10
	B. High-Vacuum Flashover and Sparkover	12
	1. General Remarks	12
	2. Uniform Field Sparkover	14
	3. Flashover	16
	4. Summary of Flashover and Sparkover Studies	25
	C. Solid Dielectric Breakdown	26
	1. Mylar Film Tests	26
	2. Electric Strength of Machinable, Low-Loss Polymers	30
	3. Summary of Dielectric Breakdown Study	34
	D. Loss Properties	34
	1. High-Vacuum Effects	34
	2. Effects of X-ray Irradiation	35
	3. Effects of Ultraviolet Radiation	49
	E. Microwave Measurements	54
IV.	Conclusions	56
V.	Recommendations	59
VI.	Cited References	60
VII.	Identification of Personnel	63

CONTENTS

VIII. Acknowledgements	64
IX. Tables	65
X. Illustrations	107

I. Purpose

A. Objective. The objective of this program was to study the effects of simulated high altitude and outer space environments on the electrical properties of electrical insulating materials.

B. Materials. The following materials were included in the program:

<u>Designation</u>	<u>Description and Supplier</u>
TFE-6	Polytetrafluoroethylene extrusion resin, commercial designation TFE-6. E.I. du Pont de Nemours and Company, Wilmington, Delaware.
TFE-7	Polytetrafluoroethylene molding resin, commercial designation TFE-7. E.I. du Pont de Nemours and Company, Wilmington, Delaware.
PF	Polytetrafluoroethylene resin which had been stored in the laboratory for about seven years. U.S. Gasket Company, Camden, New Jersey.
FEP	Copolymer of tetrafluoroethylene and hexafluoropropylene, melt processable resin, commercial designation FEP-100. E.I. du Pont de Nemours and Company, Wilmington, Delaware.
K-4	Polychlorotrifluoroethylene, commercial designation KF-6050, ASTM-1430-58T Grade II, ZST 217, pelletized, injection molding and extrusion resin. Minnesota Mining and Manufacturing Corporation, St. Paul, Minnesota.
K-5	Polychlorotrifluoroethylene, commercial designation KF-6060, ASTM-1430-58T Grade III, ZST 375, unpelletized, compression molding resin. Minnesota Mining and Manufacturing Corporation, St. Paul, Minnesota.

<u>Designation</u>	<u>Description and Supplier</u>
K-7	Copolymer of chlorotrifluoroethylene and vinylidene fluoride, commercial designation KF-5120, ASTM-1430-58T, Grade II, ZST 190, pelletized, injection molding and extrusion resin. Minnesota Mining and Manufacturing Company, St. Paul, Minnesota.
PE	Polyethylene, unpigmented. Stored in laboratory for several years. Undetermined origin.
ALATHON - 4 BK 30	Polyethylene, commercial designation ALATHON 4 BK 30 Cable Jacket Resin, high molecular weight, melt index 0.20-0.40, carbon content 2.6% \pm 0.25% (channel black not larger than 20 millimicrons average particle size). E.I. du Pont de Nemours and Company, Wilmington, Delaware.
PSC	Polystyrene, crosslinked thermosetting, commercial designation REXOLITE 1422. William Brand-Rex Division, American Enka Corporation, Concord, Massachusetts.
Mylar 130-100C	Polyester, capacitor film, commercial designation MYLAR 130-100C. E.I. du Pont de Nemours and Company, Circleville, Ohio.
Mylar 130-100T	Polyester film, commercial designation MYLAR 130-100T, highly oriented in the long, or machine direction. E.I. du Pont de Nemours and Company, Circleville, Ohio.
Mylar 130-100A	Polyester film, commercial designation MYLAR 130-100A, same composition as 130-100T but not as highly oriented.
GPG	Multiple laminate radome material consisting of Rohm and Haas PARAPLEX P-43 polyester resin and Owens-Corning Fiberglas 181 glass cloth, conforming to MIL-R-7575.
FF-95	Copper clad epoxy laminate printed circuit board with two ounce copper, commercial designation FORMICA FF-95. Formica Corporation, Cincinnati, Ohio.

<u>Designation</u>	<u>Description and Supplier</u>
FF-95C	Same as FF-95 with coating of Hysol 6233 epoxy coating material. Hysol Corporation, Olean, New York.
AL-243	Forsterite, $2\text{MgO} \cdot \text{SiO}_2$, commercial designation ALSIMAG 243. American Lava Corporation, Chattanooga, Tennessee.
ALOX	Alumina, 99% Al_2O_3 . National Beryllia Corporation, North Bergen, New Jersey.
AL-665	Steatite, $\text{MgO} \cdot \text{SiO}_2$, commercial designation ALSIMAG 665. American Lava Corporation, Chattanooga, Tennessee.
BeO	Beryllia, 99% BeO, 95% of theoretical density. Brush Beryllium Company, Cleveland, Ohio.
ECF	Polyurethane foam, commercial designation Eccofoam S, density 12 lbs per cu. ft. Emerson and Cuming, Inc., Canton, Massachusetts.

C. Electrical Properties.

1. Dielectric constant at 60 cps, 2, 18 and 100 Mc.
2. Dissipation factor at 60 cps, 2, 18 and 100 Mc.
3. Volume resistivity, d-c.
4. Surface resistivity, d-c.
5. Electric strength 60 cps, 2, 18 and 100 Mc.
6. Flashover strength 60 cps, 2, 18 and 100 Mc.
7. Microwave transmission properties at frequencies up to 10 Gc as time and facilities permitted.

D. Environmental Conditions.

1. Temperatures of -55, 25, 85 and 125C.
2. Minimum vacuum of 10^{-4} Torr.
3. Solar x-rays.

4. Solar ultraviolet.
5. Chemisphere and ionosphere conditions.

II. Abstract

Results of a study of the effects of simulated space environment on the electrical properties of solid insulating materials are reported. Equipment and techniques are described for the measurement of loss properties, flashover strength and electric strength during x-ray and ultraviolet irradiation at pressures in the 10^{-6} Torr range. Twenty-one organic and inorganic materials are included in the investigation.

High-vacuum sparkover (uniform field) and flashover measurements at d-c and 60 cps show that electrode surface roughness is the controlling factor; that the dielectric properties of the material do not influence flashover voltage; and that x-ray and ultraviolet radiation have no effect on flashover voltage. At 2 and 18 Mc high current densities at electrode edges or high losses in the solid material compromise flashover strength.

Electric strengths of low-loss polymers are not affected by x-ray irradiation in high-vacuum. High-frequency electric strength is compromised by unfavorable thermal conditions in high-vacuum.

X-ray induced a-c losses are exhibited by several materials during and after irradiation. Transient effects during irradiation cause induced 60 cps dissipation factors as high as 0.40 in some tetrafluoroethylene polymers; detailed exposure and recovery data show the effects of oxygen concentration and absorbed dose.

X-ray induced d-c polarization, absorption and conduction currents are exhibited by most materials. In some cases, recovery is not complete after several months.

Instantaneous and short-time effects of ultraviolet radiation on a-c loss properties are not large enough to be of practical importance. The d-c behavior is dominated by photoelectric effects.

Materials that are subject to moisture absorption exhibit improved electrical properties after short periods in high-vacuum.

Studies are being continued under Contract DA-36-039-SC-89147.

III. Factual Data

A. Environmental Factors.

1. Vacuum.

a. Pumping Systems. Two complete and independent high vacuum pumping systems (Kinney PW-600) were installed in the initial phase of the program to accommodate a high-voltage test cell and a loss-measurement cell. Each system consists of a 6 inch fractionating oil diffusion pump, a 15 cfm mechanical roughing and backing pump and a 2 cfm holding pump. These systems provide rapid pumping to pressures in the 10^{-6} Torr range without coolant in the trap and to pressures in the 10^{-7} Torr range with liquid nitrogen in the trap. A complete system, including a loss-measurement cell and an ultraviolet light source, is shown in Figure 1.

The block diagram of Figure 2 illustrates the essential features of the pumping system. An ion gauge tube is located at the test cell so that the pressure in the vicinity of the specimens can be measured directly. The vent on the test cell is connected to a nitrogen tank so that the cell can be filled with dry nitrogen before it is opened to the atmosphere when changing specimens. This procedure reduces the time required to reach the desired pressure when the cell is re-pumped. The improved performance results from a reduction in the amount of water vapor that is adsorbed on the walls of the cell. Once the system has been properly degassed, the cell can be pumped down to a pressure of 5×10^{-5} Torr in approximately ten minutes and 5×10^{-6} Torr in one hour.

An additional PW-600 pumping system was acquired during the third phase of the program. This unit was used in conjunction with a second loss-measurement cell.

Recent data on the variation of pressure with altitude, taken from the 1959 ARDC Model Atmosphere^{(1)*}, is shown in Figure 3. According to this curve, the vacuum equipment described above will permit the simulation of pressures over the altitude range from 0 to 240 km.

b. Loss Measurement Cells. Two similar cells were constructed to accommodate specimens for dielectric constant, dissipation factor, and d-c conductivity measurements. The interior of one of these cells is shown in Figure 4. Four 3-electrode specimens are connected to the vacuum-tight, guarded bushings which extend through the cell wall. The specimens, electrodes and bushings are similar to those previously used in studying environmental ageing effects.⁽²⁾⁽³⁾ The cell has a 12 inch inside diameter and is 14 inches in length. The cell itself is electrically isolated from the vacuum system so that it can be maintained at guard potential during measurements with the Schering bridge. The front cover-plate is designed to accommodate a quartz window for ultraviolet transmission or a beryllium window for x-ray transmission. A second cover-plate can accommodate both adaptors simultaneously.

c. High-Voltage Cell. The interior of the high-voltage cell is shown in Figure 5. Four flashover specimens are shown connected to separate high-voltage bushings in the end plate. The design of the high-voltage feed-through insulators are of interest because they are capable of withstanding higher voltages in the r-f range than commercially available glass-sealed bushings. Figure 6 shows the important features of the bushing, which consists of a polyethylene insulated center conductor, a tapered socket and a Teflon^{**} retaining cylinder.

* - Numbered references are listed on Page

** - Trademark - E. I. du Pont de Nemours and Company, Inc.

The insulated center conductor is fabricated from a short length of RG-19/U coaxial cable. The tapered section of the polyethylene insulation is pressed into the tapered socket by means of the Teflon retaining cylinder, and contact between these tapered surfaces provides a vacuum seal. The polyethylene is sealed to the copper center conductor during the cable manufacturing process, and there is no apparent leakage through this seal. The tapered socket is inserted into a clearance hole in the end-plate of the vacuum chamber, and a soft-solder joint provides the necessary vacuum seal. The air spaces between the Teflon and polyethylene parts are filled with General Electric Company SS-4005 silicone grease as a safeguard against corona. The grease remains on the outside of the vacuum seal and does not contaminate the cell. Bushings of this type perform satisfactorily at voltages up to 35 KV at 60-cps and 10 KV at 18 Mc.

2. Ultraviolet Radiation. According to revised solar spectral irradiance data obtained by the U. S. Naval Research Laboratory, the value of the solar constant is 0.140 watts/cm^2 . ⁽⁴⁾ Table 1 shows the radiation intensity at various wavelength regions. It can be seen that the total ultraviolet intensity is $10.23 \text{ milliwatts/cm}^2$, and that 99.7 per cent of the ultraviolet radiation lies in the wavelength region from 2200 to 3800 Angstroms. Consequently, in considering environmental effects, this wavelength region is of prime importance. Ultraviolet sources are available which are capable of producing the desired intensities in this wavelength region, but the shorter wavelengths can be obtained only through a prohibitive sacrifice in overall intensity.

After investigating the variety of ultraviolet sources which were available, the General Electric Company B-H6 mercury lamp appeared to be the most satisfactory one for the purposes of this investigation. The actual source of radiation in this lamp is an enclosed arc which is about 1.5 mm in diameter and 25 mm long. The power dissipation in this small volume is approximately 900 watts, so

the internal pressure builds up to about 110 atmospheres. The quartz envelope operates very near its ultimate strength under these severe loading conditions, and it is necessary to use compressed air cooling to prevent envelope failure.

Details of the lamp enclosure which was designed to accommodate the B-H6 lamp are shown in Figure 7. The manufacturer's recommendations were followed in the design of the compressed-air nozzles, which are mounted on a brass manifold directly below the lamp. A volume of about 5 1/2 cubic feet of free air per minute, at a line pressure of 19 psi, is directed through the nozzle orifices. This volume of air becomes highly ionized and would be objectionable if it were permitted to escape into the room, so it is necessary to connect the enclosure to an exhaust blower through a flexible duct, as shown in Figure 1.

In order to filter a large part of the infrared radiation, which would cause the specimens to become overheated, the beam is allowed to pass through a 1/2 inch thick layer of circulating tap-water. This water is passed through the space between two quartz windows on the front cover-plate. Figure 7 shows the front cover-plate removed; the inside quartz window and the water connections are visible. The plate is formed by joining two 1/4 inch thick brass plates which contain grooves for directing the water flow. The return water line is connected to a copper coil which is bonded to the outer wall of the enclosure, thereby providing cooling for the entire enclosure.

In Figure 8 the radiation output of the B-H6 lamp is compared to the solar radiation at the top of the earth's atmosphere. The curve showing the intensity at the surface of a specimen in the vacuum cell is based on calculated values, taking into account the absorption in the infrared filter and the quartz window of the cell.⁽⁵⁾ The integrated values over several wavelength regions are given in Table 2. It can be seen that the B-H6 lamp provides intensities in the ultraviolet region

which are high enough to permit realistic evaluation of environmental effects.

Through the courtesy of the Chemicals and Plastics Division, Food Machinery and Chemical Corporation, Baltimore, Maryland, ultraviolet transmission measurements were made on the infrared filter and other associated components. These measurements indicated that the calculated intensities were conservative for a new lamp, but represent the average values that might be expected over the life of a lamp.

3. X-rays. The average intensity of solar x-ray at the top of the earth's atmosphere is between 0.10 and 0.20 $\mu\text{w}/\text{cm}^2$, where the radiation is distributed over the wavelength interval from 7 to 60 Angstroms. ⁽⁶⁾ Such low energy x-rays would not penetrate the shell of a satellite in sufficient quantity to affect the properties of materials. Exposed components, such as antenna patterns, antenna insulators and solar cells could be affected by this radiation, however.

In order to conduct x-ray exposure tests in the laboratory it was necessary to procure an x-ray generator capable of continuous operation. Such apparatus is not available for the very soft x-rays in the 7 - 60 Angstrom range, but a generator was obtained which has a peak output intensity at approximately 0.38 Angstroms when operated at 50 KV. This unit employs two Machlett AEG-50 beryllium window tubes that are capable of continuous operation at voltages up to 50 KV and anode currents up to 50 ma. Figure 9 shows one of the x-ray tubes mounted on a beryllium window adaptor which facilitates the irradiation of loss specimens.

Several methods of measuring the intensity of the x-ray beam were considered. Since it was desirable to directly measure energy flux, and because the output of the AEG-50 tube is so high that ion recombination makes ionization measurements unreliable, ⁽⁷⁾ a

calorimeter method proved to be advantageous. Figure 10 shows the essential features of the calorimeter, which is similar in principle to those used by other workers.⁽⁸⁾ The x-ray beam enters the evacuated chamber through a beryllium window and impinges on a silver target, thereby causing a measurable increase in the target temperature. Since the target volume, mass, projected area and specific heat are known, the x-ray intensity can be computed from the measured values of temperature rise as a function of exposure time.

Silver was chosen as the target material because of its high thermal conductivity and high x-ray absorption coefficient in the wavelength region involved. To obtain maximum sensitivity, the target thickness must be small while the area exposed to the incident beam should be large. The target shown in Figure 10 is a flat, circular disc with an exposed surface area of 1.0 cm^2 , and a thickness of 0.5 mm. This thickness provides absorption of greater than 99.5 percent of the incident x-ray energy.

The temperature of the target is measured by means of a chromel-alumel thermocouple which is mounted on the back face of the target (in the shadow of the x-ray beam). Because of the low rate of energy input into the target, it is necessary to reduce the rate of heat transfer from the target to its surroundings as much as possible. Since the chamber is evacuated, the heat loss due to convection can be neglected. In order to reduce the conduction loss, the target was mounted on a thin glass rod, and very fine thermocouple wire (0.003 inch diameter) was used. The radiation loss was reduced by silver-plating and polishing the chamber walls and by making the temperature difference between the target and the chamber walls as small as possible. This was accomplished by means of a temperature-controlled, circulating-water bath. The water is pumped through a heat exchanger, where it can be heated or cooled, so that a temperature difference of less than 0.05°C is maintained between the target and the chamber, thereby

reducing the radiation loss to less than 28 μ watts during the measurements.

Intensity measurements were made at two spacings between the x-ray source and the calorimeter target, and at several output levels. The results, which are given in Tables 3 and 4, indicate that the intensity is proportional to the average anode current, but there appears to be a deviation from the inverse square law when comparing the values obtained for a given output setting at two distances. The measurements are adequate, however, for the purposes of this investigation.

In order to ensure uniform irradiation of the four specimens in the vacuum test cell, the x-ray energy distribution over the plane of the specimens was examined by exposing x-ray film. It was found that the variation in intensity was less than 20 percent over the area in question.

It is necessary to occasionally check the output of each x-ray tube in order to be sure that the tube is functioning properly and that the output for a given voltage and current setting has not changed significantly from the value determined with the calorimeter. A small ionization chamber was constructed for this purpose. It can be attached to the output-port of the tube in such a way that its position relative to the x-ray target can be accurately reproduced. The calorimeter is used to calibrate this ionization chamber, which facilitates rapid monitoring of the tube output.

B. High Vacuum Flashover and Sparkover.

1. General Remarks. The voltage at which a discharge will occur between two flat electrodes in contact with the surface of a solid dielectric is referred to as the flashover voltage. At atmospheric pressure a flashover will occur when the electrical stress in the gap between the electrodes exceeds a critical value. The magnitude of this

critical stress depends primarily on the electric strength of the surrounding medium. The voltage at which the critical stress will be reached depends upon the geometry of the electrodes and the dielectric constant of the specimen. In general, flashover voltage varies inversely with dielectric constant at the lower frequencies, as shown in a previous study. (9)

Since the electric strength of the gaseous surrounding-medium influences the flashover voltage of a given specimen, it follows that flashover strength varies with ambient pressure in accordance with the well known Paschen's Law, which states that the uniform field breakdown voltage in a gas is proportional to the product of the gas pressure, p , and the electrode separation, δ . Deviations from Paschen's Law occur at low pressures when the mean free path of the gas molecules becomes comparable to the electrode spacing, and a minimum breakdown-voltage is observed as the ambient pressure is reduced beyond this range. For air this minimum occurs at a $p\delta$ product of approximately 1.0 Torr cm. The general shape of the Paschen curve can be explained in terms of well known phenomena involving the Townsend avalanche mechanism. A recent book by F. Llewellyn-Jones contains a complete discussion of breakdown at lower gas pressures. (10)

At the low pressures encountered in space applications the mean free path of residual gas molecules is so many times greater than normal electrode (hardware) spacings that ionization phenomena no longer govern the breakdown process, and extrapolation of the Paschen curves, which would predict extremely high values of breakdown voltage, is not valid. It is certainly true that a high-vacuum medium possesses an inherently high electric-strength, but emission from metallic electrodes becomes the governing factor in high-vacuum breakdown, and sparkover is observed at stresses considerably lower than those predicted on the basis of ionization phenomena.

Erratic results were obtained in preliminary flashover and uniform field sparkover experiments, and in order to determine the extent to which the surface condition of the electrodes influenced the results, a study of uniform field sparkover was made using the smoothest electrode surfaces that could be prepared in the laboratory. These experiments and the subsequent flashover experiments are described in the following sections.

2. Uniform Field Sparkover.

a. Experimental Procedure. The most highly polished metal spheres that could be readily obtained proved to be unsatisfactory when viewed through a microscope. In order to provide very smooth electrodes, the convex surfaces of 2.3 cm diameter glass lenses were carefully polished until no scratches could be seen through a microscope under dark-field illumination. The polished lenses were then mounted in aluminum holders and placed in a vacuum chamber where evaporated silver or aluminum coatings were deposited on the polished surfaces. It was not possible to completely avoid the deposition of dust particles on the polished surfaces, and these particles were necessarily covered by the evaporated film, resulting in very small projections on the metal surface. The shape or size of these points could not be determined because they were so small (less than 0.2 microns) that only their presence and location could be determined by dark-field illumination.

The breakdown gap was formed by placing two of the metallized lenses (1.75 cm spherical radius) opposite each other in the electrode holder shown in Figure 11. To avoid scratches, the gap was set in such a way that the electrodes never touched each other. Under survey through a telescope the gap was made as small as possible, while an ohm-meter was used to ensure that the electrodes did not touch. The gap was then set at 5 mils with a micrometer, which was removed before

the electrode holder was placed in the vacuum cell. The error in setting the gap was determined to be less than 0.2 mils.

b. Experimental Results. The results of d-c breakdown tests at pressures in the 10^{-6} Torr range are summarized in Figure 12. The range of breakdown voltages corresponds to macroscopic field strengths of 0.44 to 1.7 MV/cm for silver coated lenses, and of 0.44 to 1.2 MV/cm for aluminum coated lenses. These results show that there is no marked difference in the behavior of the silver as opposed to the aluminum electrodes. At the higher voltages occasional arcs occurred at points where the macroscopic field-strength was as low as 3 percent of the field-strength in the center of the gap, but where the surface was not as smooth.

Photomicrographs of the electrode surfaces were made before and after breakdown in an effort to determine if a relationship existed between the small points (dust particles) on the electrode surfaces and the location from which the discharge occurred. No such relationship could be found because the damaged areas of the electrodes were many times the size of the points in question. Provisions for more rapid current-interruption would be required to reduce the size of the damaged areas.

It was expected that the microscopic field at the cathode would be the controlling factor in establishing the macroscopic breakdown stress in the gap. (11)(12) The results obtained with the silver coated and aluminum coated lenses indicated that, in spite of the care that was taken to provide smooth electrode surfaces, uniformly high breakdown voltages were not ensured. Consequently, it remained to be proven that macroscopic irregularities on the cathode surface were important. In order to show this, tests were made first with a roughened cathode and a smooth anode, and then with a smooth cathode and a roughened anode. The roughened electrodes were prepared by lightly sandblasting the lens before the evaporated metal film was

deposited. The results of these experiments are shown in Figure 13. In those tests where the cathode was roughened, the maximum breakdown stress (macroscopic) that was observed was 0.66 MV/cm and the breakdown occurred at values as low as 0.17 MV/cm. A comparison with the results for smooth electrodes (Figure 12) indicates that the roughened cathode causes a marked decrease in the apparent electric strength of the gap. With the roughened anode, however, the results were within the range of values exhibited by the smooth electrodes.

Since the breakdown process at very low pressures involves field emission from the electrodes, the question of the influence of surface contamination naturally arises. In the way that the electrodes were prepared it was not possible to get atomically clean surfaces,⁽¹³⁾⁽¹⁴⁾ so it was possible to study only the additional contamination due to the presence of diffusion-pump oil-vapor in the cell. Oil was evaporated at atmospheric pressure and allowed to condense on the electrodes, forming a visible film. Breakdown tests were then conducted in the vacuum chamber and the observed macroscopic field strengths varied from 0.63 to 1.6 MV/cm. These values are in the same range as those obtained without the oil film.

Having established the breakdown characteristics of the vacuum medium, it was expected that the same factors would govern flashover phenomena, where a failure is obtained in a gap formed by attaching electrodes to a solid insulating material. In order to show that this was indeed the case, the experiments described in the following section were performed.

3. Flashover.

a. Specimen Preparation. As mentioned previously, preliminary flashover experiments had yielded erratic results. In those tests the flashover gap was formed by attaching flat brass electrodes to 1/8 inch thick specimens. This test method had two disadvantages: (i) the surface condition at the edge of the washers could not be

controlled, and (ii) a small space under the washers (between the washer and the solid material) could not always be avoided. Both of these factors can lead to a large spread in results and to low values of flashover strength.⁽¹⁵⁾⁽¹⁶⁾ Therefore, in order to avoid these difficulties, electrodes were formed by depositing evaporated silver on the specimen surface in a pattern determined by an accurately machined mask. The electrode pattern and the mask are shown in Figure 14. By using this method, the space beneath the electrode was avoided, and the microscopic shape of the edge of the electrode was more precisely controlled because the same mask was used for all test specimens. The chance of the deposition of a dust particle on the critical edge of an electrode was smaller by an order of magnitude than for the deposition of a dust particle on the surface of the spherical electrodes. Therefore, less spread in results was expected for the flashover voltage measurements. The thickness of the silver film was about 0.3 microns, and the gap length was 17 mils, a distance that resulted in flashover voltages that were within the range that could be conveniently accommodated.

In view of the results obtained with the smooth spherical electrodes, it was expected that flashover strength would depend upon the roughness of the edges of the electrodes in the same manner as the uniform field strength depended upon the surface roughness of the spheres. With the flashover sample, the surface texture of the dielectric material contributes to the roughness of the edge of the evaporated electrode. One of the specimens shown in Figure 14 was chosen to demonstrate that the silver film has the same texture as the surface of the specimen. To minimize the effects of surface irregularities, glass microscope-slides with smooth surfaces were used as specimens in the first series of experiments. Consequently, the shape of the electrode edges was determined primarily by the mask through which the silver was deposited.

b. D-C Flashover Phenomena. The flashover voltages for the glass slides followed the same general pattern as for the breakdown voltages of the sphere gap. The d-c flashover voltages varied from 10 to 29 KV for the 17 mil gap and were rather uniformly distributed over this range, as shown in Figure 15. The ratio between the maximum and minimum values is 2.9 to 1.0, which is not much lower than for the spheres.

Occasional arcs were observed at locations where the distance between electrodes was as much as six times as great as the minimum distance at the center of the gap. Photomicrographs of the gap, before and after flashover, gave no correlation between the condition of the edge of the electrode and the location from which the discharge occurred. As in the case of the spheres, the damaged area was too extensive to permit such detailed examination. High-speed movie techniques would perhaps be useful in this respect.

Using the same technique described for the spherical electrodes, tests were conducted to determine if a film of oil influenced the results. No measurable effect could be found.

The next series of experiments was designed to evaluate the effects of x-ray and ultraviolet radiation on flashover voltage. Because the inherent spread in results is so large, it was necessary to proceed in the following manner:

- (i) A voltage V_1 was applied.
- (ii) The applied voltage was reduced to $(V_1 - \Delta V)$ and the specimen was exposed to the radiation.
- (iii) The radiation was removed and the voltage was increased to $V_1 + \Delta V$.
- (iv) The voltage was reduced to V_1 and the specimen was again exposed to the radiation.
- (v) The voltage was increased to $V_2 = V_1 + 2\Delta V$, and the procedure was repeated until a flashover occurred.

If a flashover did not occur at $V_n - \Delta V$ with radiation, but did occur at $V_n + \Delta V$ without radiation, then any adverse effect of the radiation could not cause a decrease in flashover voltage of more than $2\Delta V$. By an obvious modification in the procedure, it can be determined if the radiation increases the flashover voltage. The value of ΔV was adjusted to insure an experimental sensitivity of 300-volts. Since the flashover voltages range from 10 to 29 KV, but no effect was found which was as large as the stated 300 volt limit, it must be concluded that the x-ray and ultraviolet radiation had no influence on flashover voltage.

Having established the flashover behavior of the glass slide specimens, it was then necessary to determine if any additional factors might become important when the specimens were fabricated from other insulating materials with widely varying electrical and physical properties. Since it had already been shown that the roughness of the electrode surfaces that formed the gap was the controlling factor in the case of the glass slides, it was necessary to establish some control over the surface texture of the specimens in this series of measurements if effects due to electrical properties were to be detected. A group of thermoplastic materials was used in these tests because it was possible to press the specimens against glass slides and reform their surfaces by heating them in an oven. Samples that were prepared in this way were compared to samples that were made from the same material in the as-received condition. The results of these tests are shown in Figure 16 and they clearly demonstrate that the specimens with smooth surfaces and, hence, smooth electrode edges, have higher flashover strengths than the specimens with rough surfaces.

When the gaps of three K-5 samples with smooth surfaces were roughened between the electrodes, but the edges of the electrodes were undisturbed, the flashover voltages were still high (19, 20, 22 KV). However, when a smooth surface was deliberately roughened before the

silver electrodes were deposited, so that the resulting electrode edges were rough, the flashover voltages were in the vicinity of 2 KV. Similar experiments with glass slides had the same effect.

It is apparent from the foregoing experiments that the electrical properties of the specimens have little effect on flashover voltage when compared to the influence of surface texture (electrode roughness). As previously mentioned, the use of thicker metallic electrodes merely makes it more difficult to control the condition of the electrode surface, and leads to a large spread in results that are not dependent upon the electrical properties of the specimen.

c. A-C Flashover Phenomena. All of the aforementioned results were obtained with direct voltages, making it possible to separate cathode and anode effects. With alternating voltages, each electrode assumes the role of cathode and anode during successive half-cycles. Since the roughness of the cathode plays such an important part in determining the flashover voltage, it would be expected that the a-c flashover voltages would be somewhat lower than the d-c values if for no other reason than the fact that the effective cathode area is doubled, thereby increasing the chance of having a microscopic irregularity located in the critical region of the electrodes. There are, of course, other factors such as the build-up of space charge and the high local current densities due to displacement current which do not exist with direct voltages, but could be important with alternating voltages. In order to determine if these factors influence the a-c flashover behavior, measurements were made at 60 cps, 2 Mc, and 18 Mc on the various materials of the program. A detailed description of each material can be found on Pages 1, 2 and 3. The results of flashover measurements on these materials are summarized in Table 5.

In general, the a-c flashover voltages are lower than the d-c values and they decrease with increasing frequency, as shown in Table 5. When the gap was viewed through a telescope, visible glow

at the edges of the electrodes became evident at voltages below the flashover levels at 2 and 18 Mc. Both edges glowed with the same intensity and the glow pattern was identical on either side of the gap. When a d-c bias-voltage was applied in series with the a-c test-voltage, so that the polarities of the electrodes did not change during the measurement, the glow did not change in intensity and the pattern remained symmetrical. This result indicates the absence of space charge effects and, consequently, it appears that the alternating current (determined by the applied voltage and the impedance of the specimen) causes the glow by resistive heating of the thin electrode edges. Since the temperature rise depends upon the resistivity of the metallic film, it also depends upon thickness and irregularities in the film near the edges that form the gap. This temperature rise increases the field emission current, which indirectly causes a further increase in temperature, and the process becomes unstable and leads to a flashover. Dyke, Trolan and co-workers⁽¹⁴⁾⁽¹⁷⁾⁽¹⁸⁾ have found that emission current alone can cause resistive heating of small points on the surface of an electrode; thus the combined effects of the capacitive current and the enhanced emission current should cause a decrease in flashover voltage as the frequency is increased beyond 2 Mc. It has not been experimentally determined whether the temperature rise due to capacitive current is high enough to influence the flashover voltage at lower frequencies. However, no glow could be detected during the 60 cps measurements.

The temperature rise at the edges of the gap can also cause the pressure in the vicinity of the gap to increase, and this increase in pressure can lead to a decrease in flashover strength. This is particularly true with low melting point materials.

Additional thermal effects are observed in the r-f range, where the dielectric losses of some materials cause the specimen to be overheated. In several cases the specimen material melted or otherwise deformed because of excessive heating at 18 Mc, and the

test was terminated before the flashover could be obtained. This type of behavior had been encountered in previous investigations where tests were conducted at atmospheric pressure,⁽¹⁹⁾ so it was expected that the heating would be even more severe in a vacuum.

The data of Table 5 also confirm the previous remarks concerning the effect of the specimen surface texture on flashover strength. One apparent exception is AL-243, which has a relatively high flashover strength. Although this ceramic material has a surface which is not exceptionally smooth in the macroscopic sense, its microscopic texture is smooth and it is not surprising that its flashover strength is so high. Alox, on the other hand, had a low flashover strength because its microscopic texture was much rougher.

X-ray and ultraviolet radiation had no effect on the 60 cps, 2, and 18 Mc flashover behavior of any of the materials listed in Table 5. This result is in agreement with the d-c measurements previously discussed and with the results of Funfer,⁽²⁰⁾ who studied vacuum breakdown related to x-ray flash-tubes.

d. Flashover Strength of FF-95. In the first phase of the program flashover tests were made on the printed wiring board FF-95 (see Page 2 for description). With this material the electrode pattern was formed by the usual etching process. The specimens were prepared by a commercial fabricator so the smoothness of the electrode edges could not be controlled in the laboratory.

The electrode pattern shown in Figure 17 was used in measuring the flashover strength of this material. Several patterns were considered, including those used by other investigators,⁽²¹⁾ before the pattern shown in Figure 17 was devised. This particular pattern provides a field configuration approximating a condition frequently encountered in practice, and it also permits a reasonable degree of analysis. The gap length between the copper electrodes is 60-mils. The field

is graded at the edges of the gap in order to restrict the failures to the narrow region of the gap formed by the parallel conductors. The particular curvature that was used is described in Figure 18 so that it might be reproduced in any laboratory. Although this curvature is not exactly the same as the conventional Rogowski contour, it provides sufficient grading and can be reproduced by a simple geometrical construction. Another function of the curved electrodes was to provide a gap of varying length in order to determine the most probable breakdown distance for a given voltage at very low pressures. In the pδ range where the Paschen curve has a negative slope, the weakest path for a given electrode configuration does not coincide with the smallest gap spacing or the region of maximum stress.

Tests were made on uncoated and coated specimens (FF-95C). The epoxy coating (Hysol 6233) had a thickness of about 7 mils. The coating causes a significant increase in flashover strength, whereas it has little effect on other electrical properties.

The range of values that were observed at 60 cps on the uncoated specimens are given in Table 6. Under high vacuum conditions these specimens exhibit the typical spread in flashover strength that has been discussed above for the other materials of the program.

The 60 cps data for the FF-95C are given in Table 7. It can be seen that the coating greatly increases the flashover strength. However, at atmospheric pressure a visible glow appears at about 6.0 KV in the region between the electrodes where the spacing is a minimum. In high vacuum a similar visible discharge occurs at about 7.0 KV, but in this case the discharge first appears between the curved sections of the electrodes, where the gap spacing is larger. As the applied voltage is increased, the glow discharge becomes broader, extending into the area where the gap spacing is smaller. Complete breakdown does not occur until the voltage reaches a value of about 17.0 KV, the same value observed at atmospheric pressure. When failure does occur

with the coated samples, it does not follow the shortest path between the electrodes. A breakdown of the epoxy coating is involved in the flashover, and it occurs between the weak points of the coating. These weak points may be located anywhere on the coating that covers the electrodes.

A series of tests was conducted to determine whether the glow discharge was located between the coating and the printed wiring board, or on the outside of the coating. When the flashover test was conducted in sulfur hexafluoride, rather than air, the glow did not appear until much higher voltages were applied. This effect indicated that the glow discharge was located on the outside surface of the coating.

Although the pressure in the vacuum cell is measured at a point which is only a few inches away from the closest specimen, the pressure at the surface of the specimen can be considerably higher than the measured pressure when the specimen exhibits a high rate of outgassing. The epoxy coating does outgas at a higher rate than the other materials of the program, and, consequently, the pressure at the surface of the specimen can be high enough to cause a discharge to occur at a spacing where the $p\delta$ product is large enough to permit ionization phenomena to govern the breakdown process. Since the coating acts as a barrier against complete breakdown, an increase in voltage causes ionization in the region of the field where δ is smaller. This would account for the broadening of the glow discharge as described above.

In the case of the irradiated specimens, it is not possible to make visible observations during the tests, and equipment was not available for detection of the glow discharge. Consequently, there is no data presented on the effects of irradiation on the glow-discharge inception-voltage of the coated FF-95C. There is no reason, however, to suspect that the radiation causes any significant change in the phenomena that occur in the case of the unirradiated samples.

The effects which have been discussed above for FF-95 and FF-95C involve 60 cps voltages. When measurements are made at 2 and 18 Mc, the high loss factor of the base laminate causes excessive heating which leads to internal failure, rather than flashover. A 2 Mc flashover can be obtained on the uncoated materials at atmospheric pressure at a voltage of 2.0 KV. Under high vacuum conditions, however, the material suffers thermal damage after 1 minute at 3.0 KV. At 18 Mc an applied voltage of 1.2 KV leads to a thermal failure.

The coated specimens behave in a similar fashion because the epoxy coating is lossy at high-frequencies. Thermal failures involving the coating material occur at voltages somewhat lower than those mentioned above for the uncoated material. In either case, flashover is not an important consideration because of the poor high-frequency characteristics of the base material and the coating.

4. Summary of High Vacuum Flashover and Sparkover Studies.

The results obtained in the studies of flashover and sparkover indicate that, from the practical point of view, flashover at very low pressures is primarily a hardware problem, rather than a materials problem. Microscopic irregularities on the electrode surfaces are the controlling factor in determining flashover voltage. X-ray and ultraviolet radiation have no immediate effect on flashover voltage unless they cause the loss factor of a material to increase to the point where excessive heating is encountered at relatively low electrical stresses. This can, of course, be determined from loss property studies.

The designer of high-voltage components for satellites and space vehicles is faced with the problem of guarding against flashovers which are initiated by emission from metallic parts, rather than by the more familiar gas ionization process. Consequently, he cannot fully utilize the inherently high electric strength of the high vacuum environment. However, the data of Table 5 indicates that the lowest

values of flashover voltage that were encountered in the present investigation were higher than the values that would prevail at atmospheric pressure. The flashover gap was only 17 mils, a distance which would support less than 2.0 KV at atmospheric pressure. Therefore, a device which is designed to perform satisfactorily at atmospheric pressure should be safe with respect to flashover at pressures below 10^{-5} Torr. In some cases an occasional discharge of short duration might occur, particularly during the early stages of electrification, but these discharges should have a favorable conditioning effect and no permanent damage to the insulation should result. A more serious problem exists in devices which must operate for significant lengths of time at pressures in the micron range where the Paschen minima occur for most practical hardware spacings.

C. Solid Dielectric Breakdown.

1. Mylar Film Tests.

a. Graded-Field Specimen. Electric strength continues to be the most difficult dielectric property to study because its measurement is influenced by discharges that originate in the medium surrounding the solid specimen. Clearly, the effects of any environmental stress on the electric strength of an insulating material cannot be determined if the measured values are compromised by phenomena that are associated with the surrounding medium, rather than with the material in question. In previous studies concerned with the effects of moisture and temperature, breakdown measurements were made using recessed electrodes and an oil immersion medium. In the present study, where the specimen must be exposed to a high-vacuum, this high-vacuum medium automatically becomes the immersion medium for the electric strength measurements.

In the previous Section it was shown that the inherently high electric strength of a high-vacuum medium is compromised by emission from the

electrodes. This phenomenon makes it difficult to completely eliminate spurious discharges during electric strength measurements. Consequently, a great deal of care was required in preparing the specimens used in this study. There are two well known methods of eliminating discharges in the vicinity of a high-voltage electrode. The first method consists of grading the field around the high-voltage hardware, and the second method employs recessed electrodes. Both methods were used in the manner described below.

Grading of the electric field (reducing the stress) in the vicinity of the high-voltage electrode can be accomplished by reducing the surface resistivity over a portion of the specimen. The alternating-voltage gradient in a radial direction then depends on the surface resistivity (which may or may not be uniform) and the capacitance distribution of the specimen electrode system. This method has serious disadvantages when it is applied over a wide frequency range, so an alternative method was attempted which utilizes concentric conducting rings, rather than a continuous resistive film. Each ring is electrically connected to a tap of a voltage-divider network so that only a predetermined fraction of the applied voltage appears between successive rings.

This method was applied in tests on 3 mil Mylar film. One side of the film was coated with a layer of evaporated silver which served as the ground electrode. On the other side of the Mylar film a 1.25 inch diameter center-electrode and eight concentric rings were deposited by the evaporation of silver through a suitable mask. The radial distance between successive rings was increased from 0.05 to 0.20 inches as the inside radius of successive rings was increased from 0.7 to 1.9 inches. The width of each ring was about 0.05 inches. Contacts with the center electrode and each ring were made by several spring-loaded pins which were accurately positioned in a special sample-holder.

The voltage distribution between rings and between the center electrode and the first ring was adjusted by means of the voltage-divider network. It was expected that the individual voltages would be low enough to avoid surface discharges during the breakdown test, but small radial arcs were observed between the center electrode and the first ring at a total applied voltage of only 2.0 KV at 60 cps. At this total applied voltage, the voltage between the center electrode and the first ring should have been only 50 volts, a value too low to cause discharges over a 50 mil spacing. However, any discharges between larger rings (where the voltages were higher) upset the voltage distribution, thereby over-stressing the inner gaps. The difficulty was caused by small cracks which were formed in the silver coating by expansion of the Mylar film during the evaporation process. The same pattern was applied to a glass plate, which did not expand, and the first discharges did not appear until the applied voltage reached 10 KV, but even this voltage is too low for electric strength measurements on films in the mil thickness range.

Some improvement in this technique could have been made by using more rings. These experiments were discontinued, however, because the high cost and long delivery time in obtaining a suitable mask did not seem warranted in view of the complicated and time-consuming experimental procedure.

b. Composite Specimen. Since the recessed electrodes had been used successfully in previous breakdown studies, ⁽²²⁾ a specimen was designed that permitted this principle to be applied to the thin film tests. A specimen of this kind provides a high-strength material in the critical volume surrounding the high-voltage electrode. With thick specimens (1/4 inch, or more) a cavity can be formed in the material and then coated with a conducting film, which provides intimate contact with the high-voltage electrode. This type of specimen is described in the following Section. With thin specimens, however, it is not possible to

form a cavity in the test specimen itself, so a composite specimen was fabricated as shown in Figure 19. It has four parts: (i) the film specimen; (ii) a polystyrene block ($1\frac{1}{2}'' \times 1\frac{1}{2}'' \times 1\frac{1}{2}''$) with a $\frac{3}{4}$ inch diameter hole through its center; (iii) a polystyrene fillet which forms a smooth junction between the Mylar film and the cylindrical wall in the polystyrene block; and (iv) a 3 inch length of polystyrene tubing ($\frac{7}{8}''$ I. D. , $1''$ O. D.).

To form the polystyrene fillet, the polystyrene block was placed on top of the Mylar film and both parts were clamped to a small turn-table. The speed of the turn-table was adjusted so that liquid styrene resin could be transferred from a medicine dropper to the wall of the cavity without contaminating the central area (test area) of the film. This liquid formed a fillet whose shape (approximately parabolic) was determined by the viscosity and surface tension of the resin and the rotational speed of the turn-table.

After the fillet was cured the cavity and the flat side of the specimen were coated with evaporated silver. The polystyrene tube was then cemented to the block, as shown in Figure 19. The cavity was then coated again and the silver was allowed to deposit in the lower two-thirds of the tube. High-voltage contact was made by means of a circular clip which pressed against the wall of the cavity, near the polystyrene fillet. The long tube increased the voltage at which discharges occurred across the specimen surface to the ground electrode.

c. Experimental Results. In spite of the pains that were taken with these experiments, the results were not completely satisfactory, as will be shown below. On many samples the failure occurred outside of the prescribed test-area because the fillet did not form a smooth junction with the film. The difficulty was caused by changes in surface tension of the resin during the hardening process and frequent separation of the fillet from the Mylar film during the silver-evaporation process. Several modifications were tried without appreciable improvement.

A summary of the 60 cps electric strength measurements on two grades of 1 mil Mylar is given in Figure 20. The values of KV/mil indicate the stress in the thin section of the specimen. Many breakdowns occurred in the fillet, but the values of KV/mil for these tests are based on the stress in the thin section (test area) at the time the test was terminated. These values then become withstand values, so the actual range of values of electric strength would extend somewhat beyond the maximum values shown. The lower limit, however, is established by the minimum value at which the failure occurred in the test area.

Similar results for 0.5 mil Mylar are summarized in Figure 21. Again, most of the specimens failed outside of the test area. The ratio of maximum to minimum values for the valid tests was 3 to 1, a result obtained by other investigators on thin film specimens.

A series of d-c breakdown tests were conducted on the 1 mil Mylar #130-100T. Valid breakdowns were obtained over the range of 12 to 16 KV/mil and withstand values as high as 20 KV/mil were observed. These values are comparable to the peak values at 60 cps.

A simultaneous study of the effects of irradiation on the dielectric constant and dissipation factor of Mylar had indicated that no significant effects were produced during exposure periods of several hundred hours. Consequently, it was decided to postpone further studies on the electric strength of Mylar in the interest of obtaining data on other materials that had exhibited changes in loss properties during irradiation.

2. Electric Strength of Machinable, Low-Loss Polymers.

a. Specimen Preparation. This series of experiments was concerned with electric strength measurements on polystyrene (PS), polyethylene (PE) and several grades of polytetrafluoroethylene. Recessed electrodes could be applied to these materials in a more straightforward manner because the specimens were thick enough to

permit suitable cavities to be machined. Several types of cavities were tried, but the one shown in Figure 22 was most satisfactory. It has the advantage of providing a large test area (compared to a tapered cavity) and the thick section at the center of the cavity does not have to be carefully machined. The machining was done in a lathe, using a properly shaped tool with rounded cutting blades.

Evaporated silver coatings served as the electrodes. A brass insert shaped as shown in Figure 22 reduced the sharp field at the rim of the cavity, thereby eliminating discharges from this troublesome area. Contact between the brass piece and the silver coating was made with a helical clock-spring at a point in the base of the cavity where the material was about five times thicker than it was in the test area.

In spite of the precautions that were taken, occasional arcs occurred between the high-voltage hardware and the ground electrode. To keep these discharges from actuating the thyatron switching circuit, a guard cylinder was placed around the ground electrode as shown in Figure 22. As mentioned in a previous section, the discharges that occur at relatively low stresses in a high-vacuum have a favorable conditioning effect and do not recur as the voltage is increased. Consequently, these discharges did not influence the breakdown tests as long as they were not permitted to trigger the thyatron.

b. Breakdown Data (Unirradiated Specimens). A summary of the 60 cps measurements on specimens that were placed in the vacuum chamber, but not irradiated, is given in Table 8. These values are based on tests where a sharp puncture was obtained in the thin section of the specimen. The spread in results is not unusual for high-strength materials. Just how much of this spread is characteristic of the material itself is difficult to evaluate. Certainly a property such as electric strength, which involves a localized catastrophic event, will exhibit a greater spread than a property such as dielectric constant, which depends on the average behavior of all mechanisms in the active

volume of a specimen. The additional contribution to the spread caused by handling of the specimen and by electrode effects, cannot be readily evaluated.

Similar results were obtained in tests on PE and PF using positive direct-voltage, i.e. the high-voltage electrode was positive with respect to the ground electrode. The average value of d-c electric strength for PE was 2.3 KV/mil and the maximum and minimum values were 3.0 and 1.9 KV/mil respectively. For PF the results were 2.6 KV/mil average, 3.3 KV/mil maximum and 1.8 KV/mil minimum.

Tests in the radio-frequency range, even on these low-loss materials, resulted in considerable heating in the critical volume of the specimen. Thermal failures were observed at 2 Mc and 18 Mc on PE, PS and the fluoroethylene polymers. The failure stresses are given in Table 9. These tests were conducted under severe thermal conditions because very little of the heat which was developed in the critical volume of the specimen could be conducted away by the thin silver coating and the vacuum medium provided no significant cooling. These same materials exhibit sharp, pin-point punctures at frequencies up to 100 Mc when the tests are conducted in an oil immersion medium and the electrodes are made of solid brass.⁽²³⁾ Furthermore, under more favorable thermal conditions, the failure stresses are two or three times greater than those shown in Table 9. These results illustrate how much the test method can affect measured values of electric strength. They further indicate the importance of thermal considerations in high-frequency applications, particularly in a high-vacuum medium.

c. Effects of X-ray Irradiation on Electric Strength. To determine the immediate effects of x-ray irradiation on electric strength, tests were conducted at 60 cps in the manner described for the flash-over experiments (see page 18). No effect could be detected for any of the materials listed in Table 8.

Long-time radiation effects were investigated by conducting the breakdown test on each specimen after a given exposure period. The tests were made while the specimens were still being irradiated. These tests are very time-consuming because each specimen yields only one breakdown value at the end of the exposure period.

The results obtained on PE, TFE-6, TFE-7, and FEP-100 are summarized in Figures 23 - 26 respectively. Any effects that might be produced over the dosage ranges shown are masked by the spread in results. Consequently, the results only show that no large effects were detected. This result was expected for PE and FEP-100 but not for TFE-6 and TFE-7. The loss properties of the TFE materials were drastically affected by x-ray irradiation (see Section III, D, 2). Values of 60 cps $\tan\delta$ as high as 0.40 for TFE-6 and 0.17 for TFE-7 were observed after absorbed doses of approximately 2.5 and 1.0 megarads respectively. Consequently, it was expected that such high values of induced dissipation factor would cause thermal effects to influence the electric strength measurements. Surprisingly, however, temperature rise in the test-area was found to be less than that predicted on the basis of the high dissipation factors. To resolve this discrepancy, dissipation factor measurements were made on breakdown specimens during irradiation. However, the results of these approximate measurements confirmed the existence of very high dissipation factors for both materials.

One effect that would explain the apparent improvement in behavior during the breakdown test is a dependence of $\tan\delta$ on applied voltage. Time did not permit a thorough study of this effect, but a circuit was assembled which served to show that $\tan\delta$ (60 cps) was indeed a decreasing function of voltage for irradiated TFE-6 and TFE-7. Furthermore, the variation with voltage was reversible. This suggests that the radiation-induced loss-mechanism could be one that is hindered and, therefore, contributes to the loss for only a part of

each half-cycle at the higher voltages. Further experiments could aid in identifying the particular mechanism involved, but they could not be conducted in time to be included in this report.

3. Summary of Dielectric Breakdown Study. The breakdown study has revealed no significant effects on electric strength as a result of x-ray irradiation under high-vacuum. However, the study is not complete. Only one class of materials, the low-loss polymers, has been investigated. Future studies involving the electric strength of solids in a high-vacuum environment have been planned. Emphasis will be placed on determining the extent to which various factors influence the spread in results. The objective of this study will be two-fold: (i) to permit detection of small (but significant) changes in electric strength caused by pertinent environmental stresses, so that short-time exposure data can be used in predicting high-stress effects under service conditions; and (ii) to gain a better understanding of the mechanisms involved in breakdown under the exposure conditions of the program.

D. Loss Properties.

1. High-Vacuum Effects. As a matter of convenience the term "loss properties" is used in this report to include dielectric constant, dissipation factor ($\tan\delta$), d-c surface resistivity and d-c volume resistivity — the properties which do, indeed, govern the loss characteristics of a material. These properties are not dependent upon the electrical characteristics of the medium which surround a specimen (in contrast to flashover strength); but the composition of the surrounding medium can, of course, influence the loss properties of a solid by causing changes in the composition of the solid material. In a vacuum environment such changes can be caused by the removal of moisture and other volatile products from the solid material.

In general, the effects of high-vacuum exposure result in improved loss properties. The largest changes occur during the early stages of exposure. The rate of change depends on the pressure in the vacuum chamber, the specimen temperature and the previous conditioning of the specimen.

Since these changes in electrical properties are not degradative, there is no reason to be concerned about insulation-life in a high-vacuum environment unless the physical properties of a material are impaired. However, when stability is an important consideration, any change in electrical properties can be undesirable. A decrease in dielectric constant, for instance, can affect the performance of a component and thereby change the operating characteristics of a device. Consequently, even the changes that result in improved electrical properties must be considered undesirable in some cases.

When x-ray irradiation is introduced, the resulting changes in electrical properties are not usually beneficial. These effects are discussed in the following Section. In the irradiation experiments each specimen was exposed to high-vacuum for about two days before the irradiation was introduced. Measurements were made before pump-down and again at the end of the two day period. In the tables of exposure data these values are referred to as "Initial" and "Pump-down" respectively.

The initial loss properties of all the materials included in this program are summarized in Tables 10 and 11. These values were measured under room condition, on specimens that were stored in the laboratory for at least two weeks.

2. Effects of X-ray Irradiation on Loss Properties.

a. General Remarks. A considerable amount of research has been reported on the effects of radiation on materials. Charlesby,⁽²⁶⁾ in a recent book, summarizes the important publications in this field

and discusses the mechanisms involved in radiation effects for several polymers. Moody, ⁽²⁷⁾ in an REIC Memorandum, points out that most of the published work pertains to physical and chemical properties, rather than electrical properties. However, Charlesby does include a short chapter on electrical conductivity, based primarily on the work of Fowler. ⁽²⁸⁾

In several of the investigations where electrical properties have been studied, measurements were made before and after irradiation, but meaningful measurements could not be made during irradiation. In this program, measurements of dielectric constant and dissipation factor were made during irradiation while the specimens were in a high-vacuum (10^{-5} - 10^{-6} Torr). Transient effects were observed which would not have been evident if significant time intervals had elapsed between irradiation and measurement.

The three-electrode specimens that were used in this study are normally used for measurements of dielectric constant, dissipation factor, d-c surface resistivity and d-c volume resistivity. However, during irradiation the ionization currents in the residual gas and the photoelectric currents from the electrodes were larger than the d-c currents in the specimen (a condition that does not seem to be adequately accounted for in some published investigations). Consequently, d-c measurements could only be made while the x-ray generator was temporarily turned off. A lack of pumping time and cell space would not permit the use of separate specimens for d-c measurements only.

Recovery measurements were made while the specimens remained in the vacuum environment for at least 24 hours. Subsequent recovery measurements were made at atmospheric pressure (room-condition) because of the prohibitive pumping-time required to make such measurements in the high-vacuum cell.

The results for each type of material are discussed below.

b. Tetrafluoroethylene Polymers. The most striking radiation effects were those exhibited by the TFE polymers. Polytetrafluoroethylene has received a great deal of attention in irradiation studies because of its poor radiation resistance in contrast to its excellent thermal and chemical stability. The TFE polymers and the FEP copolymer exhibit similar electrical properties under normal ambient conditions, but their behavior in the presence of x-ray irradiation differs markedly.

Figure 27 shows the drastic effect of x-ray irradiation on the dissipation factors of TFE-6 and TFE-7 at 60 cps and 1 kc. The detailed data are given in Table 12. The 60 cps dissipation factor of TFE-6 increased rapidly during the early stages of exposure, reaching a maximum value of 0.408 at an absorbed dose of 2.5 megarads. It decreased during the remainder of the exposure period to a value of 0.081 at a total absorbed dose of 6.6 megarads. TFE-7 exhibited a similar transient effect, reaching a maximum value of 0.169 after only 29 hours (0.91 megarads). For both materials the effect is greatly moderated at 1 kc, indicating that the induced loss is associated with a relatively large, slow-moving mechanism.

Corresponding changes in dielectric constant were observed for both materials, as shown in Figure 28. In the case of TFE-7 the change in 1 kc dielectric constant was less than 1.0 percent throughout the exposure period. The detailed data are given in Table 13.

In these experiments the radiation intensity was approximately $150 \mu\text{watts/cm}^2$ and the ambient pressure was about 5.0×10^{-6} Torr. Measurements were made with the beam on, and frequent checks were made with the beam off to verify the fact that the observed values were representative of the specimen behavior. These checks showed that extraneous effects, such as gas ionization and photoelectric currents, did not affect the measurements. Furthermore, simultaneous measurements of FEP-100 and PF showed no significant induced loss for either of these materials. Consequently, there could be no question concerning

the validity of the measurements, but there remained some doubt concerning the purity of the TFE specimens.

New lots of TFE-6 and TFE-7 samples were prepared by the manufacturer and the irradiation experiments were repeated. The results were essentially the same as those obtained in the original experiments. Consequently, the presence of accidental impurities in the specimens was very unlikely.

Measurements of d-c conductivity were also made during the irradiation exposure period. As mentioned previously, the x-ray beam was temporarily interrupted during the d-c measurements. However, only five minutes was allowed for each measurement because the specimens do exhibit significant recovery characteristics. Experiments showed that during the five minute electrification the current decayed to within 20 percent of the value remaining after 24 hours of electrification. The results of these measurements are given in Table 14.

These data show that measurable conduction currents were induced by the x-ray irradiation, but no attempt was made to study this phenomenon in detail. A considerable amount of work has been done on radiation-induced conductivity by other workers. Warner⁽²⁹⁾ reported in 1951 on the induced conductivity in high-quality materials and Warner, Muller and Nordlin⁽³⁰⁾ reported further on this subject in 1954. Fowler⁽²⁸⁾ discusses the mechanism of radiation-induced conductivity, being primarily concerned with recovery characteristics.

The recovery data of Table 14 indicate that there was no steady decay of induced conductivity during 1170 hours of recovery. Although these measurements include polarization currents that might have existed after 24 hours of electrification, they are of practical significance. The results of Fowler for much smaller absorbed doses indicate that induced conductivity decays rapidly. However, this should not be interpreted to mean that the effects of radiation on the total induced current will disappear shortly after the removal of radiation.

The behavior during recovery depends upon the absorbed dose and the period of electrification. A more detailed study would be required to determine the effects of specimen thickness (diffusion), ambient oxygen concentration and dose rate on the decay of induced conductivity for high dose rates.

Recovery measurements of a-c loss properties on TFE-6 and TFE-7 indicate that a rapid decrease in $\tan\delta$ occurs when the radiation is discontinued. This decrease in $\tan\delta$ continues during 96 hours of recovery in high-vacuum, as shown in Figure 27. In a later series of measurements, which are discussed below, it was found that when TFE specimens were removed from the vacuum chamber, the low frequency $\tan\delta$ increased (sometimes erratically) to values as high as 0.01 at 100 cps. Subsequent decay was very slow, some specimens showing measurable induced losses after 35 days recovery at room condition.

These results demonstrate the importance of ambient constituents in studies of radiation effects. Wall and Florin⁽³¹⁾ found that gamma radiation caused rapid loss of tensile strength in polytetrafluoroethylene film when specimens were irradiated in air, but the material was relatively resistant to radiation in high vacuum. They attribute this behavior to the difference in oxygen concentration. Florin and Wall⁽³²⁾ discuss their work in greater detail in a more recent publication dealing with the radiation chemistry of fluorocarbon polymers. They include a list of 62 references which provides a valuable summary of the published work in this specialized area.

In view of the drastic effects observed during irradiation of the TFE polymers in vacuum, where it was expected that radiation effects would be moderated, it seemed most desirable to conduct similar experiments in air. This was done and the dissipation factor and dielectric constant data are shown in Figures 29 and 30. Here the induced losses increase to the same high level as the maximum values observed in the vacuum irradiation, but this high level is then maintained throughout the exposure period (720 hours). This behavior is in

sharp contrast to the steady decrease in $\tan\delta$ for both TFE polymers during the latter stages of irradiation in vacuum. These results further demonstrate the influence of oxygen concentration. However, they also indicate that the induced reactions are not simple ones and must occur in discrete stages with significant time-lags between reactions.

The observed behavior is summarized in the curves of Figures 31 and 32, which show the changes in $\tan\delta$ for TFE-6 under three different experimental conditions: (i) irradiation in air (Curve A); (ii) irradiation in vacuum (Curve B); and (iii) irradiation in vacuum using a specimen that had been previously irradiated (8.5 megarads) and allowed to recover in air for ten months (Curve C).

It is generally agreed that irradiation of TFE polymers produces free radicals which are readily oxidized and hydrolyzed. The loss data suggest that the free radicals are not directly responsible for the very high values of $\tan\delta$. The largest contribution to the induced losses is probably associated with the oxidized products. This is evidenced by the steady high-losses observed in air, as opposed to the transient behavior exhibited in high vacuum. It is further demonstrated by the sudden increase in $\tan\delta$ that is observed when irradiated specimens are exposed to air (see recovery data Figure 32).

The data also show that these groups are capable of contributing to the induced losses for only a short period of time. Their elimination or rearrangement in the polymer structure results in a decrease in $\tan\delta$. This is demonstrated by the recovery data for the specimens irradiated in air (Curve A, Figure 32), and by the transient nature of the vacuum irradiation effects. The concentration of these groups depends upon their mean life, the x-ray dose rate, the G-value for the production of free radicals (number of reactions per 100 ev of absorbed energy), and the oxygen concentration.

Since it is known that radiation causes crosslinking and degradation in TFE polymers, it is possible that oxidized groups

ultimately become attached to long chain molecules in such positions that they no longer contribute to the high induced losses.

After very long recovery periods the physical and optical changes caused by crosslinking and degradation are still evident. The induced losses, however, are not measurable after several months of recovery in air. Consequently, these structural changes do not significantly affect electrical properties and may, indeed, provide the means by which the high-loss mechanism is eliminated, as mentioned above.

During both the latter stages of exposure and the five day recovery in vacuum, the dissipation factor of the specimen which had been previously irradiated (Curve C) remained constant. This indicates that interaction with the radiation was no longer contributing to the induced losses during the latter period of exposure. Upon exposure of the specimen to the atmosphere, however, $\tan\delta$ immediately increased and then remained constant for 30 days. The specimen that was being irradiated for the first time (Curve B) experienced an abrupt decrease in $\tan\delta$ as soon as the radiation was discontinued, but then showed no further change during recovery in vacuum. Upon exposure to the atmosphere this specimen also exhibited a sudden increase in $\tan\delta$, followed by a somewhat erratic decrease to a level which then remained constant for the next two weeks.

This difference in behavior cannot be explained solely on the basis of oxygen concentration because both specimens were simultaneously exposed to the same environment. However, the difference in total absorbed dose is significant and both specimens would probably have exhibited comparable losses if the exposure had been prolonged. The specimen irradiated in air showed no saturation effect after absorbing 12 megarads, but this is still a smaller dose than the cumulative dose absorbed by the specimen of Curve C. It is to be expected that the G-values for most radiation products would decrease as the absorbed dose increases, and this would lead to a lower concentration of the groups that cause the high induced losses.

Attempts to relate the observed phenomena to specific reactions described by other workers have not been completely satisfactory. The most serious difficulty lies in the completely different behavior of PF, which has the same basic structure as the TFE-6 and TFE-7 polymers. The PF material, which is a polytetrafluoroethylene polymer that had been stored in the laboratory for several years, showed no measurable induced loss for absorbed doses up to 9.3 megarads. This difference in behavior is so striking, when compared to the high dissipation factors exhibited by the TFE polymers, that explanation of the TFE behavior based on the reactions which are initiated by breaking C-C and C-F bonds must be viewed with caution. The same kinds of bonds are subject to scission in both types of materials, but the PF material exhibits no induced loss. This suggests that end groups and impurities could play important roles in radiation induced losses.

Specimens of TFE-6 which contained different added impurities were available and experiments were conducted to determine the effects of these bulk additives. One-percent loadings of zirconia, silica or carbon had no marked effect on the radiation sensitivity or recovery characteristics of TFE-6. However, these granular materials are not representative of the kinds of impurities that might be included during production of the polymers.

All of the detailed results that have been accumulated in the course of this study on TFE are not included in the tables of this report. The important effects have been described and enough typical data have been given to demonstrate the normal spread in results. To include all of the measured values would serve no useful purpose.

Further studies of the effect of irradiation on the low frequency loss properties of TFE should include measurements on thin specimens that have been baked under vacuum before radiation is introduced. During recovery periods the ambient relative humidity should be controlled so that moisture absorption does not complicate the results. (29)

It should be noted that the electrical behavior during irradiation is only one consideration in selecting insulating materials for use in a radiation environment. Degradation of physical properties is also an important consideration. It has been found that TFE resins enjoy an increase in zero-strength-time (ZST) during the early stages of exposure to gamma radiation, but then exhibit lower values of ZST as the exposure time is prolonged.⁽³²⁾ This transient effect could be related to the observed peak in $\tan\delta$, and it would be of special interest to study dynamic mechanical properties during irradiation.

c. FEP-100. The a-c loss properties of the copolymer FEP were unaffected by x-ray irradiation. An induced d-c conductivity was observed, however, during vacuum irradiation. The volume and surface resistivity data are given in Table 15. These data demonstrate the existence of an induced conductivity, but experiments could not be conducted to study this effect in greater detail.

The physical and optical properties of FEP-100 were permanently affected by the x-ray irradiation, but no quantitative measurements were taken, as previously explained.

d. Polychlorotrifluoroethylene. Two grades of polychlorotrifluoroethylene, designated K-4 and K-5, and one grade of the copolymer of chlorotrifluoroethylene and vinylidene fluoride, designated K-7, were examined. These materials are described in detail on Pages 1 and 2, and their initial properties are given in Tables 10 and 11.

Both K-4 and K-5 showed decreases in 60 cps $\tan\delta$ during and after irradiation as shown by the data of Table 16. The low values of 0.001 after 1920 hours of recovery in air were of particular interest because they are about one decade lower than the initial values. However measurements at the end of 6700 hours (16 months) indicate that the dissipation factors are slowly increasing, but are still about 50 percent of the initial values.

The d-c resistivity data are given in Tables 17 and 18.

Visual inspection indicated that the x-ray irradiation caused a yellow color-change in K-4 and a slight change in index of refraction in K-5.

The more recent measurements on K-7 indicate that the a-c loss properties of the copolymer were unaffected by x-ray doses up to 27.8 megarads. The exposure and recovery data are given in Tables 19 and 20.

Induced d-c conductivity was observed as shown by the volume and surface resistivity data of Table 21.

No visual changes in physical or optical properties were evident as a result of the irradiation.

e. Polyethylene (Alathon 4 BK 30). This material is a high molecular weight polyethylene which contains approximately 2.6 percent carbon channel black. It was exposed for 94 hours to a total dose of 0.69 megarads. No changes in a-c properties were detected and only slight changes in d-c conductivity were observed, as shown in Table 22. Fowler has measured x-ray induced conductivity in polyethylene and discusses his results in detail in Reference 28. A polyethylene comparable to that used by Fowler has not been included in the program, so that a direct comparison of results is not possible. The conduction currents observed in both cases were in the 10^{-14} ampere range, but his specimens had a larger area-to-thickness ratio.

f. Crosslinked Polystyrene (PSC). The a-c loss properties of PSC were unaffected by irradiation in vacuum for doses up to 4.5 megarads. Induced conductivities were observed as shown by the data of Table 23. The initial values are of particular interest because they are considerably lower than those exhibited by conventional polystyrene.

The radiation resistance of polystyrene is known to be high, so it was not expected that the crosslinked material would be affected by the x-ray irradiation. The only visual evidence of physical effects was a slight change of color.

g. Mylar. Measurements were made on two grades of Mylar; 130-100C capacitor film and 130-100T highly oriented, tensilized film. The largest changes in a-c loss properties of these 1 mil films occurred during the pump-down period prior to irradiation. These changes consisted of decreases in dissipation factor and dielectric constant, as shown in Tables 24 and 25. The removal of moisture accounts for the improved electrical properties. It will be noted that corresponding increases in loss properties occurred when the specimens were again exposed to the atmosphere.

The d-c volume and surface resistivity data are given in Tables 26 and 27. The observed decreases in these properties were limited to approximately one decade throughout the exposure period.

The irradiation caused a slight yellowing of the transparent films and they became somewhat stiffer (more brittle).

h. Glass Polyester Laminate, (GPG). This material exhibited changes in a-c and d-c properties during vacuum x-ray irradiation. No changes in dielectric constant were observed, but rapid increases in 60 cps and 1 kc dissipation factor occurred during the early stages of irradiation, as shown by the data of Table 28. During the remainder of the exposure period there was little change in dissipation factor, and there was no rapid decay during the recovery period.

The d-c data are given in Table 28 and it will be noted that the first measurements were made after 68 hours of irradiation. Earlier measurements would have been made except for an unavoidable situation which made it impossible to do so. However, it can be seen that the largest change in conductivity had occurred prior to the first measure-

ment and relatively little change was observed during the remainder of the exposure period. During the 960 hour recovery period the volume and surface resistivities remained essentially constant, i. e. they showed no definite decay.

The material, which is a light green translucent laminate, experienced a yellowing color change during irradiation. This color change is further evidence of a permanent degradation during exposure. Since this material is intended for use in radomes, it would seem advisable to determine the effects of irradiation on its mechanical properties.

i. Copper-Clad Glass-Epoxy Laminate (FF-95). At the time the irradiation study of FF-95 was made the upper limits of d-c volume and surface resistivity that could be measured were 1.8×10^{14} ohm-cm and 4.0×10^{13} ohms per square. Consequently, no induced conductivity was detected during the exposure period. Specimens of FF-95 coated with HYSOL 6233 were also examined under the same conditions and exhibited no induced conductivity.

No changes in a-c loss properties were observed for FF-95 or the coated material FF-95C during a 48 hour exposure period.

Further tests on this material were planned for the last phase of the program. It is just as well that these additional tests were not conducted because it is now understood that significant changes in the material have been made by the manufacturer, so the data would be of questionable value.

j. Forsterite, Alsimag-243 (2 MgO.SiO₂). In general, the ceramics are more resistant to ionizing radiation than organic materials. No drastic changes in the electrical properties of AL-243 were observed during a 95 hour x-ray exposure period. The dielectric constant and dissipation factor values remained constant and are, therefore, not presented in tabular form. Slight changes in d-c

resistivity are given in Table 29. Throughout the exposure and recovery periods the volume and surface resistivities remained very close to the limit of measurement, a result that was expected on the basis of the known behavior of such materials in a radiation environment.

Visual inspection of the specimens indicated very little or no darkening as the result of color center formation.

k. Alox (Al_2O_3). The electrical behavior of Alox was similar to that of AL-243 during vacuum x-ray exposure. No changes were detected in a-c loss properties, but slight changes in d-c resistivity were observed, as shown by the data of Table 30. Alox is one of the few materials that exhibited an initial d-c conductivity that was within the range of measurement. The resistivity of one specimen was consistently higher than the other one, and this specimen showed virtually no change during exposure. This variation among specimens is typical, and is not peculiar to Alox alone by any means.

The x-ray irradiation produced a drastic color change in Alox, from white to brown. This change is the result of color center formation associated with the absorption of energy from the incident x-ray radiation. Upon exposure to visible light, the specimens are bleached to their original color, but in the absence of light, the induced color centers are retained indefinitely. The recovery data of Table 30 were obtained with specimens that were stored in a dark area, but were not kept in complete darkness during the actual recovery measurements. Therefore, it is possible that the low values of resistivity that were observed during recovery might have been influenced by photoconduction.⁽³³⁾ However, it should be noted that in spite of the high concentration of color centers, the properties of Alox were not drastically affected.

l. Steatite, Alsimag-665 ($\text{MgO} \cdot \text{SiO}_2$). This ceramic also showed high resistance to x-ray irradiation. Its a-c properties were

virtually unaffected during irradiation, but showed some variation during recovery in air, as shown in Table 31. These slight changes in $\tan\delta$ could be caused by fluctuations in ambient relative humidity, which was not controlled during the recovery period.

The d-c resistivity data shown in Table 32, indicate that no steady increase in conductivity was exhibited. The spread in results and the fluctuations over a long period of time are typical of d-c resistivity measurements, particularly with ceramics.

Only a slight change in color was produced by the x-ray irradiation.

m. Beryllium Oxide (BeO). Exposure data on dissipation factor, dielectric constant, and d-c resistivity are given in Tables 33, 34 and 35 respectively. Detailed results are shown for two specimens. Specimen 1 was the best sample in a lot of 50 pieces and Specimen 2 was typical of most of the samples in that same lot. All of the specimens were refired at a temperature of 1350°C to remove any contamination caused by the grinding operation. Particular care was taken to avoid surface contamination while handling the specimens in the laboratory, but the variation in electrical properties among samples was still quite large. This condition was also encountered with the high-purity alumina described above. The two BeO specimens exhibited radically different behavior during exposure. Specimen 1 was virtually unaffected, while Specimen 2 showed a marked improvement in loss properties. The largest changes in the properties of Specimen 2 occurred during the pump-down period prior to irradiation. The properties of the two samples became more nearly alike during the exposure period and they remained unchanged during the recovery period in vacuum. However, when the specimens were exposed to the atmosphere, the loss properties of Specimen 2 increased to their initial values and became somewhat erratic during the remainder of the recovery period.

This behavior indicates that Specimen 2 was highly sensitive to ambient relative humidity, while Specimen 1 was unaffected by the same changes in environmental conditions. Consequently, it must be concluded that the effects of vacuum exposure on the electrical properties of BeO depend on the presence of impurities and surface contaminants.

The x-ray irradiation caused severe discoloration in BeO, from white to dark grey. This effect could be important in applications where emissivity is a design consideration.

n. Eccofoam S, (ECF). This material is a polyurethane foam which has a density of 12 lbs per cu. ft. Like other low density materials, it has a low dielectric constant and a low dissipation factor over a wide frequency range. The fact that so much of the volume is occupied by air accounts for the low values of measured dielectric constant and dissipation factor. Actually, the solid material itself does not possess particularly good electrical properties. The initial values of d-c volume and surface resistivity are given in Table 36. These values indicate that the solid material has a relatively high conductivity, since the measured conduction current flows only in the cellular structure and not in the gaseous portion of the specimen.

Specimens of ECF were exposed to x-ray irradiation under high vacuum for 94 hours. No changes in a-c properties were detected during this period, but some variations in d-c resistivity were observed, as shown by the data of Table 36. For the most part, the exposure had a beneficial effect, which was probably associated with the removal of moisture and other volatile products.

3. Effects of Ultraviolet Radiation on Loss Properties.

a. General Remarks. In space applications ultraviolet radiation presents a less severe environmental stress than x-ray or higher energy radiation because it is so readily absorbed by most materials

that it can interact only with the surfaces of exposed components. Consequently, greater emphasis was placed on the x-ray irradiation study during this program.

A few experiments conducted during the first phase of the program indicated that thermal effects were contributing to the observed changes in loss properties during ultraviolet irradiation.

In the second phase of the program a specimen holder was designed which permitted the ultraviolet radiation to pass through a transparent electrode and impinge on the active area of the loss specimen. Provision was made to compensate for the specimen temperature rise in order to separate thermal effects from those caused by interaction with the radiation. Although no drastic effects were observed, the experiments are described below in order to provide a description of the technique. Results are also given for measurements that were made before and after exposure, where electrodes were not applied to the specimen during irradiation.

b. Ultraviolet Measurements During Irradiation. The specimen holder used in these experiments utilizes a quartz high-voltage electrode to permit the radiation to impinge on the active area of the loss specimen. The transparent electrode is a 2 1/2 inch diameter, 1/8 inch thick quartz plate with a conductive coating of tin oxide which has a resistivity of approximately 2.2×10^4 ohms per square. The coating was applied by Dr. N. M. Bashara, University of Nebraska, Lincoln, Nebraska, who is using this type of electrode in a study of discharges in dielectric voids. ⁽³⁴⁾

The specimen holder is shown in Figure 33. The transparent high-voltage electrode is mounted in the large brass cylinder on the left. The measurement electrode is shown in a raised position to make it distinguishable from the guard ring which surrounds it. Two typical specimens are shown in the foreground. The radiation intensity at the specimen surface is given in Table 2.

Experiments were conducted to determine the extent to which the resistivity of the tin oxide coating would influence loss measurements. It was found that no error was introduced at frequencies up to 10 kc. At higher frequencies the equivalent series resistance of the cell would cause a significant error.

To determine the effectiveness of the contact between the coated electrode and the bare specimen, measurements were made on several materials before and after the application of evaporated silver electrodes. Significant errors were found to occur only with badly warped specimens.

Since it is possible to have small air spaces between the transparent electrode and the specimen surface, it was necessary to determine if these voids introduced errors when measurements were made in the presence of intense ultraviolet radiation. In these experiments the coated electrode was deliberately held at a distance of 3 mils from the specimen surface, while measurements were made with and without ultraviolet radiation. Using polystyrene samples it was found that the bridge balance did not change as the ultraviolet source was switched on and off.

One of the disadvantages of the cell is its relatively large mass, which gives it a long thermal time-constant. The cell was designed for use with a sensitive temperature control network which would maintain the specimen temperature constant ($\pm 0.5^{\circ}\text{C}$) throughout an extended period in which the ultraviolet beam was on for only a part of the time. In order to accomplish this, it was necessary to allow several hours for the cell to reach an equilibrium temperature a few degrees higher than it would normally attain with the beam on. An incandescent lamp in the vacuum cell was used to supply the required thermal energy to raise the temperature of the cell. The response time of the control circuit was such that after the final temperature was reached, the ultraviolet source could be turned on and the

incandescent lamp would then supply only enough energy to maintain a constant specimen temperature. A similar arrangement for temperature control was used with a conventional three-electrode specimen, where the metal electrode shielded the active volume of the specimen from the ultraviolet beam.

Measurements were made on the radome material GPG using both types of electrode systems. Before the ultraviolet source was turned on, both samples had reached thermal equilibrium and their dielectric constants had stabilized at a value approximately 9 percent above room temperature value. The exposure and recovery data are given in Table 37. Both samples showed an increase in dielectric constant when the beam was turned on. The conventional specimen exhibited the greater change during irradiation, but the maximum increase was less than 4 percent and the difference between specimens was about 2 percent. When the measurements were repeated with specimens of PSC and Alathon 4 BK 30, no changes in loss properties were observed. Similar measurements were made on the printed circuit laminate FF-95 by stripping the copper film from one side. No changes in loss properties were observed after thermal equilibrium was established.

Time would not permit further investigation of the behavior exhibited by GPG. The observed changes were small, but they do pose an interesting academic question. However, it was necessary to proceed with other experiments to determine if important effects were produced during longer exposure periods.

c. Measurements Before and After Irradiation. Since it was desirable to gain the maximum amount of information in the limited time available for ultraviolet exposure studies, a series of measurements was made on specimens before and after irradiation. Silver paint electrodes were applied to the specimens and initial measurements were made. The electrodes were then removed before the

specimens were placed in the vacuum cell. This method permitted four specimens to be irradiated simultaneously. After exposure for about 335 hours, the specimens were removed and new electrodes were applied.

The results of these tests showed that the ultraviolet radiation produced no significant changes in dielectric constant, $\tan\delta$ and d-c surface and volume resistivity of Mylar 130-100 T, Mylar 130-100 C, AL-665, BeO and PSC. The exposure times for these materials varied from 334 to 338 hours. Although the 1 mil Mylar specimens showed no changes in electrical properties, they did suffer severe physical degradation, as evidenced by brittleness and yellow coloring.

d. Insulation Resistance Measurements FF-95. Experiments were conducted on the printed circuit board FF-95, using the comb-type insulation resistance specimen shown in Figure 34. This specimen, described in Signal Corps Technical Requirements SCL-6225 (10 July 1957), has a two-electrode system that consists of six sharply defined parallel conductors 0.030 inches \pm 0.003 inches wide, spaced 0.030 inches \pm 0.003 inches apart and 3.0 inches in length. Alternate conductors are connected to terminal areas at opposite ends of the board.

Measurements of d-c insulation resistance could not be made during irradiation because the photoelectric current was many times greater than the combined surface and volume conduction currents. When the beam was turned off, the current immediately decayed to a value beyond the range of measurement. No permanent effects were produced by the irradiation.

e. Summary of Ultraviolet Irradiation Study. As mentioned previously, the x-ray irradiation study received far greater effort than the ultraviolet study. The experiments that have been discussed above show that the instantaneous and short-time effects of ultraviolet irradiation on a-c loss properties are not large enough to be of practical

importance. Photoelectric effects dominate the d-c behavior and, in most instances, it would not be possible to expose metal circuit elements or hardware to solar ultraviolet radiation if a high level of insulation resistance must be maintained.

The long-time degradative effects of ultraviolet radiation in high-vacuum remain to be studied. Other laboratories are studying such effects, but there is no program primarily concerned with electrical properties. It is reasonable to expect, however, that physical degradation will be a more important consideration in selecting materials that must be exposed to solar radiation.

E. Microwave Measurements. A used Microwave Dielectrometer, Model 2, manufactured by Central Research Laboratories, Inc., Red Wing, Minnesota, was acquired during the program. This equipment is designed to facilitate measurement of dielectric constant and dissipation factor in the frequency range from 1.0 to 8.6 Gc.

The equipment was repaired and put into operation during the second phase of the program. Its performance was evaluated by a series of measurements on materials whose microwave properties have been well established. Long-time stability of the equipment was found to be satisfactory requiring only minor adjustments to maintain proper operation. However, short-time fluctuations caused by temperature and line voltage variations were great enough to make it necessary to perform four measurements on each specimen. Instability is not a problem with high dielectric constant, high loss materials.

A second series of measurements was made on specimens of TFE and polystyrene before and after x-ray irradiation in high-vacuum. Surface layer doses of 5.7 and 3.2 megarads respectively produced no measurable changes in loss properties at 3.0 Gc.

To eliminate a great deal of the time-consuming calculations involved in reducing the data, simplifications were made which

permitted the manipulation of real quantities only. To achieve further reduction in the time required for calculations a computer program was designed to provide values which could be plotted to form a series of charts that permit rapid reduction of data from instrument readings. This program was run on an IBM 7090 computer at the Johns Hopkins Applied Physics Laboratory.

Further studies of microwave properties of materials under space environmental conditions will be made in the next program.

IV. Conclusions

This program has served as an introduction to the study of the effects of space environment on the electrical properties of insulating materials. Many aspects of this broad subject have been examined, but only a few specific effects could be studied in detail. Future programs will be concerned with the unanswered questions that have been raised during this investigation.

Several important results were obtained, however, and they are summarized below:

1. Flashover in high-vacuum depends upon electrode roughness in the same way as uniform field sparkover. The breakdown process is governed by field emission rather than a Townsend ionization mechanism, and the condition of the cathode surface dominates the phenomenon.
2. X-ray or ultraviolet radiation have no immediate effect on high-vacuum sparkover or flashover.
3. X-ray irradiation caused no significant effects on the electric strengths of the low-loss polymers examined.
4. Thermal effects dominate the high-frequency breakdown of solid materials when the electric strength measurements are made in high-vacuum with lightweight electrodes. Thermal conditions are so unfavorable that even the low-loss polymers exhibit excessive heating at stresses considerably lower than their electric strengths as measured in an oil immersion medium.
5. Exposure to high-vacuum causes changes in loss properties in those materials that are subject to

moisture absorption. The removal of moisture and other volatile products results in improved electrical properties. The largest changes occur during the early stages of evacuation, and the magnitude of the changes depend on the specimen temperature and the previous environmental history of the specimen.

6. X-ray irradiation causes induced d-c conduction, polarization and absorption currents which may decay very slowly after the radiation is removed. The recovery characteristics depend upon the period of electrification used in making the measurements.
7. Low-frequency loss properties of the TFE polymers are drastically affected by x-ray irradiation. The increases in dielectric constant and $\tan\delta$ depend upon ambient oxygen concentration during exposure and recovery. Induced losses were measured after 35 days recovery in air. The induced losses decrease with increasing frequency above 60 cps and the 60 cps dissipation factor decreases with increasing voltage; these two effects indicate the presence of a large loss-mechanism whose motion is hindered. The a-c loss properties of PF were unaffected by x-ray irradiation although this material has the same basic structure as the TFE polymers.
8. The effects of x-ray irradiation on the loss properties of the other materials of the program were much smaller than those exhibited by TFE. Results on each material are discussed in Section III, D, 2.
9. Instantaneous and short-time effects of ultraviolet radiation on a-c loss properties are not large enough to be of practical importance.

10. Photoelectric effects dominate d-c behavior in the presence of ultraviolet radiation. Shielding of hardware would be required wherever high insulation resistance must be maintained.

V. Recommendations

The investigation of the effects of space environment on the electrical properties of insulating materials will be continued under Contract DA-36-039-SC-89147. Emphasis will be placed on studying the phenomena associated with environmental effects, rather than further accumulation of exposure data on additional materials. Special consideration will be given to the detection of small, but significant, changes in properties which can be applied to predictions of component and material reliability under extended service conditions. In this regard, long-time exposure will also be conducted as time and facilities allow.

Refinements in techniques and apparatus will be made to provide for:

1. More effective trapping of molecules which escape from specimen surfaces.
2. The introduction of temperature as a test parameter.
3. The determination of weight loss during exposure.

New cells and accessories will be designed and constructed for use with a 40-liter Vac-Ion pump. This equipment will provide a limited amount of data at pressures in the 10^{-8} to 10^{-9} Torr range, but will be used primarily in obtaining information required in planning future experimental work.

VI. Cited References

1. R. A. Minzner, K. S. W. Champion and H. L. Pond, The ARDC Model Atmosphere, 1959. Airforce Surveys in Geophysics, No. 115, AFCRC-TR-59-267, August 1959.
2. J. J. Chapman, L. F. Blickley and E. A. Szymkowiak, Surface and Volume Dielectric Losses. AIEE Transactions, Vol. 74, Pt. I, July 1955, pp. 343-9.
3. J. J. Chapman and L. J. Frisco, A Practical Interpretation of Dielectric Measurements Up To 100-Mc. Final Report of Contract DA-36-039-SC-73156, December 31, 1958.
4. F. S. Johnson, The Solar Constant. Journal of Meteorology, Vol. 11, No. 6, pp. 431-9
5. L. R. Koller, Ultraviolet Radiation, John Wiley and Sons, New York (1952).
6. Technical Memorandum NR. M-1747, The Environment of an Earth Satellite, 15 November 1956, USASRDL, Ft. Monmouth, New Jersey.
7. G. L. Clark, Applied X-rays, McGraw-Hill Book Co., New York (1955).
8. G. J. Hine and G. L. Brownell, Radiation Dosimetry, Academic Press, Inc., New York (1956).
9. L. J. Frisco and J. J. Chapman, The Flashover Strength of Solid Dielectrics. Power Apparatus and Systems, No. 23, April 1956, pp. 77-83.
10. F. Llewellyn-Jones, Ionization and Breakdown in Gases. Methuen and Co. Ltd., London and John Wiley and Sons, Inc., New York (1957).
11. K. Hashimoto, Figures on the Surface of Metal Electrodes Produced By Breakdown In High-Vacuum. J. Phys. Soc. Japan, 2, 71-5 (1947).
12. H. Tuzek, Contribution to the Explanation of High Vacuum Breakdown From Field Emission Pictures. Z. angew. Phys., 9, No. 8, 338-94 (1957). In German.
13. F. G. Allen, J. Eisinger, H. D. Hagstrum, and J. T. Law, Cleaning of Silicon Surfaces by Heating in High-Vacuum. J. Appl. Phys., 30, No. 10, 1563-71 (1959).

14. W.P. Dyke and J.K. Trolan, Field Emission: Large Current Densities, Space Charge, and the Vacuum Arc. Phys. Rev., 89, No. 4, 799-808 (1953).
15. M.J. Kofoed, Phenomena at the Metal-Dielectric Junction of High-Voltage Insulators in Vacuum and Magnetic Field. Power App. and Syst., No. 51, 991-9 (1960).
16. M.J. Kofoed, Effect of Metal-Dielectric Junction Phenomena on High-Voltage Breakdown Over Insulators in Vacuum. Power App. and Syst., No. 51, 999-1004 (1960).
17. W.P. Dyke, J.K. Trolan, E.E. Martin, and J.P. Barbour, The Field Emission Initiated Vacuum Arc I, Experiments on Arc Initiation. Phys. Rev., 91, No. 5, 1043-54 (1953).
18. W.W. Dolan, W.P. Dyke, and J.K. Trolan, The Field Emission Initiated Vacuum Arc II, The Resistivity Heated Emitter. Phys. Rev., 91, No. 5, 1054-57 (1953).
19. L.J. Frisco and J.J. Chapman, The Flashover Strength of Solid Dielectrics. Power App. and Syst., No. 23, 77-83 (1956).
20. E. Funfer, High-Vacuum Breakdown and Its Application to X-ray Flash-Tubes. Z. angew. Phys., 5, No. 11, 426-40 (1953). In German.
21. W.H. Klippel and E.J. Lorentz, Materials and Design Factors In Printed Wiring Applications. Electrical Manufacturing, Vol. 58, No. 1, July 1956, pp. 62-9.
22. J.J. Chapman, L.J. Frisco and J.S. Smith, Dielectric Breakdown Techniques. Electrochemical Journal, 102, No. 2, 67-72 (1955).
23. J.J. Chapman, L.J. Frisco and J.S. Smith, Dielectric Failure of Volume and Surface Types. AIEE Transactions, 74, Pt. I, 349-56 (1955).
24. A.L. Alexander, F.M. Noonan, J.E. Cowling and Suzanne Stokes, The Degradation of Polymers By Ultraviolet Irradiation. NRL Memorandum Report 914, April 1959.
25. A. Charlesby, Effect of Radiation on Behavior and Properties of Polymers. Chapter 10 of The Effects of Radiation on Materials, edited by J.J. Harwood, H.H. Hausner, J.G. Morse and W.G. Rauch. Reinhold Publishing Corp., New York (1958).

26. A. Charlesby, Atomic Radiation and Polymers. Pergamon Press, London (1960).
27. J.W. Moody, The Effect of Nuclear Radiation on Electrical Insulating Materials. REIC Memorandum 14, March 31, 1959, Radiation Effects Information Center, Battelle Memorial Institute, Columbus, Ohio.
28. J.F. Fowler, X-ray Induced Conductivity In Insulating Materials. Proc. Royal Soc., 236A, 468-80 (1956).
29. A.J. Warner, The Effect of Ionizing Radiation on High Quality Insulating Materials. Annual Report 1951 Conference on Electrical Insulation (NAS-NRC), p. 26-28 (1952).
30. A.J. Warner, F.A. Muller and H.G. Nordlin, Electrical Conductivity Induced by Ionizing Radiation in Some Polymeric Materials. J. Applied Physics, 25, No. 1, 131 (1954).
31. L.A. Wall and R.E. Florin, Polytetrafluoroethylene - A Radiation Resistant Polymer. Letter to the Editor, J. Appl. Polymer Sci., Vol. II, No. 5, p.251 (1959).
32. R.E. Florin and L.A. Wall, Gamma Irradiation of Fluorocarbon Polymers. J. Research National Bureau of Standards, 65A, No. 4, 375-87 (1961).
33. R.B. Gordon, Color Centers in Crystals, American Scientist, 47, No. 3, 361-75 (1959).
34. N.M. Bashara, The Study of Discharges in Dielectric-Voids By Photomultiplier Methods. AIEE Transactions Paper No. 61-249, (1961).

VII. Identification of Personnel

L. J. Frisco	Research Contract Director, M. Sc. in Electrical Engineering. Full time.
A. M. Muhlbaum	Research Associate, Dipl. in Engineering Physics (Technical University of Delft, Netherlands). Full time.
E. A. Szymkowiak	Research Staff Assistant, B. E. in Electrical Engineering. Full time.
Andreas Rannestad	Research Assistant, B. E. in Electrical Engineering, candidate for advanced degree in Electrical Engineering. Full time June 15, 1959 to September 30, 1959; 25% of full time from October 1, 1959 to April 30, 1960; 52% of full time from May 1, 1960 to January 31, 1961.
D. J. D. Chu	Research Assistant, M. E. in Electrical Engineering, candidate for advanced degree in Electrical Engineering. Full time from June 6, 1961 to September 30, 1961.
W. G. Baumann	Research Technician. Full time.
Duncan McCulloch	Research Technician. Full time.
C. L. Woodward	Secretary. Full time.

VIII. Acknowledgements

The investigation of radiation effects on polytetrafluoroethylene was conducted in close cooperation with the Polychemicals Department, E.I. du Pont de Nemours and Company, Wilmington, Delaware. Their assistance and keen interest in the program is appreciated.

The following organizations contributed specimens and offered technical assistance whenever it was requested:

Minnesota Mining and Manufacturing Company,
St. Paul, Minnesota

Formica Corporation, Cincinnati, Ohio

William Brand-Rex Division, American Enka
Corporation, Concord, Massachusetts

Brush Beryllium Company, Cleveland, Ohio

E.I. du Pont de Nemours and Company, Polyester
Film Research and Development Department,
Circleville, Ohio

The National Beryllia Corporation, North Bergen, New Jersey, supplied specimens of Alox on a no-profit basis.

Thanks is also due Dr. N.M. Bashara, University of Nebraska, Lincoln, Nebraska, for processing the coated quartz plates that were used as transparent electrodes, and to the Chemicals and Plastics Division, Food Machinery and Chemical Corporation, Baltimore, Maryland, for measuring the ultraviolet transmission of several components.

IX. Tables

<u>Table</u>	<u>Description</u>	<u>Page</u>
1	Solar spectral irradiance data.	69
2	Comparative UV intensities at 30 cm from lamp.	70
3	Output intensity of AEG-50 x-ray tube at 220 mm distance.	71
4	Output intensity of AEG-50 x-ray tube at 155 mm distance.	72
5	Summary of flashover data.	73
6	FF-95 flashover strength.	74
7	FF-95C flashover strength.	75
8	60 cps electric strength of low-loss polymers.	76
9	Radio-frequency breakdown data.	77
10	Initial values; dielectric constant.	78
11	Initial values; dissipation factor.	79
12	TFE-6 and TFE-7 dissipation factor; vacuum x-ray exposure data.	80
13	TFE-6 and TFE-7 dielectric constant; vacuum x-ray exposure data.	81
14	TFE-6 and TFE-7 volume resistivity; vacuum x-ray exposure data.	82
15	FEP-100 volume and surface resistivity; vacuum x-ray exposure data.	83
16	K-4 and K-5 dissipation factor; vacuum x-ray exposure data.	84
17	K-4 and K-5 volume resistivity; vacuum x-ray exposure data.	85

IX. Tables (continued)

<u>Table</u>	<u>Description</u>	<u>Page</u>
18	K-4 and K-5 surface resistivity; vacuum x-ray exposure data.	86
19	K-7 dissipation factor; vacuum x-ray exposure data.	87
20	K-7 dielectric constant; vacuum x-ray exposure data.	88
21	K-7 volume and surface resistivity; vacuum x-ray exposure data.	89
22	Alathon 4 BK 30 volume and surface resistivity; vacuum x-ray exposure data.	90
23	PSC volume and surface resistivity; vacuum x-ray exposure data.	91
24	Mylar dissipation factor; vacuum x-ray exposure data.	92
25	Mylar dielectric constant; vacuum x-ray exposure data.	93
26	Mylar volume resistivity; vacuum x-ray exposure data.	94
27	Mylar surface resistivity; vacuum x-ray exposure data.	95
28	GPG loss properties; vacuum x-ray exposure data.	96
29	AL-243 volume and surface resistivity; vacuum x-ray exposure data.	97
30	ALOX volume and surface resistivity; vacuum x-ray exposure data.	98
31	AL-665 dielectric constant and dissipation factor; vacuum x-ray exposure data.	99

IX. Tables (continued)

<u>Table</u>	<u>Description</u>	<u>Page</u>
32	AL-665 volume and surface resistivity; vacuum x-ray exposure data.	100
33	BeO dissipation factor; vacuum x-ray exposure data.	101
34	BeO dielectric constant; vacuum x-ray exposure data.	102
35	BeO volume and surface resistivity; vacuum x-ray exposure data.	103
36	ECF volume and surface resistivity; vacuum x-ray exposure data.	104
37	GPG dielectric constant and dissipation factor; ultraviolet exposure data.	105

Table 1. Solar Spectral Irradiance Data*.

<u>Wavelength Region</u> <u>(Angstroms)</u>	<u>Intensity</u> <u>(milliwatts/cm²)</u>
Below 2200	0.03
2200-3800	10.2
3800-7000	59.5
7000-10,000	29.5
10,000-20,000	32.2
20,000-70,000	7.4

* - Computed from Reference 4.

Table 2. Comparative Ultraviolet Intensities (mw/cm²)
At 30-cm Distance From Lamp.

<u>Wavelength Band</u> <u>(Angstroms)</u>	<u>Bare</u>	<u>Filtered</u>	<u>Filtered</u> <u>B-H6 and</u> <u>Coated Electrode*</u>	<u>Solar</u>
	<u>B-H6</u>	<u>B-H6*</u>		
Below 2262	0	0	0	0.04
2262-2800	3.31	1.21	0.68	0.67
2800-3165	7.62	3.61	2.39	2.05
3165-3800	10.84	5.31	4.13	7.41
Total U. V.	21.77	10.13	7.20	10.17

* - Intensity at specimen surface

Table 3. Output Intensity of AEC-50 X-ray Tube
(mw/cm²) at 220-mm Distance.

<u>Anode Current</u> <u>(ma)</u>	<u>Peak Voltage</u> <u>50-KV</u>	<u>Peak Voltage</u> <u>40-KV</u>	<u>Peak Voltage</u> <u>30-KV</u>
50.0	1.10	0.76	0.30
25.0	0.49		
12.5	0.24		
6.25	0.13		

Table 4. Output Intensity of AEG-50 X-ray Tube
(mw/cm²) at 155-mm Distance.

<u>Anode Current</u> <u>(ma)</u>	<u>Peak Voltage</u> <u>50-KV</u>	<u>Peak Voltage</u> <u>40-KV</u>	<u>Peak Voltage</u> <u>30-KV</u>
50.0	1.60	1.10	0.63
25.0	0.80	0.60	0.25
12.5	0.40		
6.25	0.20		

Table 5. Flashover Voltages; 17 mil Gap, Evaporated Silver Electrodes, 10^{-6} Torr Pressure Range.

<u>Material</u>	<u>D-C (KV)</u>	<u>60-cps (KV peak)</u>	<u>2-Mc (KV peak)</u>	<u>18-Mc (KV peak)</u>
K-4	7.0-1.4	2.7-6.0	2.1-2.5	<1.4*
K-5	4.0-16	2.7-4.5	2.2-3.1	<1.4*
K-5(S)	17-24			
4 BK 30	7.0-17			<1.4*
4 BK 30(S)	10.25	2.7-14	1.5-4.0	
FEP-100	4.5-13	2.5-6.5	2.5-3.0	1.1-2.0
FEP-100(S)	13-20			
TFE-6	6.5-13	3.2-4.5	2.2-3.0	1.4-2.0
TFE-7	5.5-20	2.1-5.6	1.7-2.7	1.1-2.1
GPG	5.0-8.0	4.0-11	1.8-3.8	<0.7
AL-243	7.5-26	4.0-12	2.1-3.4	1.4-1.5
Alox	2.0-9.0	4.0-8.7	1.7-2.4	2.1-2.8
Glass Slides	10-29	4.5-15		

(S) - Smooth surface, see page 19.

* - Test terminated because of excessive heating of material in the gap.

Table 6. FF-95 Flashover Strength; 60-cps Exposure Data.

<u>Pressure Torr</u>	<u>Radiation</u>	<u>rms-KV</u>
760	none	3.6-3.7
10 ⁻⁵	none	2.5-6.0
10 ⁻⁵	UV	2.8-7.2
10 ⁻⁵	x-ray	4.6-7.2

Table 7. FF-95C Flashover Strength; 60-cps Exposure Data.

<u>Pressure Torr</u>	<u>Radiation</u>	<u>rms-KV*</u>
760	none	17
10^{-5}	none	16-18
10^{-5}	UV	13-16
10^{-5}	x-ray	8-15

* - Actual failure voltages. Visible glow occurs at lower voltages. See text.

Table 8. Initial Values of 60-cps Electric Strength In High-
Vacuum, No Irradiation; (rms KV/mil).

<u>Material</u>	<u>Thickness (mils)</u>	<u>No. of Tests</u>	<u>Average</u>	<u>Max.</u>	<u>Min.</u>
PE	12	11	2.2	2.5	1.7
PS	8	31	3.5	5.1	1.9
PF	12	31	1.5	2.2	0.9
TFE-6	12	5	1.6	1.8	1.3
TFE-7	12	7	2.4	2.5	1.7
FEP-100	12	1	2.2		

Table 9. Thermal Failure Stress at Radio-Frequencies;
Recessed Electrodes In High Vacuum, No
Irradiation; (rms KV/mil).

<u>Material</u>	<u>Thickness</u> <u>(mils)</u>	<u>2-Mc</u>	<u>18-Mc</u>
PE	12	0.2	0.1
PS	8	0.4	0.1
PF	12	0.4	0.1

Table 10. Initial Values; Dielectric Constant.

<u>Material</u>	<u>60-cps</u>	<u>100-cps</u>	<u>1-kc</u>	<u>10-kc</u>	<u>100-kc</u>	<u>2-Mc</u>	<u>18-Mc</u>	<u>100-Mc</u>
PSC	2.57	2.57	2.57	2.57	2.57			
4 BK 30	2.56		2.52	2.50	2.47	2.45	2.44	2.43
TFE-6	2.08	2.08	2.08	2.07	2.06	2.05	2.04	2.03
TFE-7	2.09	2.08	2.05	2.04	2.03	2.02	2.01	2.00
FEP-100	2.11	2.11	2.11	2.11	2.11	2.10	2.09	2.08
K-4	2.73		2.65	2.54	2.50	2.48	2.47	2.45
K-5	2.67		2.57	2.45	2.44	2.43	2.41	2.37
K-7		2.79	2.68	2.55	2.46			
Mylar C	3.11		3.10	3.09				
Mylar T	3.38		3.34	3.33				
FF-95	5.05		4.98	4.91	4.80	4.25	4.22	4.20
FF-95C	5.05		4.98	4.91	4.80	4.25	4.22	4.20
GPG	4.27		4.18	4.16	4.13	3.91	3.89	3.87
ECF	1.10		1.10	1.09	1.06			
AL-243	6.74		6.69	6.64	6.64	6.57	6.47	6.44
AL-665	6.00		5.99	5.98				
Alox	10.38		10.31	10.16	10.15	9.33	9.10	8.85
BeO	7.07		6.57	6.48				

Table 11. Initial Values; Dissipation Factor.

<u>Material</u>	<u>60-cps</u>	<u>100-cps</u>	<u>1-kc</u>	<u>10-kc</u>	<u>100-kc</u>	<u>2-Mc</u>	<u>18-Mc</u>	<u>100-Mc</u>
PSC	.0002	.0002	.0002	.0003	.0003			
4 BK 30	L		L	L	.006	.001	.005	.005
TFE-6	.0003	.0003	.0003	.0003	.0003	L	L	L
TFE-7	.0002	.0002	.0002	.0003	.0003	L	L	L
FEP-100	.0003	.0003	.0003	.0002	.0002			
K-4	.008		.025	.028	.018	.012	.007	.006
K-5	.011		.024	.027	.014	.002	.003	.003
K-7		.018	.026	.025	.017			
Mylar C	.004		.005	.0002				
Mylar T	.003		.005	.0002				
FF-95	.004		.009	.016	.038	.018	.015	.004
FF-95C	.003		.009	.016	.038	.018	.017	.004
GPG	.003		.006	.010	.023	.014	.013	.010
ECF	L		L	L	L			
AL-243	.002		.002	.002	L	L	.015	.020
AL-665	.0002		.0008	.0005				
Alox	.001		.003	.004	.005	.004	.008	.009
BeO	.053		.033	.006				

L - Less than 0.001

Table 12. TFE-6 and TFE-7 Dissipation Factor;
Vacuum X-Ray Exposure Data.

<u>Dose</u> <u>(Mrads)</u>	<u>TFE-6</u>		<u>TFE-7</u>	
	<u>60-cps</u>	<u>1-kc</u>	<u>60-cps</u>	<u>1-kc</u>
0	L	L	L	L
0.06	.002	L	L	L
0.16	.024	.003	L	L
0.71	.144	.017	.120	.014
0.84	.160	.020	.147	.016
0.94	.170	.023	.169	.017
1.49	.239	.036	.143	.018
1.72	.291	.040	.141	.018
2.27	.377	.047	.129	.016
2.40	.390	.048	.124	.015
3.11	.408	.048	.095	.011
3.24	.404	.047	.092	.010
4.02	.334	.040	.085	.008
5.38	.226	.026	.031	.006
5.51	.216	.025	.027	.005
5.61	.208	.024	.025	.005
6.16	.168	.019	.019	.003
6.28	.158	.018	.019	.003
6.38	.152	.017	.019	.003
6.90	.116	.015	.019	.003
7.07	.109	.014	.019	.003
7.16	.105	.014	.019	.003
7.72	.081	.011	.019	.003
<u>Recovery</u> <u>Time</u> <u>(Hours)</u>				
2	.063	.010	.016	.002
6	.049	.009	.009	.002
24	.015	.003	.007	L
96	.001	L	.001	L

L - Less than .001

Table 13. TFE-6 and TFE-7 Dielectric Constant;
Vacuum X-Ray Exposure Data.

<u>Dose</u> <u>(Mrads)</u>	<u>TFE-6</u>		<u>TFE-7</u>	
	<u>60-cps</u>	<u>1-kc</u>	<u>60-cps</u>	<u>1-kc</u>
0	2.08	2.08	2.09	2.05
0.06	2.08	2.08	2.09	2.05
0.16	2.08	2.08	2.11	2.05
0.71	2.12	2.08	2.15	2.05
0.84	2.14	2.08	2.15	2.05
0.94	2.14	2.10	2.15	2.05
1.49	2.23	2.12	2.15	2.05
1.72	2.25	2.12	2.15	2.05
2.27	2.31	2.12	2.13	2.05
2.40	2.31	2.12	2.13	2.05
3.11	2.33	2.12	2.13	2.05
3.24	2.33	2.12	2.13	2.05
4.02	2.29	2.12	2.13	2.05
5.38	2.23	2.10	2.13	2.05
5.51	2.23	2.10	2.13	2.05
5.61	2.23	2.10	2.13	2.05
6.16	2.20	2.08	2.13	2.05
6.28	2.18	2.08	2.13	2.05
6.38	2.18	2.08	2.13	2.05
6.90	2.16	2.08	2.13	2.05
7.07	2.16	2.08	2.13	2.05
7.16	2.16	2.08	2.13	2.05
7.72	2.12	2.08	2.13	2.05
<u>Recovery</u> <u>Time</u> <u>(Hours)</u>				
2	2.12	2.08	2.13	2.05
6	2.12	2.08	2.11	2.05
24	2.08	2.08	2.09	2.05
96	2.08	2.08	2.09	2.05

Table 14. TFE-6 and TFE-7 Volume Resistivity (ohm-cm);
Vacuum X-Ray Exposure Data.

Dose (Mrads)	TFE-6		TFE-7	
	Sample 1	Sample 2	Sample 1	Sample 2
0	A	A	A	A
0.06	6.9×10^{17}	3.9×10^{16}	1.4×10^{17}	2.0×10^{16}
0.16	1.1×10^{17}	6.3×10^{16}	9.8×10^{16}	1.1×10^{17}
0.71	3.1×10^{16}	3.9×10^{15}	1.2×10^{17}	1.1×10^{17}
0.84	1.8×10^{16}	4.9×10^{15}	9.2×10^{16}	1.1×10^{17}
0.94	7.7×10^{15}	7.7×10^{15}	1.9×10^{16}	1.2×10^{17}
1.49	6.9×10^{15}	7.7×10^{15}	3.6×10^{16}	1.5×10^{17}
1.72	3.5×10^{16}	8.6×10^{15}	1.6×10^{16}	1.6×10^{17}
2.27	3.5×10^{16}	7.7×10^{15}	1.5×10^{16}	1.6×10^{17}
2.40	3.5×10^{16}	8.1×10^{15}	2.2×10^{16}	2.8×10^{16}
3.11	2.3×10^{16}	8.6×10^{15}	2.5×10^{16}	5.0×10^{16}
3.24	1.2×10^{17}	8.1×10^{15}	1.8×10^{16}	6.0×10^{16}
4.02	6.9×10^{17}	8.1×10^{15}	1.8×10^{16}	4.6×10^{16}
5.38	6.9×10^{17}	2.8×10^{15}	1.7×10^{16}	2.8×10^{16}
5.51	3.9×10^{15}	5.1×10^{15}	2.1×10^{16}	8.1×10^{16}
5.61	5.2×10^{15}	3.7×10^{15}	6.6×10^{16}	1.3×10^{17}
6.16	1.7×10^{16}	5.5×10^{15}	4.1×10^{16}	5.2×10^{16}
6.28	1.8×10^{16}	1.2×10^{15}	2.5×10^{16}	2.8×10^{16}
6.38	1.6×10^{16}	4.9×10^{15}	2.0×10^{16}	4.6×10^{17}
6.90	1.5×10^{15}	1.9×10^{15}	1.5×10^{16}	4.6×10^{17}
7.07	9.2×10^{15}	4.2×10^{15}	1.8×10^{16}	A
7.16	6.9×10^{16}	2.6×10^{15}	1.6×10^{16}	A
7.72	3.1×10^{16}	4.1×10^{15}	2.8×10^{16}	5.8×10^{16}
Recovery Time (Hours)				
2	3.1×10^{15}	4.1×10^{15}	2.0×10^{16}	2.9×10^{16}
6	4.9×10^{13}	4.1×10^{15}	1.5×10^{16}	A
24	4.1×10^{14}	1.6×10^{16}	2.0×10^{16}	2.7×10^{16}
96	3.6×10^{15}	3.6×10^{16}	4.8×10^{16}	2.6×10^{16}
168	6.3×10^{15}	8.6×10^{14}	3.5×10^{14}	2.5×10^{14}
360	2.2×10^{16}	6.3×10^{15}	2.5×10^{14}	2.8×10^{14}
1170	4.0×10^{17}	3.5×10^{17}	9.2×10^{15}	5.8×10^{15}

A - Greater than 1×10^{18} ohm-cm

Note: Samples removed from vacuum chamber after 96 hours

Table 15. FEP-100 D-C Volume and Surface Resistivity;
Vacuum X-Ray Exposure Data.

Dose (Mrads)	Volume Resistivity (ohm-cm)		Surface Resistivity (ohms per square)	
	Sample 1	Sample 2	Sample 1	Sample 2
0	A	A	B	B
0.06	A	A	B	B
0.16	A	A	B	B
0.75	1.1×10^{17}	8.1×10^{16}	B	2.9×10^{17}
0.94	6.0×10^{16}	3.5×10^{16}	B	5.8×10^{16}
1.55	1.8×10^{16}	1.0×10^{15}	3.4×10^{16}	2.2×10^{15}
1.72	2.4×10^{16}	1.1×10^{15}	3.9×10^{16}	1.9×10^{15}
2.30	6.6×10^{15}	6.6×10^{15}	2.2×10^{16}	3.9×10^{14}
2.49	7.7×10^{15}	5.1×10^{15}	2.1×10^{16}	3.9×10^{14}
3.08	4.8×10^{15}	5.5×10^{15}	7.2×10^{15}	2.1×10^{14}
Recovery Time (Hours)				
3	3.6×10^{15}	8.1×10^{15}	5.8×10^{16}	1.4×10^{15}
5	1.8×10^{16}	1.1×10^{15}	B	5.3×10^{15}
72	1.2×10^{17}	1.1×10^{15}	1.9×10^{17}	2.9×10^{17}

A - Greater than 1×10^{18} ohm-cm

B - Greater than 5×10^{17} ohms per square

Table 16. K-4 and K-5 Dissipation Factor;
Vacuum X-Ray Exposure Data.

<u>Dose</u> <u>(Mrads)</u>	<u>K-4</u>		<u>K-5</u>	
	<u>60-cps</u>	<u>1-kc</u>	<u>60-cps</u>	<u>1-kc</u>
0	.008	.025	.011	.024
0.34	.008	.026	.010	.025
0.56	.005	.028	.007	.028
2.46	.005	.029	.007	.029
4.92	.005	.029	.007	.028
5.37	.005	.029	.007	.028
7.60	.005	.029	.007	.028
8.06	.005	.029	.007	.028
10.3	.005	.028	.006	.028
21.0	.005	.028	.004	.028
<u>Recovery</u> <u>Time</u> <u>(Hours)</u>				
24	.005	.026	.004	.027
1920	.001	.029	.001	.028

Note: Samples removed from vacuum chamber after
72 hours

Table 17. K-4 and K-5 D-C Volume Resistivity (ohm-cm);
Vacuum X-ray Exposure Data.

Dose (Mrads)	<u>K-4</u>		<u>K-5</u>	
	<u>Sample 1</u>	<u>Sample 2</u>	<u>Sample 1</u>	<u>Sample 2</u>
0	A	A	A	A
0.56	5.7×10^{17}	A	2.9×10^{17}	2.3×10^{17}
4.92	1.9×10^{17}	3.9×10^{16}	A	2.3×10^{16}
7.60	1.9×10^{17}	1.9×10^{17}	1.6×10^{17}	8.8×10^{17}
10.3	4.8×10^{16}	2.1×10^{16}	2.9×10^{17}	5.7×10^{17}
21.0	3.8×10^{16}	A	A	2.3×10^{17}
Recovery				
Time				
<u>(Hours)</u>				
24	1.5×10^{16}	1.9×10^{17}	A	5.7×10^{17}
312	2.3×10^{17}	2.0×10^{16}	1.3×10^{16}	1.0×10^{17}
672	1.6×10^{17}	3.6×10^{16}	7.6×10^{16}	1.6×10^{17}
1920	2.3×10^{17}	8.8×10^{16}	1.4×10^{17}	2.9×10^{17}

A - Greater than 1×10^{18} ohm-cm

Note: Samples removed from vacuum chamber after 72 hours

Table 18. K-4 and K-5 D-C Surface Resistivity (ohms per square);
Vacuum X-Ray Exposure Data.

Dose (Mrads)	<u>K-4</u>		<u>K-5</u>	
	<u>Sample 1</u>	<u>Sample 2</u>	<u>Sample 1</u>	<u>Sample 2</u>
0	B	B	B	B
0.56	3.0×10^{15}	4.5×10^{15}	4.9×10^{16}	1.3×10^{15}
4.92	3.6×10^{15}	4.2×10^{15}	4.5×10^{16}	1.4×10^{15}
7.60	3.4×10^{15}	4.2×10^{15}	4.2×10^{16}	1.7×10^{15}
10.3	3.6×10^{15}	4.2×10^{15}	4.2×10^{16}	1.8×10^{15}
21.0	5.4×10^{15}	6.0×10^{15}	5.4×10^{16}	2.9×10^{15}
Recovery Time (Hours)				
24	4.9×10^{15}	6.4×10^{15}	6.0×10^{16}	2.4×10^{15}
312	5.4×10^{16}	1.1×10^{16}	1.4×10^{17}	1.1×10^{17}
672	6.0×10^{16}	1.1×10^{17}	5.4×10^{16}	2.7×10^{17}
1920	1.4×10^{17}	1.2×10^{17}	B	B

B - Greater than 5×10^{17} ohms per square

Note: Samples removed from vacuum chamber after 72 hours

Table 19. K-7 Dissipation Factor; Vacuum X-Ray Exposure Data.

<u>Exposure Time (Hours)</u>	<u>100-cps</u>	<u>1-kc</u>	<u>10-kc</u>	<u>100-kc</u>	<u>Dose (Mrads)</u>
Initial	.0180	.0264	.0251	.0168	
Pump-Down	.0189	.0264	.0251	.0166	0
6	.0190	.0266	.0262	.0168	0.52
24	.0191	.0267	.0250	.0175	2.08
47	.0186	.0266	.0249	.0175	4.08
90	.0186	.0266	.0249	.0175	7.81
161	.0186	.0266	.0253	.0175	13.95
183	.0183	.0266	.0255	.0180	15.88
207	.0180	.0266	.0251	.0179	17.95
229	.0189	.0266	.0245	.0179	19.85
251	.0189	.0266	.0238	.0180	21.7
321	.0187	.0264	.0248	.0178	27.8
<u>Recovery Time - Days</u>					
1	.0191	.0263	.0234	.0170	
2	.0199	.0262	.0234	.0170	
3	.0196	.0262	.0235	.0173	
4	.0178	.0263	.0235	.0170	
14	.0183	.0261	.0246	.0169	

Table 20. K-7 Dielectric Constant; Vacuum X-Ray Exposure Data.

<u>Exposure Time (Hours)</u>	<u>100-cps</u>	<u>1-kc</u>	<u>10-kc</u>	<u>100-kc</u>	<u>Dose (Mrads)</u>
Initial	2.794	2.682	2.551	2.464	
Pump-Down	2.742	2.642	2.542	2.455	0
6	2.776	2.668	2.568	2.470	0.52
24	2.763	2.660	2.555	2.470	2.08
47	2.763	2.660	2.555	2.470	4.08
90	2.763	2.660	2.555	2.464	7.81
161	2.763	2.660	2.555	2.464	13.95
183	2.763	2.660	2.555	2.464	15.85
207	2.750	2.658	2.555	2.464	17.95
229	2.750	2.650	2.555	2.464	19.85
251	2.750	2.640	2.550	2.464	21.7
321	2.746	2.640	2.550	2.464	27.8
 <u>Recovery Time - Days</u>					
1	2.746	2.640	2.550	2.464	
2	2.746	2.640	2.550	2.464	
3	2.746	2.640	2.550	2.464	
4	2.746	2.640	2.550	2.464	
14	2.746	2.635	2.542	2.464	

Table 21. K-7 D-C Volume and Surface Resistivity;
Vacuum X-Ray Exposure Data.

Dose (Mrads)	Volume Resistivity (ohm-cm)		Surface Resistivity (ohms per square)	
	Sample 1	Sample 2	Sample 1	Sample 2
0	4.1×10^{18}	2.1×10^{18}	7.3×10^{17}	9.1×10^{17}
2.08	5.0×10^{16}	7.3×10^{16}	2.8×10^{17}	4.6×10^{17}
4.08	4.9×10^{16}	6.1×10^{16}	3.6×10^{17}	B
7.81	3.7×10^{16}	5.4×10^{16}	3.3×10^{17}	B
13.95	2.9×10^{16}	3.9×10^{16}	1.1×10^{17}	3.6×10^{17}
15.85	2.5×10^{16}	3.3×10^{16}	1.6×10^{17}	3.6×10^{18}
17.95	2.4×10^{16}	2.4×10^{16}	1.8×10^{17}	B
19.85	1.9×10^{16}	2.3×10^{16}	2.4×10^{17}	1.8×10^{18}
21.7	1.9×10^{16}	2.4×10^{16}	3.3×10^{17}	B
27.8	1.1×10^{16}	1.5×10^{16}	1.3×10^{17}	1.8×10^{18}
Recovery Time (Days)				
1	4.1×10^{16}	4.9×10^{16}	1.1×10^{17}	1.8×10^{18}
2	5.8×10^{16}	6.9×10^{16}	1.6×10^{17}	3.6×10^{18}
3	9.2×10^{16}	9.3×10^{16}	2.3×10^{17}	1.8×10^{18}
4	9.2×10^{16}	9.5×10^{16}	9.9×10^{16}	4.6×10^{17}
14	3.7×10^{17}	2.7×10^{17}	1.5×10^{17}	5.2×10^{17}

B - Greater than 3.6×10^{18} ohms per square

Table 22. Alathon 4 BK 30 D-C Volume and Surface Resistivity;
Vacuum X-Ray Exposure Data.

Dose (Mrads)	Volume Resistivity (ohm-cm)		Surface Resistivity (ohms per square)	
	Sample 1	Sample 2	Sample 1	Sample 2
0	A	A	B	B
0.06	A	A	B	B
0.41	2.0×10^{17}	2.3×10^{17}	B	B
0.53	1.5×10^{17}	6.9×10^{16}	2.9×10^{17}	8.3×10^{16}
0.83	2.3×10^{17}	6.9×10^{16}	5.0×10^{17}	2.9×10^{17}
0.93	4.6×10^{16}	1.7×10^{17}	5.0×10^{17}	5.0×10^{17}
1.27	9.2×10^{16}	2.6×10^{17}	5.0×10^{17}	B
1.37	1.5×10^{17}	5.1×10^{16}	B	9.7×10^{16}
1.71	A	2.6×10^{17}	B	2.9×10^{17}

Recovery
Time
(Hours)

5	A	A	5.0×10^{17}	B
72	A	A	B	B

A - Greater than 1×10^{18} ohm-cm

B - Greater than 5×10^{17} ohms per square

Table 23. PSC Volume and Surface Resistivity;
Vacuum X-Ray Exposure Data.

Dose (Mrads)	Volume Resistivity (ohm-cm)		Surface Resistivity (ohms per square)	
	Sample 1	Sample 2	Sample 1	Sample 2
0	A	2.1×10^{18}	3.6×10^{17}	1.3×10^{17}
0.34	3.6×10^{17}	3.6×10^{17}	3.6×10^{16}	1.3×10^{17}
0.67	3.9×10^{17}	4.3×10^{17}	5.0×10^{16}	2.3×10^{17}
1.28	3.9×10^{17}	4.8×10^{17}	5.5×10^{16}	3.0×10^{17}
2.26	3.9×10^{17}	2.5×10^{16}	4.4×10^{16}	1.8×10^{17}
2.57	4.3×10^{17}	4.8×10^{17}	6.6×10^{16}	2.8×10^{17}
2.91	4.3×10^{18}	4.8×10^{17}	6.3×10^{16}	2.8×10^{17}
3.23	3.6×10^{17}	3.9×10^{17}	5.9×10^{16}	2.8×10^{17}
3.53	5.4×10^{17}	5.4×10^{17}	6.5×10^{16}	2.4×10^{17}
4.51	4.3×10^{17}	4.3×10^{17}	8.3×10^{16}	3.6×10^{17}
<u>Recovery</u> <u>Time - Days</u>				
1	6.1×10^{18}	7.2×10^{17}	9.9×10^{16}	3.0×10^{17}
2	4.3×10^{17}	7.2×10^{17}	6.3×10^{16}	1.9×10^{17}
3	1.4×10^{18}	1.4×10^{18}	1.1×10^{17}	3.6×10^{17}
4	4.3×10^{17}	1.7×10^{17}	3.6×10^{16}	8.3×10^{16}
14	6.1×10^{17}	6.2×10^{17}	4.4×10^{16}	1.3×10^{17}

A - Greater than 4.3×10^{18} ohm-cm

Table 24. Mylar 130-100-C and Mylar 130-100-T Dissipation Factor;
Vacuum X-Ray Exposure Data.

<u>Exposure Time (Hours)</u>	<u>Mylar 130-100-C</u>		<u>Mylar 130-100-T</u>		<u>Dose (Mrads)</u>
	<u>60-cps</u>	<u>1-kc</u>	<u>60-cps</u>	<u>1-kc</u>	
Initial	.0040	.0045	.0035	.0056	
Pump-Down	.0023	.0045	.0023	.0058	0
24	.0022	.0044	.0028	.0055	0.43
32	.0022	.0044	.0028	.0055	0.57
77	.0022	.0044	.0028	.0055	1.37
149	.0022	.0043	.0028	.0055	2.65
168	.0022	.0043	.0028	.0056	2.98
193	.0022	.0045	.0028	.0057	3.42
212	.0022	.0043	.0028	.0056	3.75
231	.0022	.0043	.0028	.0055	4.08
300	.0022	.0042	.0028	.0054	5.31
<u>Recovery Time (Days)</u>					
1	.0022	.0042	.0028	.0054	
2	.0022	.0044	.0028	.0058	
3	.0022	.0048	.0028	.0063	
4	.0028	.0049	.0029	.0064	
7	.0040	.0049	.0029	.0062	
8	.0040	.0048	.0029	.0060	
9	.0040	.0048	.0029	.0060	

Note: samples removed from vacuum chamber after 3 days

Table 25. Mylar 130-100-C and Mylar 130-100-T Dielectric Constant;
Vacuum X-Ray Exposure Data.

<u>Exposure Time (Hours)</u>	<u>Mylar 130-100-C</u>		<u>Mylar 130-100-T</u>		<u>Dose (Mrads)</u>
	<u>60-cps</u>	<u>1-kc</u>	<u>60-cps</u>	<u>1-kc</u>	
Initial	3.115	3.072	3.360	3.296	
Pump-Down	3.070	3.050	3.325	3.282	0
24	3.070	3.050	3.340	3.284	0.43
32	3.070	3.050	3.340	3.284	0.57
77	3.070	3.050	3.340	3.284	1.37
149	3.070	3.050	3.332	3.284	2.65
168	3.070	3.050	3.328	3.284	2.98
193	3.070	3.050	3.324	3.282	3.42
212	3.070	3.050	3.324	3.280	3.75
231	3.070	3.050	3.326	3.280	4.08
300	3.070	3.050	3.328	3.280	5.31
<u>Recovery</u>					
<u>Time (Days)</u>					
1	3.066	3.048	3.326	3.282	
2	3.066	3.046	3.324	3.280	
3	3.066	3.046	3.322	3.278	
4	3.125	3.100	3.392	3.356	
7	3.104	3.090	3.366	3.324	
8	3.104	3.090	3.360	3.316	
9	3.104	3.090	3.360	3.312	

Note: Samples removed from vacuum chamber after 3 days

Table 26. Mylar 130-100-C and Mylar 130-100-T
D-C Volume Resistivity (ohm-cm);
Vacuum X-ray Exposure Data.

<u>Dose</u> <u>(Mrads)</u>	<u>Mylar 130-100-C</u>		<u>Mylar 130-100-T</u>	
	<u>Sample 1</u>	<u>Sample 2</u>	<u>Sample 1</u>	<u>Sample 2</u>
0	3.9×10^{19}	5.4×10^{19}	2.7×10^{19}	3.6×10^{19}
0.43	6.4×10^{18}	5.5×10^{18}	4.3×10^{18}	3.6×10^{18}
0.57	6.7×10^{18}	6.4×10^{18}	3.6×10^{19}	5.1×10^{18}
1.37	6.1×10^{18}	5.3×10^{18}	3.4×10^{18}	3.6×10^{18}
2.65	5.8×10^{18}	5.1×10^{18}	3.4×10^{18}	3.4×10^{18}
3.42	6.4×10^{18}	5.5×10^{18}	3.4×10^{18}	2.9×10^{18}
3.75	5.3×10^{18}	5.1×10^{18}	3.0×10^{18}	3.0×10^{18}
4.08	1.7×10^{19}	1.7×10^{19}	3.0×10^{18}	3.0×10^{18}
5.31	5.8×10^{18}	5.3×10^{18}	3.3×10^{18}	3.6×10^{18}
<u>Recovery</u> <u>Time</u> <u>(Days)</u>				
1	1.3×10^{19}	9.8×10^{18}	1.5×10^{18}	6.4×10^{18}
2	1.8×10^{19}	1.1×10^{19}	1.3×10^{18}	9.8×10^{18}
3	1.8×10^{19}	1.7×10^{19}	1.1×10^{19}	1.3×10^{19}
4	3.9×10^{18}	3.9×10^{18}	3.0×10^{18}	3.2×10^{18}
7	7.1×10^{18}	5.3×10^{18}	4.4×10^{18}	4.6×10^{18}
8	1.5×10^{19}	7.3×10^{18}	4.8×10^{18}	4.7×10^{18}
9	2.0×10^{19}	9.5×10^{18}	5.3×10^{18}	5.1×10^{18}

Note: Samples removed from vacuum chamber after 3 days

Table 27. Mylar 130-100-C and Mylar 130-100-T
D-C Surface Resistivity (ohms per square);
Vacuum X-Ray Exposure Data.

Dose (Mrads)	Mylar 130-100-C		Mylar 130-100-T	
	Sample 1	Sample 2	Sample 1	Sample 2
0	B	2.6×10^{17}	9.1×10^{17}	B
0.43	B	1.9×10^{16}	9.1×10^{17}	B
0.57	B	2.1×10^{16}	B	B
1.37	9.0×10^{17}	1.8×10^{16}	B	B
2.65	4.5×10^{16}	1.5×10^{16}	1.2×10^{17}	B
3.42	3.0×10^{16}	1.5×10^{16}	1.0×10^{17}	B
3.75	8.6×10^{16}	1.3×10^{16}	2.6×10^{17}	B
4.08	1.2×10^{17}	1.0×10^{16}	4.0×10^{16}	7.0×10^{17}
5.31	9.0×10^{17}	2.0×10^{16}	3.9×10^{16}	B

Recovery
Time
(Days)

1	B	5.0×10^{16}	B	B
2	B	2.6×10^{17}	B	B
3	B	9.0×10^{17}	B	B
4	B	B	B	B
7	3.6×10^{16}	B	B	B
8	9.0×10^{17}	B	B	B
9	B	B	B	B

B - Greater than 1.8×10^{18} ohms per square

Note: Sample removed from vacuum chamber after 3 days

Table 28. GPG Loss Properties; Vacuum X-ray Exposure Data.

<u>Exposure Time (Hours)</u>	<u>$\tan\delta$ 60-cps</u>	<u>$\tan\delta$ 1-kc</u>	<u>D-C Volume Resistivity (ohm-cm)</u>	<u>D-C Surface Resistivity (ohms per square)</u>
0	.003	.006	A	B
2	.010	.011		
7	.011	.011		
24	.013	.011		
31	.014	.011		
68	.019	.010	3.0×10^{15}	1.3×10^{15}
72	.019	.010		
91	.019	.009	3.7×10^{15}	8.1×10^{15}
97	.019	.009		
116	.019	.009	3.7×10^{15}	7.4×10^{14}
120	.019	.009		
139	.018	.009	9.9×10^{15}	1.6×10^{15}
<u>Recovery Time (Hours)</u>				
24	.015	.009	3.1×10^{15}	2.4×10^{15}
120	.010	.007	1.7×10^{15}	6.8×10^{14}
168			1.9×10^{15}	1.1×10^{15}
960			1.6×10^{15}	9.8×10^{14}

A - Greater than 1×10^{18} ohm-cm

B - Greater than 5×10^{17} ohms per square

Note: Samples removed from vacuum chamber after 48 hours

Table 29. AL-243 D-C Volume and Surface Resistivity;
Vacuum X-Ray Exposure Data.

Dose (Mrads)	Volume Resistivity (ohm-cm)		Surface Resistivity (ohms per square)	
	Sample 1	Sample 2	Sample 1	Sample 2
0	A	A	B	B
0.28	A	A	B	B
0.69	3.6×10^{17}	A	1.9×10^{17}	B
3.19	A	A	B	B
4.03	4.6×10^{17}	5.9×10^{17}	9.6×10^{16}	1.9×10^{17}
6.65	A	A	1.9×10^{17}	1.9×10^{17}
7.35	A	A	1.9×10^{17}	1.9×10^{17}
9.85	A	A	1.9×10^{17}	1.9×10^{17}
10.7	1.0×10^{18}	6.9×10^{17}	1.9×10^{17}	1.9×10^{17}
13.2	A	A	1.9×10^{17}	1.9×10^{17}
Recovery Time (Hours)				
3	A	A	1.9×10^{17}	1.9×10^{17}
5	A	A	2.9×10^{17}	1.9×10^{17}
72	A	A	1.9×10^{17}	1.9×10^{17}

A - Greater than 1×10^{18} ohm-cm

B - Greater than 5×10^{17} ohms per square

Table 30. ALOX D-C Volume and Surface Resistivity;
Vacuum X-Ray Exposure Data.

Dose (Mrads)	Volume Resistivity (ohm-cm)		Surface Resistivity (ohms per square)	
	Sample 1	Sample 2	Sample 1	Sample 2
0	9.2×10^{16}	6.9×10^{17}	4.2×10^{16}	3.0×10^{16}
5.98	3.3×10^{16}	4.6×10^{17}	3.4×10^{15}	1.0×10^{16}
8.02	4.2×10^{16}	4.6×10^{17}	2.3×10^{15}	3.4×10^{16}
10.2	3.5×10^{15}	6.9×10^{17}	2.3×10^{15}	2.2×10^{16}
12.3	6.9×10^{16}	4.6×10^{17}	3.0×10^{15}	3.9×10^{16}
Recovery				
Time				
(Hours)				
24	1.7×10^{16}	2.0×10^{17}	3.9×10^{15}	2.9×10^{16}
120	2.6×10^{15}	6.6×10^{15}	3.9×10^{15}	9.0×10^{16}
168	3.2×10^{15}	1.2×10^{16}	1.2×10^{16}	1.4×10^{17}
960	1.8×10^{15}	1.1×10^{16}	4.5×10^{15}	1.5×10^{16}

Note: Samples removed from vacuum chamber after 24 hours

Table 31. Steatite AL-665 Dielectric Constant and Dissipation Factor;
Vacuum X-Ray Exposure Data.

Exposure Time (Hours)	60-cps		1-kc		Dose (Mrads)
	ϵ'	$\tan\delta$	ϵ'	$\tan\delta$	
Initial	5.99	.0002	5.98	.0011	
Pump-Down	6.00	.0002	5.98	.0009	0
4	6.00	.0002	5.98	.0009	0.37
21	6.00	.0002	5.98	.0009	1.96
41	6.01	.0002	5.98	.0008	3.83
61	6.01	.0003	5.98	.0007	5.69
81	6.01	.0003	5.98	.0006	7.56
150	6.00	.0004	5.98	.0006	14.0
172	6.00	.0004	5.99	.0007	16.0
193	6.00	.0004	5.99	.0008	18.0
212	6.00	.0004	5.99	.0009	19.8
234	6.00	.0004	5.99	.0009	21.8
303	6.00	.0004	5.98	.0009	28.3
Recovery					
Time (Days)					
1	6.00	<.0002	5.98	.0009	
2	6.00	<.0002	5.98	.0009	
3	6.00	<.0002	5.98	.0009	
4	5.99	<.0002	5.98	.0009	
7	5.99	.0006	5.98	.0009	
8	6.00	.0006	5.99	.0008	
9	6.00	.0006	5.99	.0008	
10	6.00	.0006	5.99	.0007	
11	6.00	.0006	5.99	.0007	
15	6.00	.0003	5.99	.0004	
16	6.00	.0003	5.99	.0003	
18	6.01	.0002	5.99	.0002	
21	6.01	<.0002	5.99	<.0002	
23	6.01	<.0002	5.99	<.0002	
25	6.01	<.0002	5.99	<.0002	

Note: Samples removed from vacuum chamber after 7 days

Table 32. Steatite AL-665 D-C Volume and Surface Resistivity;
Vacuum X-Ray Exposure Data.

Dose (Mrads)	Volume Resistivity (ohm-cm)		Surface Resistivity (ohms per square)	
	Sample 1	Sample 2	Sample 1	Sample 2
Initial	4.3×10^{17}	A	1.5×10^{18}	1.8×10^{18}
0	6.1×10^{17}	A	1.8×10^{18}	B
1.96	1.4×10^{17}	1.1×10^{17}	B	2.1×10^{17}
3.83	2.1×10^{17}	1.0×10^{17}	B	9.6×10^{16}
5.69	3.3×10^{17}	8.1×10^{16}	5.2×10^{17}	7.7×10^{16}
7.56	5.3×10^{17}	7.7×10^{16}	9.1×10^{17}	2.6×10^{17}
14.0	1.4×10^{18}	2.7×10^{17}	4.5×10^{17}	6.1×10^{16}
16.0	3.6×10^{17}	5.4×10^{16}	4.5×10^{17}	7.3×10^{16}
18.0	4.3×10^{17}	8.0×10^{16}	1.8×10^{18}	1.0×10^{17}
19.8	3.9×10^{17}	8.0×10^{16}	5.2×10^{17}	7.6×10^{16}
21.8	3.3×10^{17}	6.4×10^{16}	9.1×10^{17}	8.7×10^{16}
28.3	2.9×10^{17}	6.0×10^{16}	5.2×10^{17}	6.5×10^{16}
Recovery				
Time				
(Days)				
1	3.6×10^{17}	2.4×10^{17}	3.0×10^{17}	1.4×10^{17}
2	2.7×10^{17}	3.3×10^{17}	4.5×10^{17}	B
3	3.3×10^{17}	2.2×10^{18}	5.3×10^{17}	B
4	3.1×10^{17}	2.2×10^{18}	2.8×10^{17}	B
7	3.9×10^{17}	A	5.2×10^{17}	B
8	1.9×10^{17}	1.2×10^{17}	9.1×10^{16}	1.0×10^{16}
9	1.9×10^{17}	1.7×10^{17}	1.6×10^{17}	7.6×10^{16}
10	2.5×10^{17}	1.8×10^{17}	2.8×10^{17}	1.0×10^{17}
11	2.7×10^{17}	2.5×10^{17}	4.0×10^{17}	2.3×10^{17}
15	2.7×10^{17}	1.8×10^{17}	2.8×10^{17}	4.9×10^{16}
16	3.6×10^{17}	2.4×10^{17}	3.6×10^{17}	2.3×10^{17}
18	1.9×10^{17}	2.1×10^{17}	1.0×10^{17}	2.4×10^{17}
21	2.5×10^{17}	1.8×10^{17}	8.3×10^{16}	1.2×10^{15}
23	4.3×10^{17}	3.3×10^{17}	4.5×10^{17}	3.6×10^{17}
25	4.3×10^{17}	3.6×10^{17}	6.1×10^{17}	6.0×10^{16}

A - Greater than 4.3×10^{18} ohm-cm

B - Greater than 3.6×10^{18} ohms per square

Note: Samples removed from vacuum chamber after 7 days

Table 33. BeO Dissipation Factor; Vacuum X-Ray Exposure Data.

Exposure Time (Hours)	60-cps		1-kc		Dose (Mrads)
	Sample 1	Sample 2	Sample 1	Sample 2	
Initial	.0020	.098	.0010	.042	
Pump-Down	.0010	.0040	.0007	.0056	0
4	.0010	.0040	.0006	.0056	0.08
21	.0009	.0038	.0006	.0054	0.41
41	.0007	.0030	.0006	.0046	0.82
61	.0006	.0029	.0006	.0044	1.21
81	.0005	.0028	.0006	.0040	1.61
150	.0005	.0023	.0006	.0037	2.99
172	.0004	.0022	.0006	.0035	3.42
193	.0004	.0020	.0006	.0032	3.84
212	.0004	.0019	.0006	.0032	4.22
234	.0004	.0018	.0006	.0030	4.66
303	.0004	.0013	.0006	.0030	6.03
Recovery					
Time (Days)					
1	.0004	.0013	.0006	.0030	
2	.0004	.0013	.0006	.0030	
3	.0004	.0013	.0006	.0030	
4	.0004	.0012	.0006	.0030	
7	.0004	.0012	.0006	.0030	
8	.0003	.115	.0008	.060	
9	.0003	.142	.0008	.074	
10	.0002	.154	.0008	.073	
11	.0002	.169	.0008	.065	
15	.0002	.159	.0008	.069	
16	.0002	.161	.0008	.068	
18	.0002	.173	.0008	.077	
21	.0002	.199	.0007	.077	
23	.0002	.125	.0005	.060	
25	.0002	.109	.0005	.049	

Note: Samples removed from vacuum chamber after 7 days

Table 34. BeO Dielectric Constant; Vacuum X-Ray Exposure Data.

Exposure Time (Hours)	60-cps		1-kc		Dose (Mrads)
	Sample 1	Sample 2	Sample 1	Sample 2	
Initial	6.50	7.71	6.48	6.71	
Pump-Down	6.48	6.54	6.47	6.47	0
4	6.48	6.52	6.47	6.47	0.08
21	6.48	6.51	6.47	6.47	0.41
41	6.48	6.48	6.46	6.46	0.82
61	6.48	6.48	6.46	6.46	1.21
81	6.48	6.48	6.46	6.46	1.61
150	6.48	6.48	6.46	6.46	2.99
172	6.48	6.48	6.46	6.46	3.42
193	6.48	6.48	6.46	6.46	3.84
212	6.47	6.47	6.45	6.45	4.22
234	6.47	6.47	6.45	6.45	4.66
303	6.47	6.47	6.45	6.45	6.03
Recovery					
Time (Days)					
1	6.47	6.47	6.45	6.45	
2	6.47	6.47	6.45	6.45	
3	6.47	6.47	6.45	6.45	
4	6.47	6.47	6.45	6.45	
7	6.47	6.47	6.45	6.45	
8	6.48	7.91	6.47	6.49	
9	6.48	7.95	6.47	7.00	
10	6.48	7.82	6.47	7.00	
11	6.48	7.03	6.47	6.92	
15	6.48	7.43	6.47	7.00	
16	6.48	7.36	6.47	6.97	
18	6.48	7.53	6.47	7.07	
21	6.48	7.36	6.47	7.08	
23	6.48	7.87	6.47	6.88	
25	6.48	7.77	6.48	6.78	

Note: Samples removed from vacuum chamber after 7 days

Table 35. BeO D-C Volume and Surface Resistivity;
Vacuum X-Ray Exposure Data.

Dose (Mrads)	Volume Resistivity (ohm-cm)		Surface Resistivity (ohms per square)	
	Sample 1	Sample 2	Sample 1	Sample 2
Initial	1.2×10^{17}	1.1×10^{15}	1.8×10^{18}	4.5×10^{16}
0	1.9×10^{17}	3.4×10^{16}	1.8×10^{18}	B
0.41	4.7×10^{17}	1.0×10^{16}	1.7×10^{17}	B
0.82	4.8×10^{16}	1.2×10^{16}	1.8×10^{17}	9.1×10^{17}
1.21	5.4×10^{16}	1.0×10^{16}	3.3×10^{17}	2.6×10^{17}
1.61	5.4×10^{16}	1.3×10^{16}	3.6×10^{17}	1.0×10^{17}
2.99	5.0×10^{16}	1.5×10^{16}	4.0×10^{17}	2.6×10^{17}
3.42	4.7×10^{16}	1.4×10^{16}	3.3×10^{17}	1.2×10^{17}
3.84	4.9×10^{16}	1.5×10^{16}	1.2×10^{18}	2.3×10^{17}
4.22	4.4×10^{16}	1.5×10^{16}	2.8×10^{17}	1.2×10^{18}
4.66	4.3×10^{16}	1.3×10^{16}	3.6×10^{17}	9.1×10^{17}
6.03	4.4×10^{16}	1.5×10^{16}	2.3×10^{17}	9.1×10^{17}
Recovery				
Time (Days)				
1	4.3×10^{16}	1.6×10^{16}	3.6×10^{17}	5.2×10^{17}
2	5.1×10^{16}	1.6×10^{16}	5.2×10^{17}	1.8×10^{18}
3	5.2×10^{16}	1.5×10^{16}	1.2×10^{18}	B
4	5.6×10^{16}	1.5×10^{16}	B	B
7	6.1×10^{16}	2.0×10^{16}	B	B
8	3.9×10^{16}	8.8×10^{12}	9.8×10^{15}	1.1×10^{15}
9	3.3×10^{16}	7.6×10^{12}	1.4×10^{16}	1.4×10^{15}
10	3.5×10^{16}	8.2×10^{12}	6.3×10^{16}	6.3×10^{15}
11	4.2×10^{16}	2.1×10^{13}	1.1×10^{17}	5.2×10^{17}
15	3.5×10^{16}	5.9×10^{12}	2.4×10^{15}	2.0×10^{15}
16	4.2×10^{16}	1.4×10^{13}	1.2×10^{17}	3.6×10^{16}
18	3.5×10^{16}	3.1×10^{12}	1.0×10^{17}	9.1×10^{14}
21	3.5×10^{16}	2.4×10^{12}	1.0×10^{17}	3.8×10^{16}
23	5.1×10^{16}	4.4×10^{13}	2.4×10^{17}	4.2×10^{16}
25	5.2×10^{16}	1.6×10^{14}	3.3×10^{17}	5.3×10^{17}

B - Greater than 3.6×10^{18} ohms per square

Note: Samples removed from vacuum chamber after 7 days

Table 36. ECF D-C Volume and Surface Resistivity;
Vacuum X-Ray Exposure Data.

<u>Exposure Time (Hours)</u>	<u>Volume Resistivity (ohm-cm)</u>		<u>Surface Resistivity (ohms per square)</u>	
	<u>Sample 1</u>	<u>Sample 2</u>	<u>Sample 1</u>	<u>Sample 2</u>
0	1.2×10^{16}	4.5×10^{16}	3.2×10^{15}	5.7×10^{16}
3	4.6×10^{16}	1.7×10^{17}	3.8×10^{15}	5.7×10^{16}
22	A	3.7×10^{16}	7.0×10^{15}	3.4×10^{16}
29	2.8×10^{17}	9.2×10^{16}	8.2×10^{15}	2.5×10^{16}
46	1.4×10^{17}	5.8×10^{16}	1.3×10^{16}	2.8×10^{16}
51	1.2×10^{17}	9.8×10^{16}	1.7×10^{16}	2.6×10^{16}
70	2.3×10^{17}	3.9×10^{16}	3.1×10^{16}	1.9×10^{16}
75	1.2×10^{17}	4.2×10^{16}	2.6×10^{16}	9.7×10^{15}
94	A	6.9×10^{16}	3.6×10^{16}	6.8×10^{15}
Recovery				
<u>Time (Hours)</u>				
5	3.5×10^{17}	3.5×10^{17}	2.9×10^{17}	1.2×10^{17}
72	A	6.0×10^{16}	5.0×10^{17}	1.7×10^{16}

A - Greater than 1×10^{18} ohm-cm

Table 37. GPG 60-cps Dielectric Constant and Dissipation Factor;
Ultraviolet Exposure In High Vacuum.

<u>Exposure Time (Hours)</u>	<u>Metallic Electrode</u>		<u>Transparent H. V. Electrode</u>	
	<u>K</u>	<u>Tanδ</u>	<u>K</u>	<u>Tanδ</u>
0	4.67	.027	4.67	.027
0.25	4.77	.028	4.70	.027
0.50	4.80	.029	4.71	.028
0.75	4.80	.029	4.72	.027
1.0	4.81	.030	4.72	.027
1.5	4.83	.030	4.75	.029
2.0	4.82	.036	4.76	.028
3.0	4.81	.037	4.77	.030
4.0	4.80	.030	4.79	.027
6.0	4.77	.030	4.76	.029
<u>Recovery Time (Hours)</u>				
0.3	4.64	.023	4.74	.025
0.75	4.64	.020	4.71	.025
1.0	4.64	.019	4.71	.025
1.5	4.64	.019	4.69	.025

Note: At T=0, specimen had reached equilibrium temperature. Temperature change during remainder of experiment was less than 0.5°C.

X. Illustrations

<u>Figure</u>	<u>Description</u>	<u>Page</u>
1	Vacuum system, loss measurement cell and ultraviolet source.	111
2	Block diagram of vacuum pumping system.	112
3	Variation of pressure with geometric altitude.	113
4	Interior of loss measurement cell with specimens in place.	114
5	Interior of high-voltage cell with flashover specimens in place.	115
6	High-voltage feed-through bushing.	116
7	B-H6 ultraviolet lamp enclosure.	117
8	Comparison of B-H6 output intensity to solar radiation.	118
9	Vacuum system, loss measurement cell and x-ray tube.	119
10	Calorimeter for measurement of x-ray intensity.	120
11	Vacuum sparkover electrode holder with coated-lens electrodes.	121
12	D-c uniform-field sparkover voltages in high-vacuum (10^{-6} Torr range) for 5 mil gap.	122
13	Effect of electrode roughness on high-vacuum uniform-field sparkover. Evaporated silver electrodes, 5 mil gap.	123
14	Flashover specimen and mask for depositing evaporated metal electrodes.	124
15	Vacuum flashover voltages for 17 mil gap on glass slides with evaporated silver electrodes.	125

X. Illustrations (continued)

<u>Figure</u>	<u>Description</u>	<u>Page</u>
16	Effect of specimen surface texture on high-vacuum flashover voltage.	126
17	Printed wiring board flashover specimen.	127
18	Geometrical construction of printed wiring board flashover electrode.	128
19	Thin film electric strength specimen with polystyrene fillet.	129
20	Summary of 60 cps breakdown tests on 1 mil Mylar using composite specimen of Figure 19.	130
21	Summary of 60 cps breakdown tests on 0.5 mil Mylar 130-100A using composite specimen of Figure 19.	131
22	Electric strength specimen with recessed electrode in machined cavity.	132
23	Effect of x-ray irradiation in vacuum on the 60 cps electric strength of PE.	133
24	Effect of x-ray irradiation in vacuum on the 60 cps electric strength of TFE-6.	134
25	Effect of x-ray irradiation in vacuum on the 60 cps electric strength of TFE-7.	135
26	Effect of x-ray irradiation in vacuum on the 60 cps electric strength of FEP-100.	136
27	Effect of x-ray irradiation in vacuum on the dissipation factor of TFE-6 and TFE-7.	137
28	Effect of x-ray irradiation in vacuum on the dielectric constant of TFE-6 and TFE-7.	138
29	Effect of x-ray irradiation in air on the dissipation factor of TFE-6 and TFE-7.	139

X. Illustrations (continued)

<u>Figure</u>	<u>Description</u>	<u>Page</u>
30	Effect of x-ray irradiation in air on the dielectric constant of TFE-6 and TFE-7.	140
31	Effect of x-ray irradiation on TFE-6. <u>Curve A</u> - irradiated in air; <u>Curve B</u> - irradiated in vacuum; <u>Curve C</u> - irradiated in vacuum after previous dose of 8.5 megarads, followed by 10 months recovery in air.	141
32	Recovery characteristics of TFE-6 specimens after x-ray irradiation as shown in Figure 31.	142
33	Loss-specimen holder with transparent high-voltage electrode.	143
34	Printed wiring board insulation resistance specimen.	144

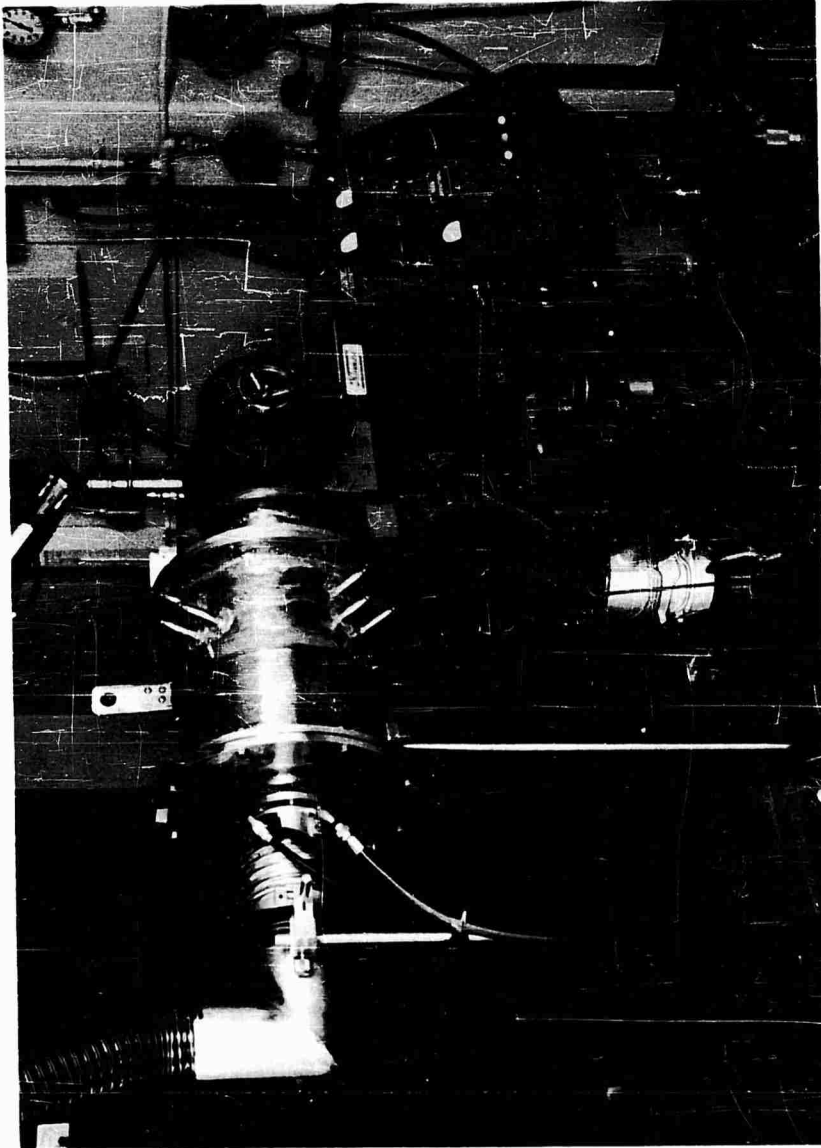


Figure 1. Vacuum system, loss measurement cell and ultraviolet source.

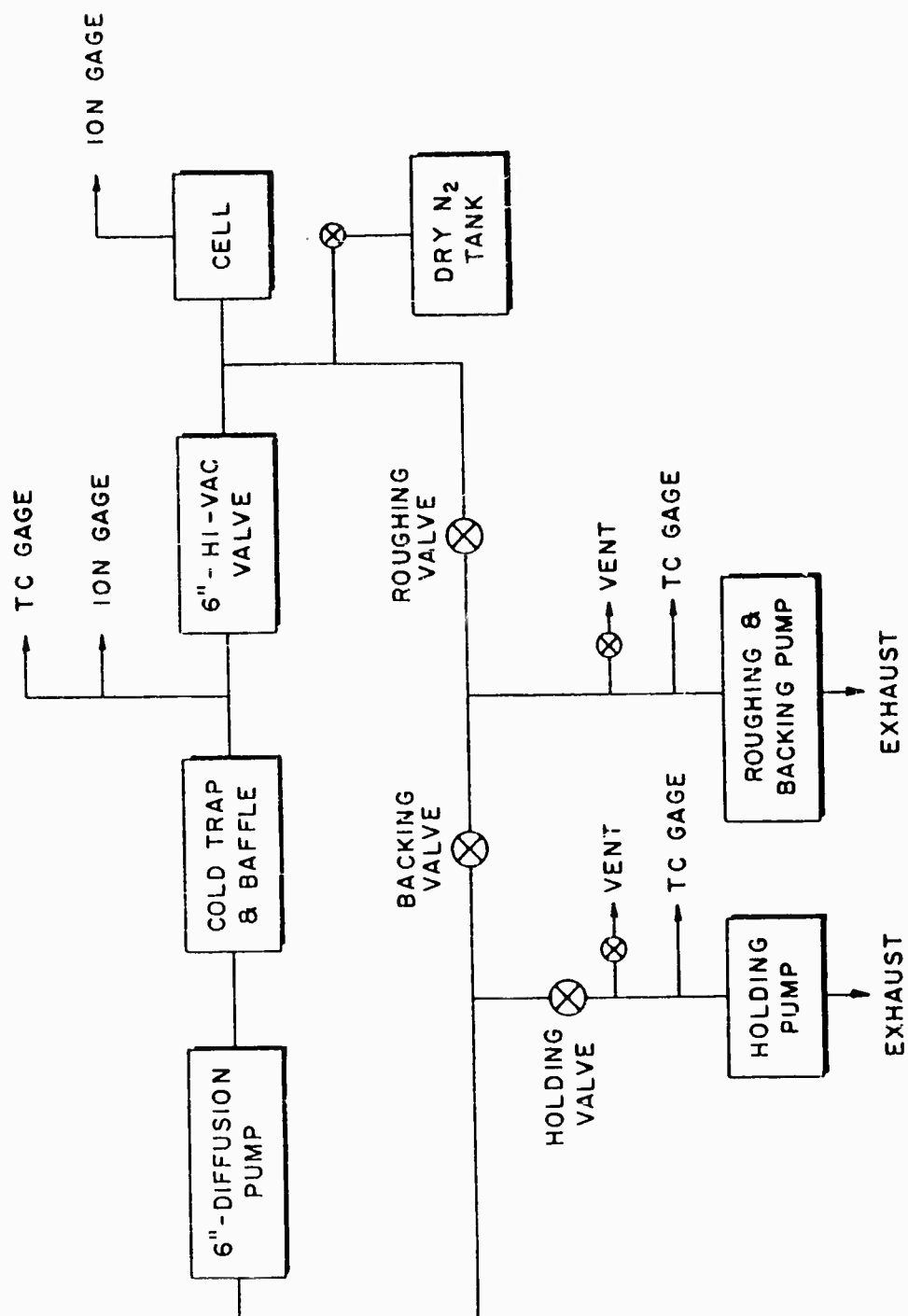


Figure 2. Block diagram of vacuum pumping system.

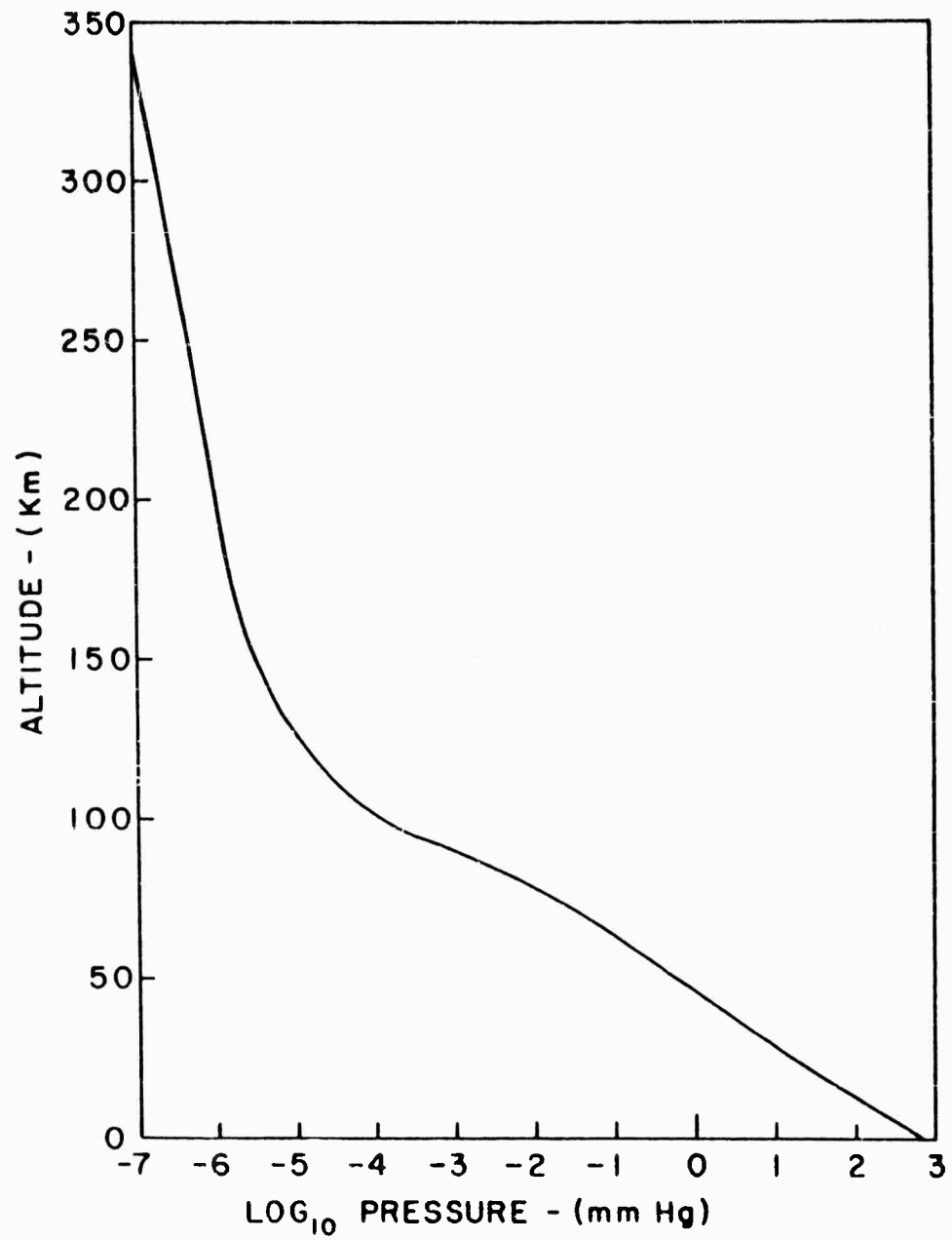


Figure 3. Variation of pressure with geometric altitude.



Figure 4. Interior of loss measurement cell with specimens in place.

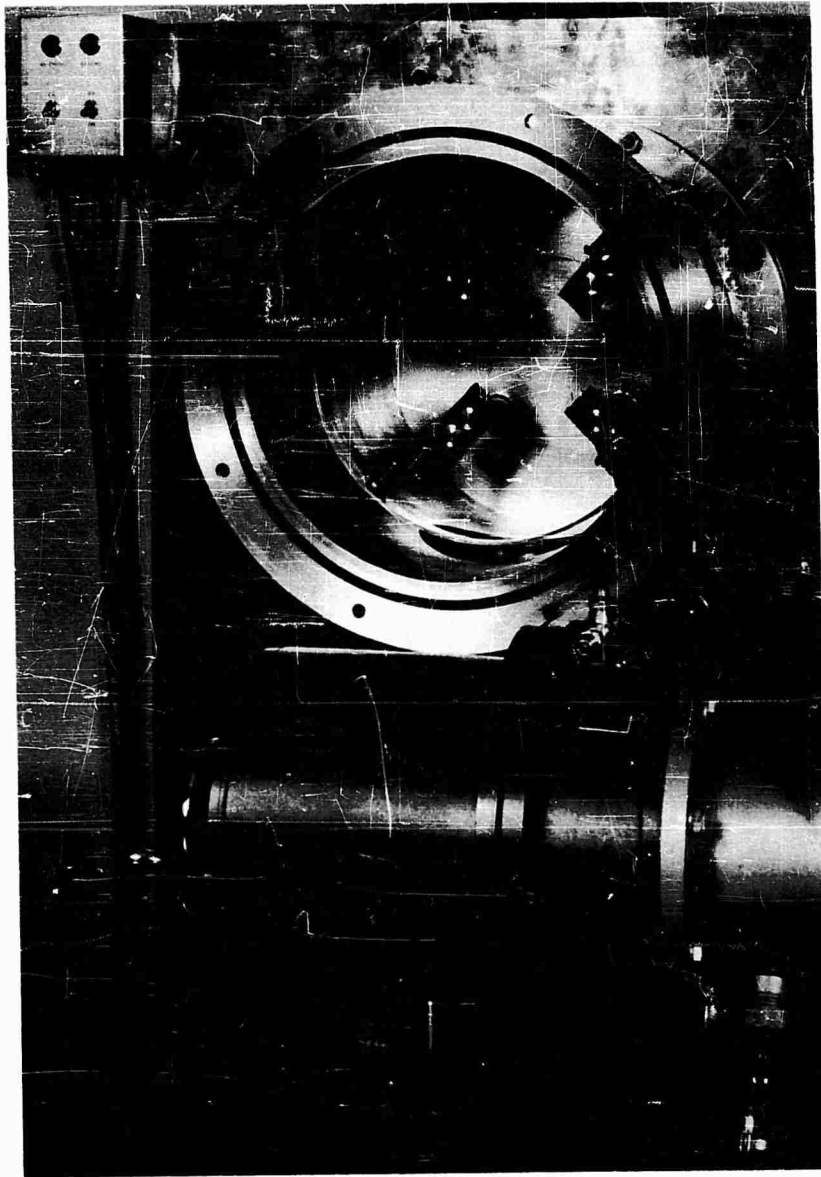


Figure 5. Interior of high-voltage cell with flashover specimens in place.

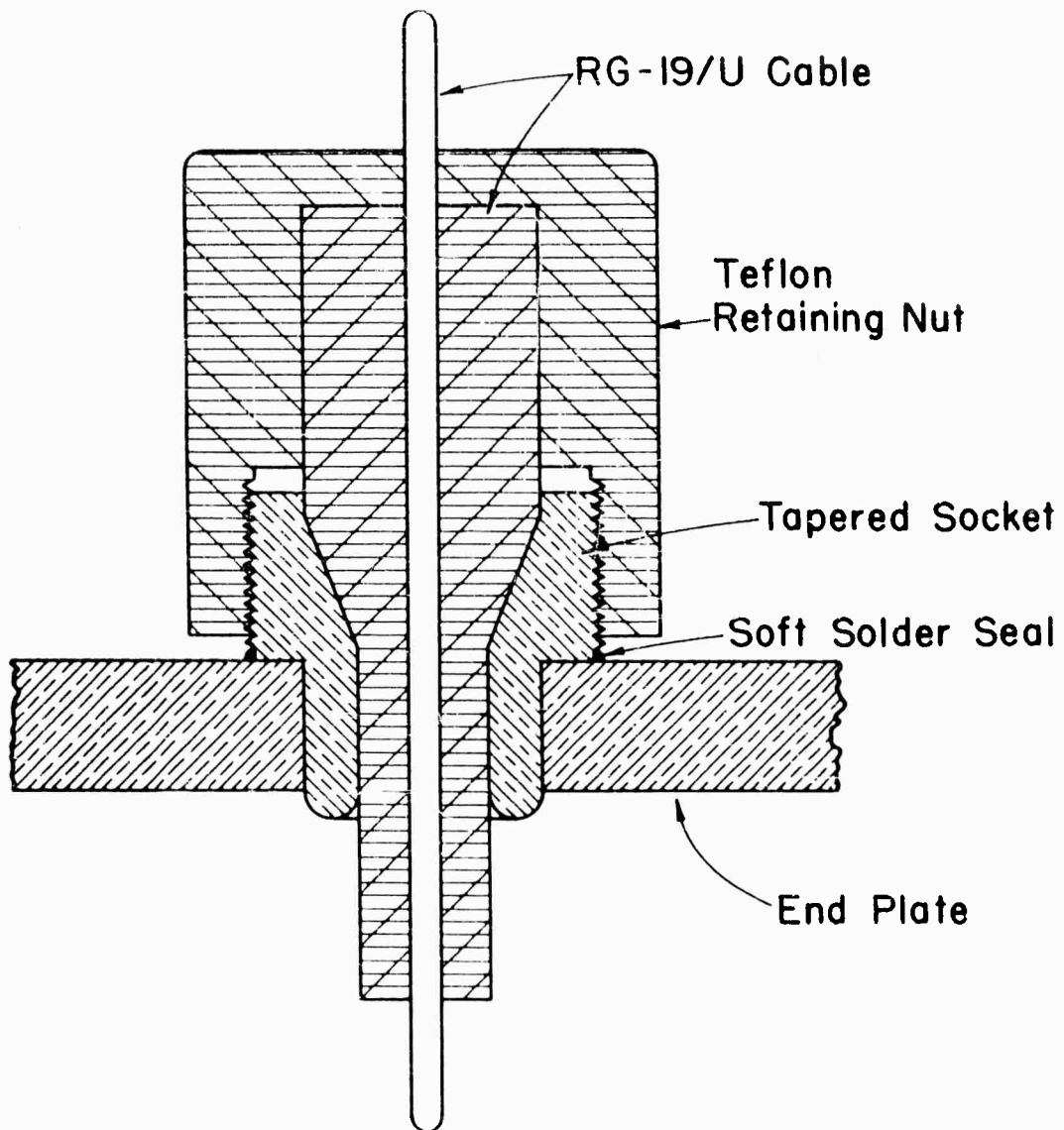


Figure 6. Modified high-voltage bushing.

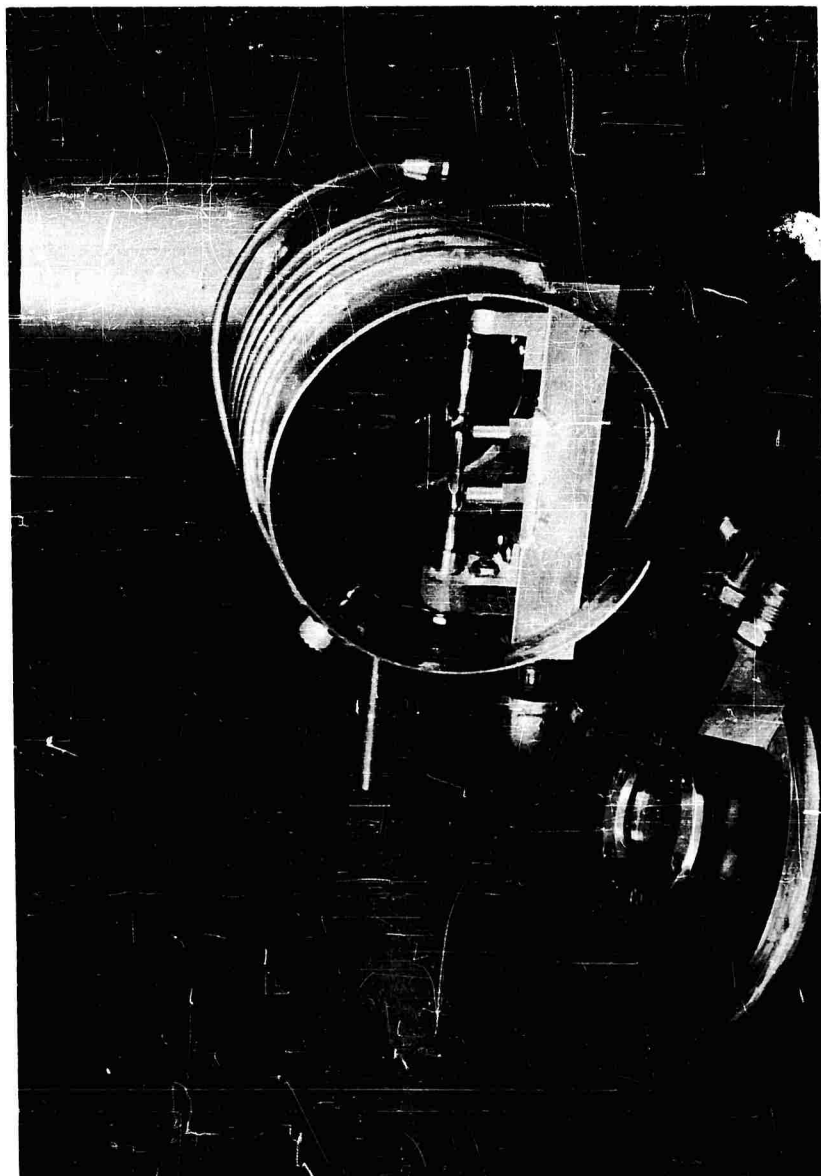


Figure 7. B-H6 ultraviolet lamp enclosure.

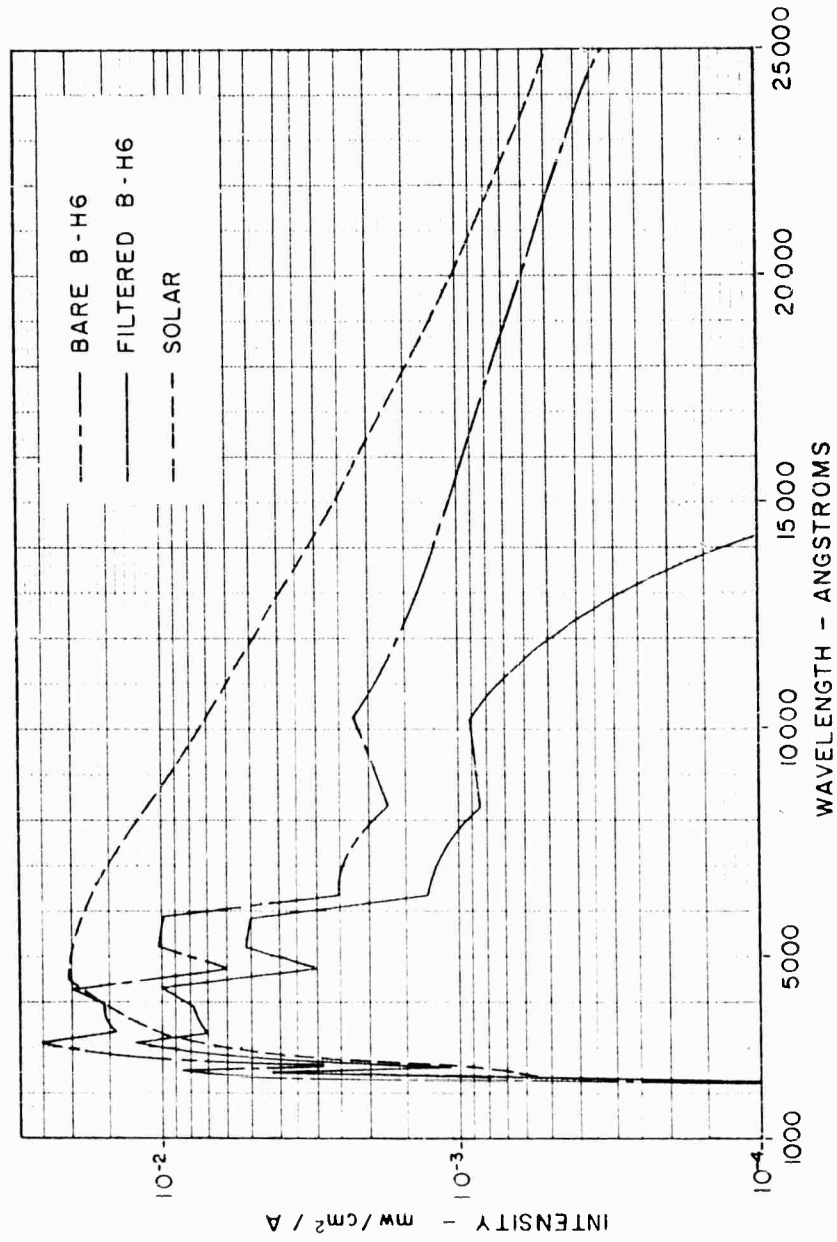


Figure 8. Comparison of B-H6 output intensity to solar radiation.

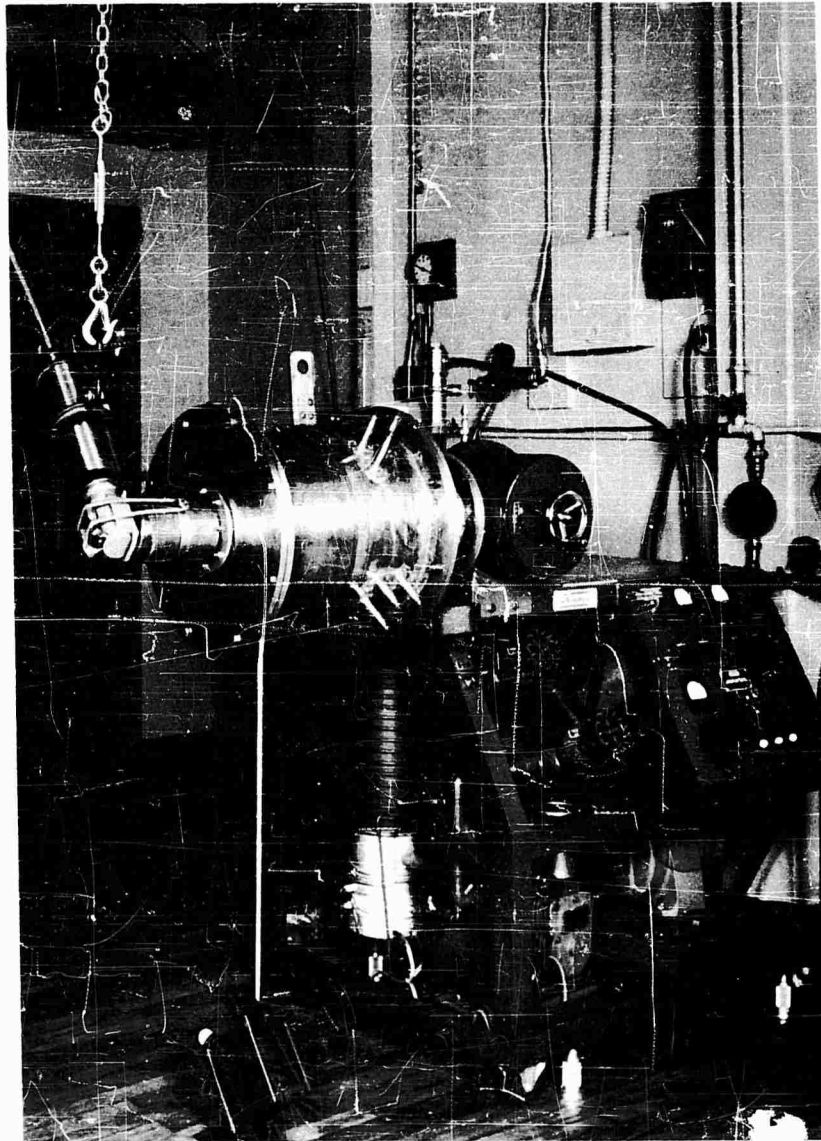


Figure 9. Vacuum system, loss measurement cell and x-ray tube.

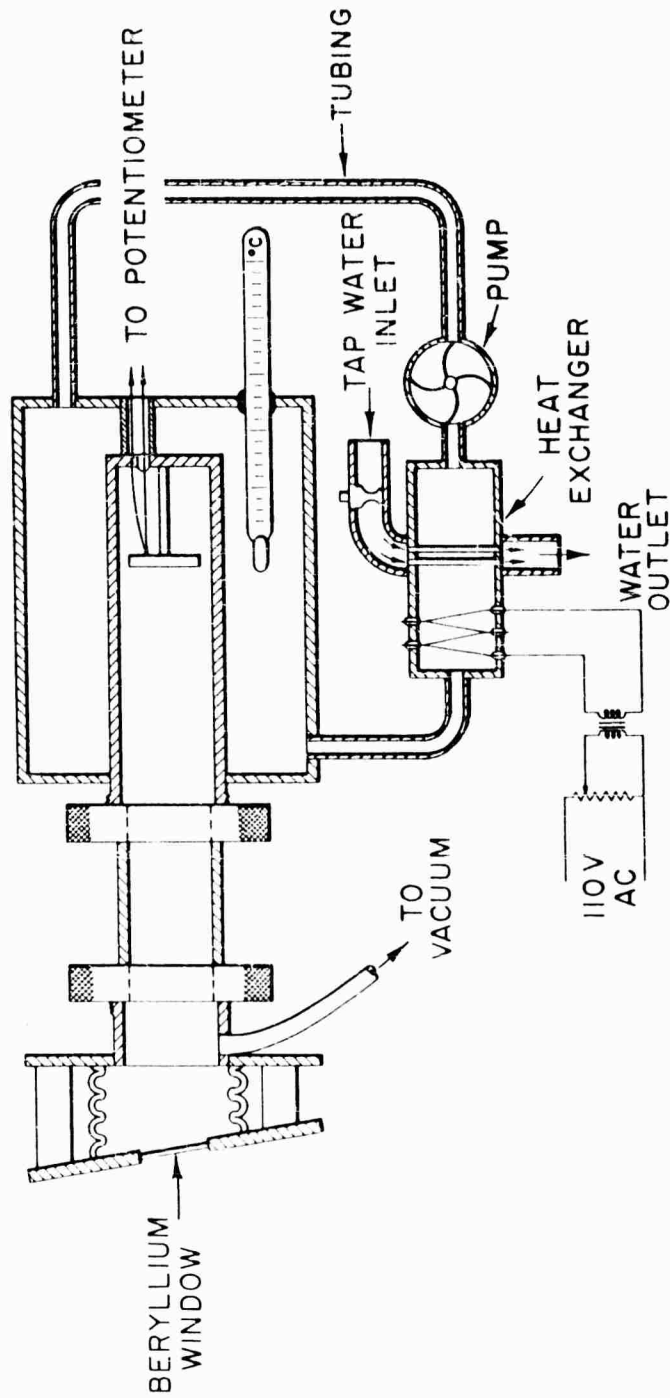


Figure 10. Calorimeter for measurement of x-ray intensity.

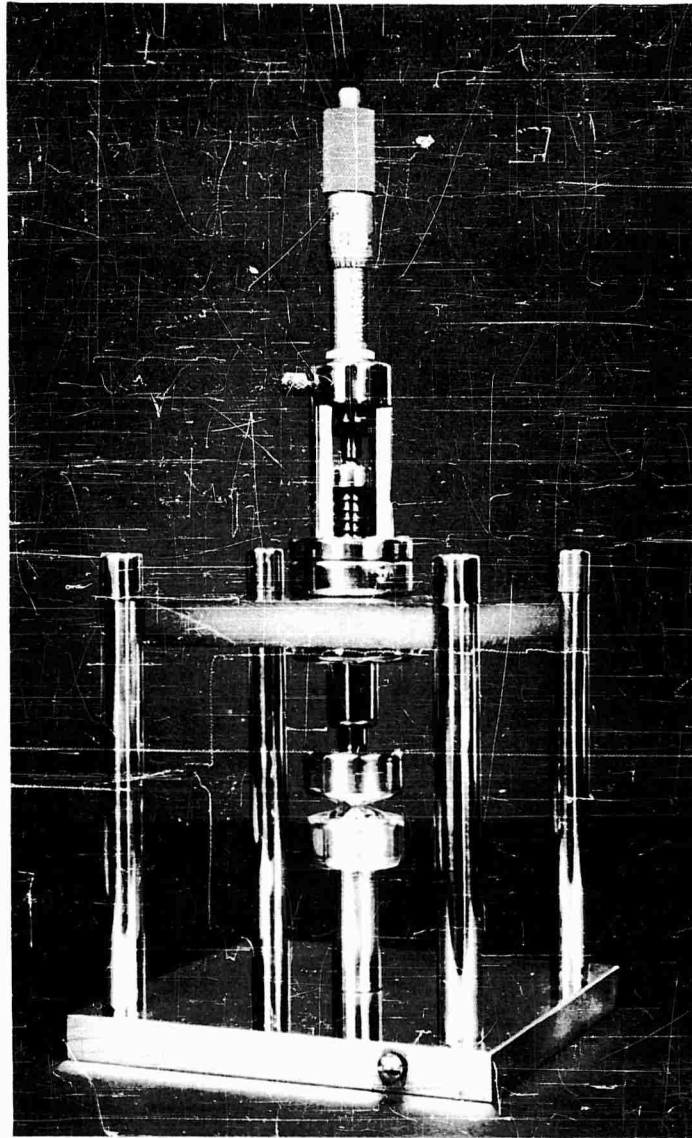


Figure 11. Vacuum sparkover electrode holder with coated-lens electrodes.

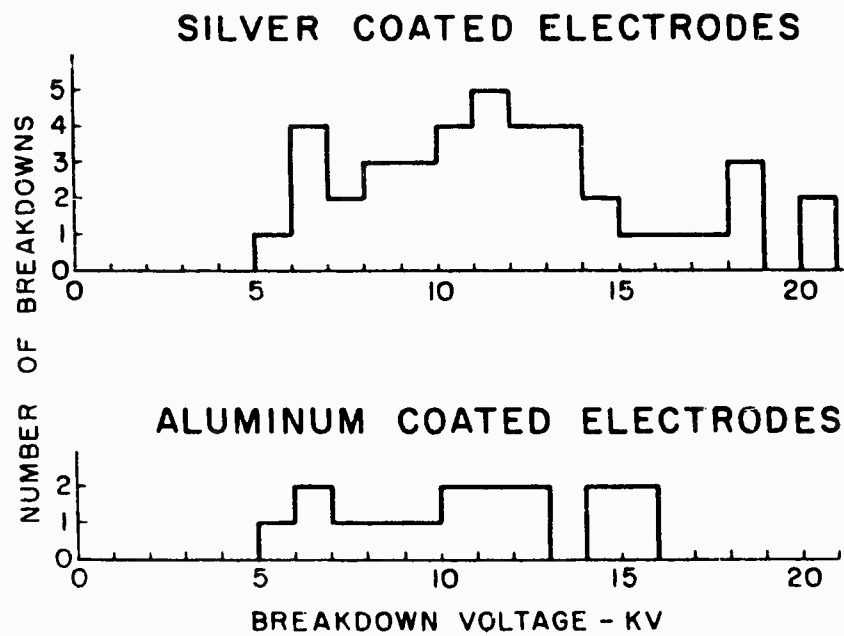


Figure 12 D-c uniform field breakdown voltages for 5-mil gap in 10^{-6} Torr range.

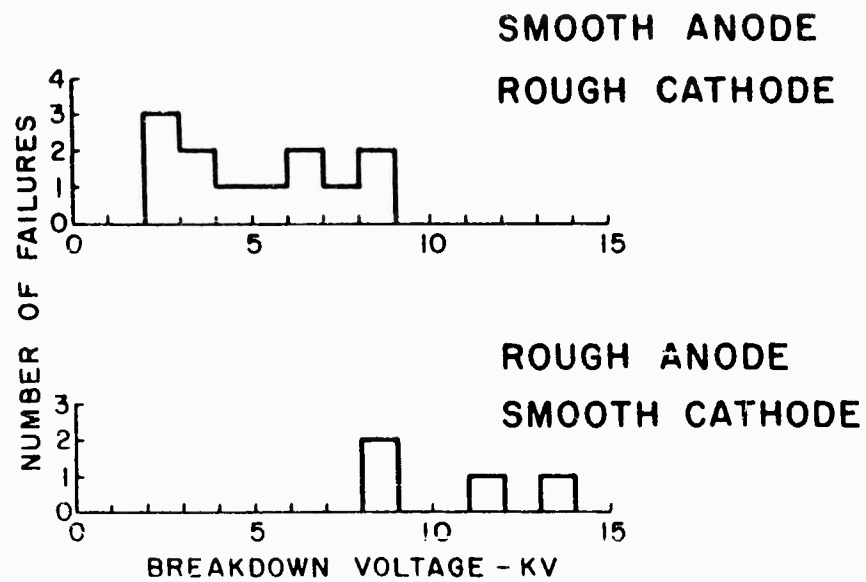


Figure 13. Effect of electrode roughness on high vacuum breakdown. Evaporated silver electrodes, 5-mil gap.



Figure 14. Flashover specimen and mask for depositing evaporated metal electrodes.

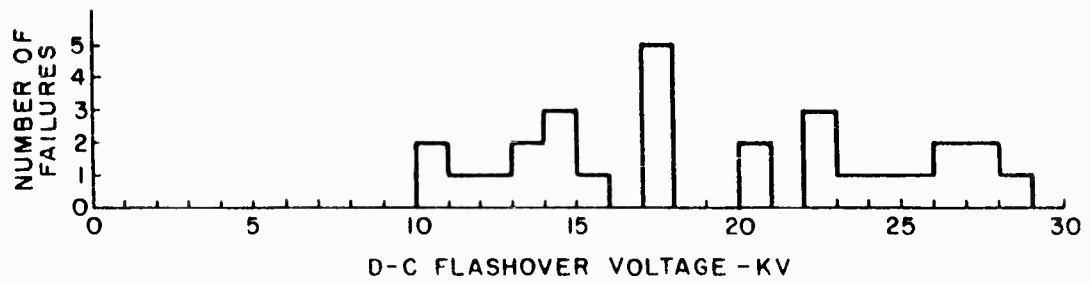


Figure 15. Vacuum flashover voltages for 17-mil gap on glass slides with evaporated silver electrodes.

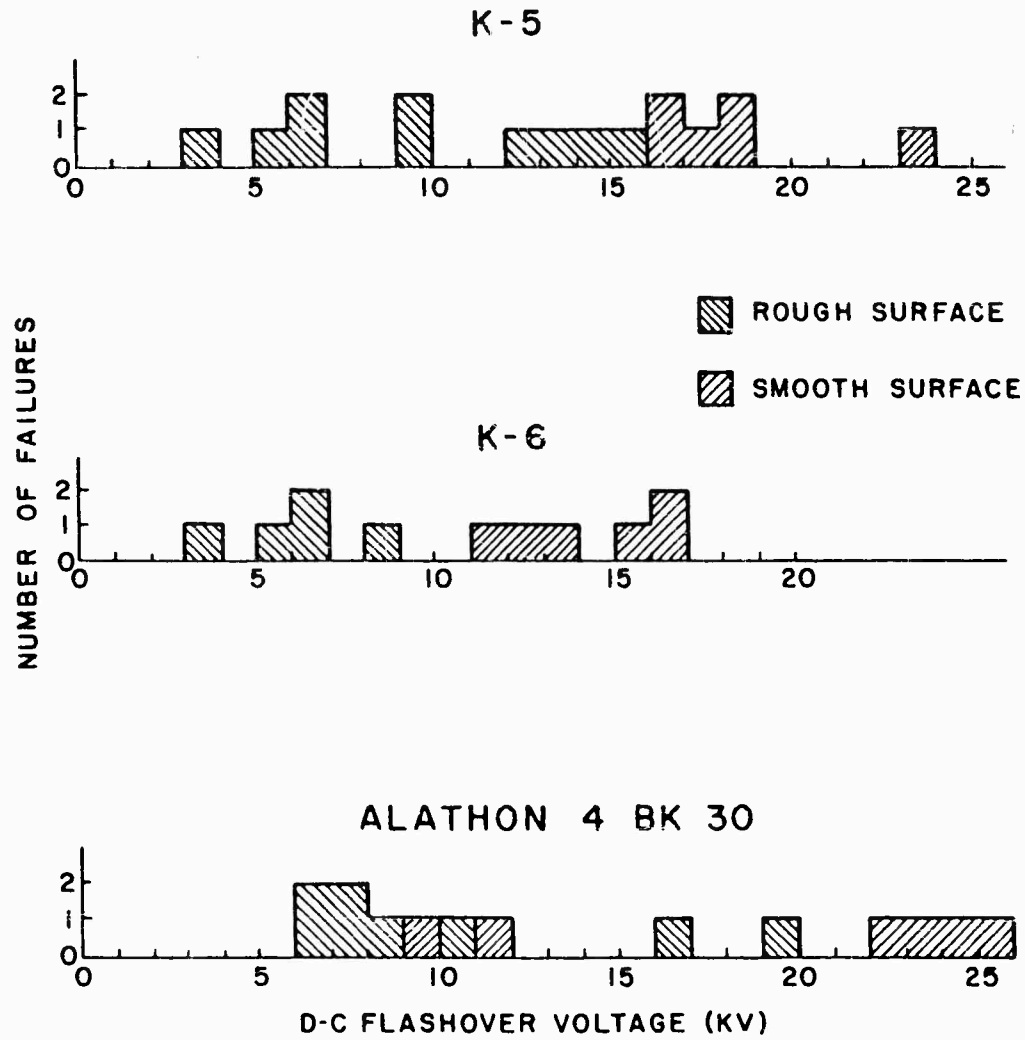


Figure 16. Effect of specimen surface texture on high-vacuum flashover voltage.

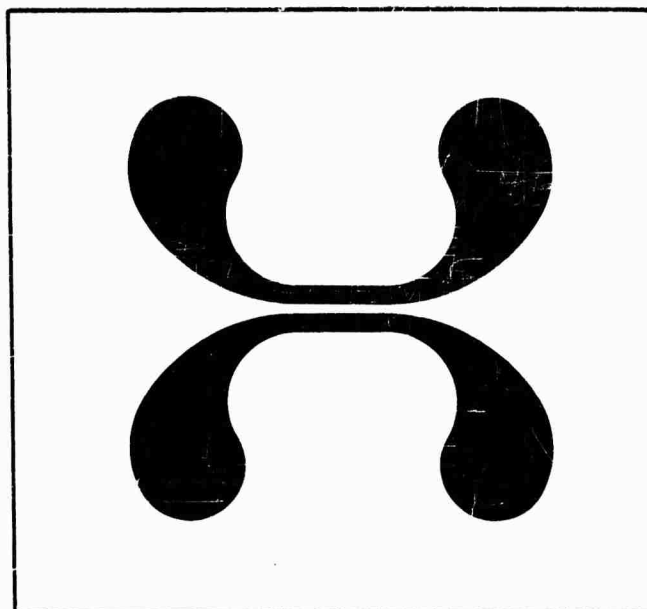


Figure 17. Printed wiring board flashover specimen.

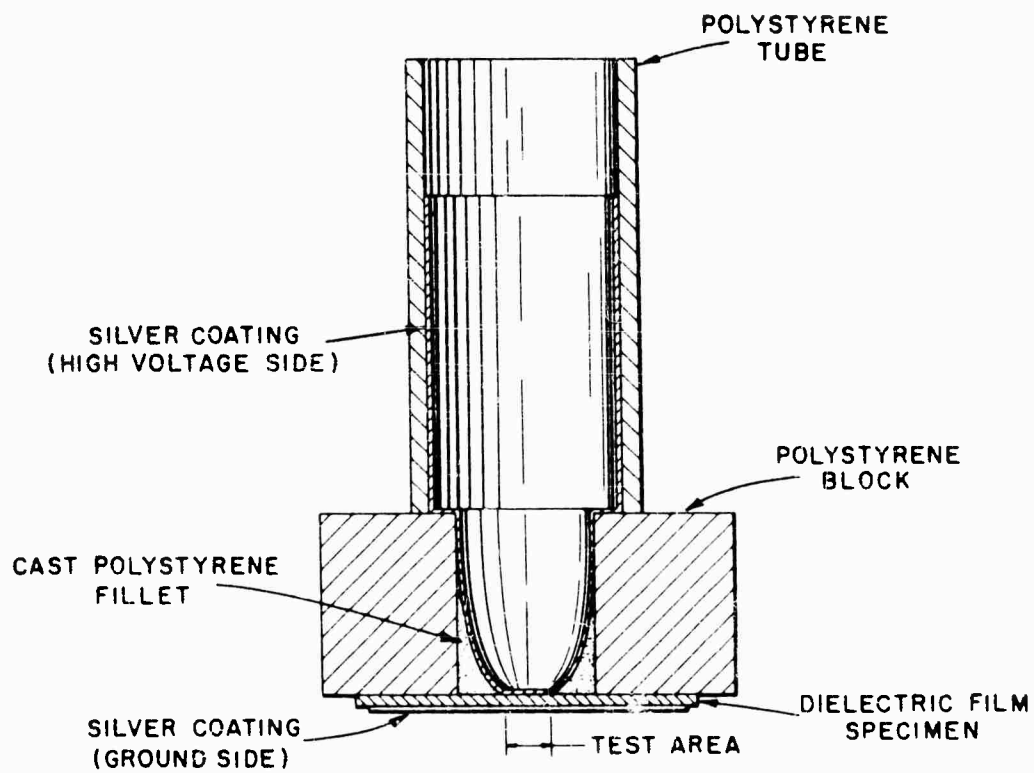


Figure 19. Thin film electric strength specimen with polystyrene fillet.

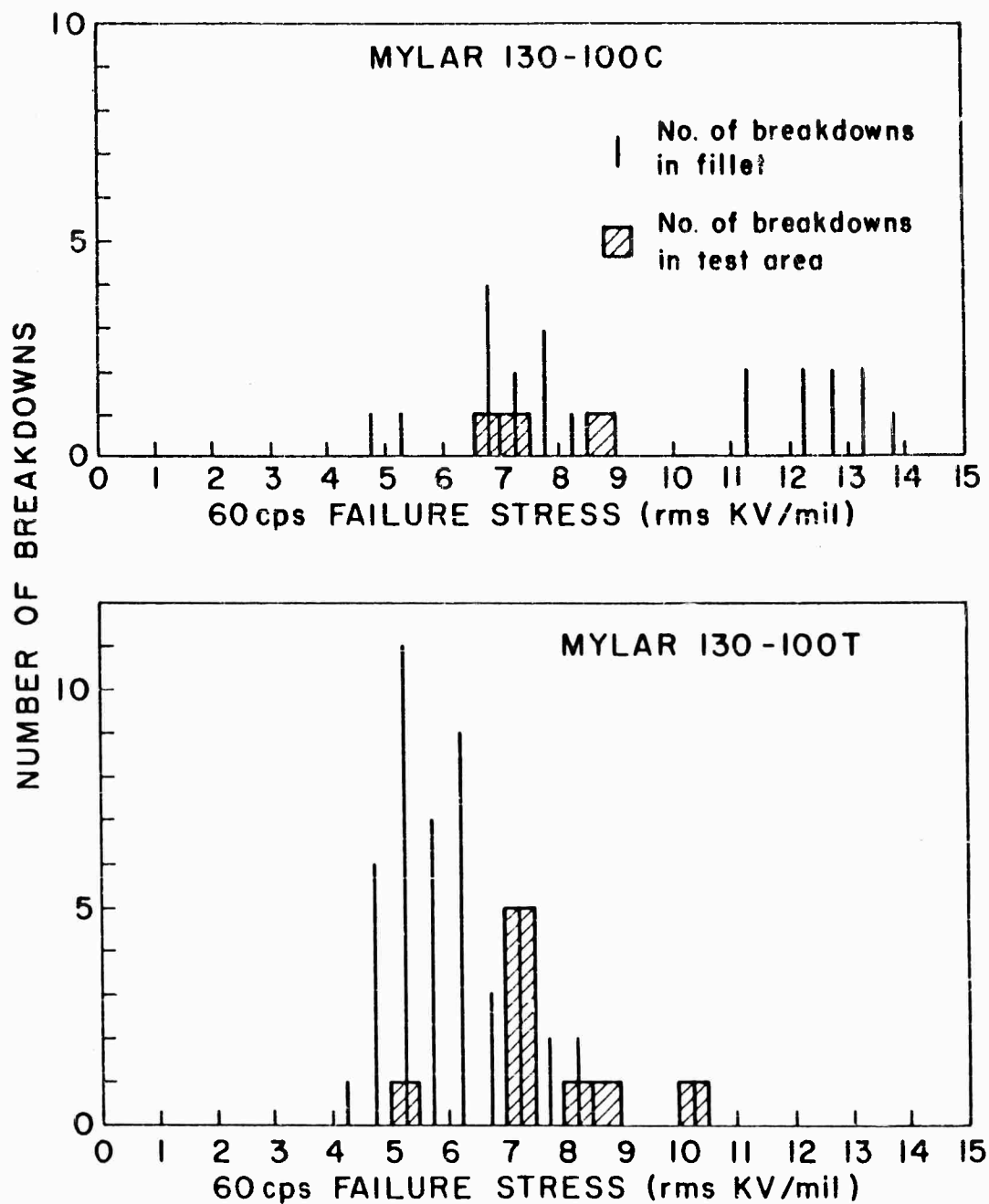


Figure 20. Summary of 60 cps breakdown tests on 1 mil Mylar using composite specimen of Figure 19.

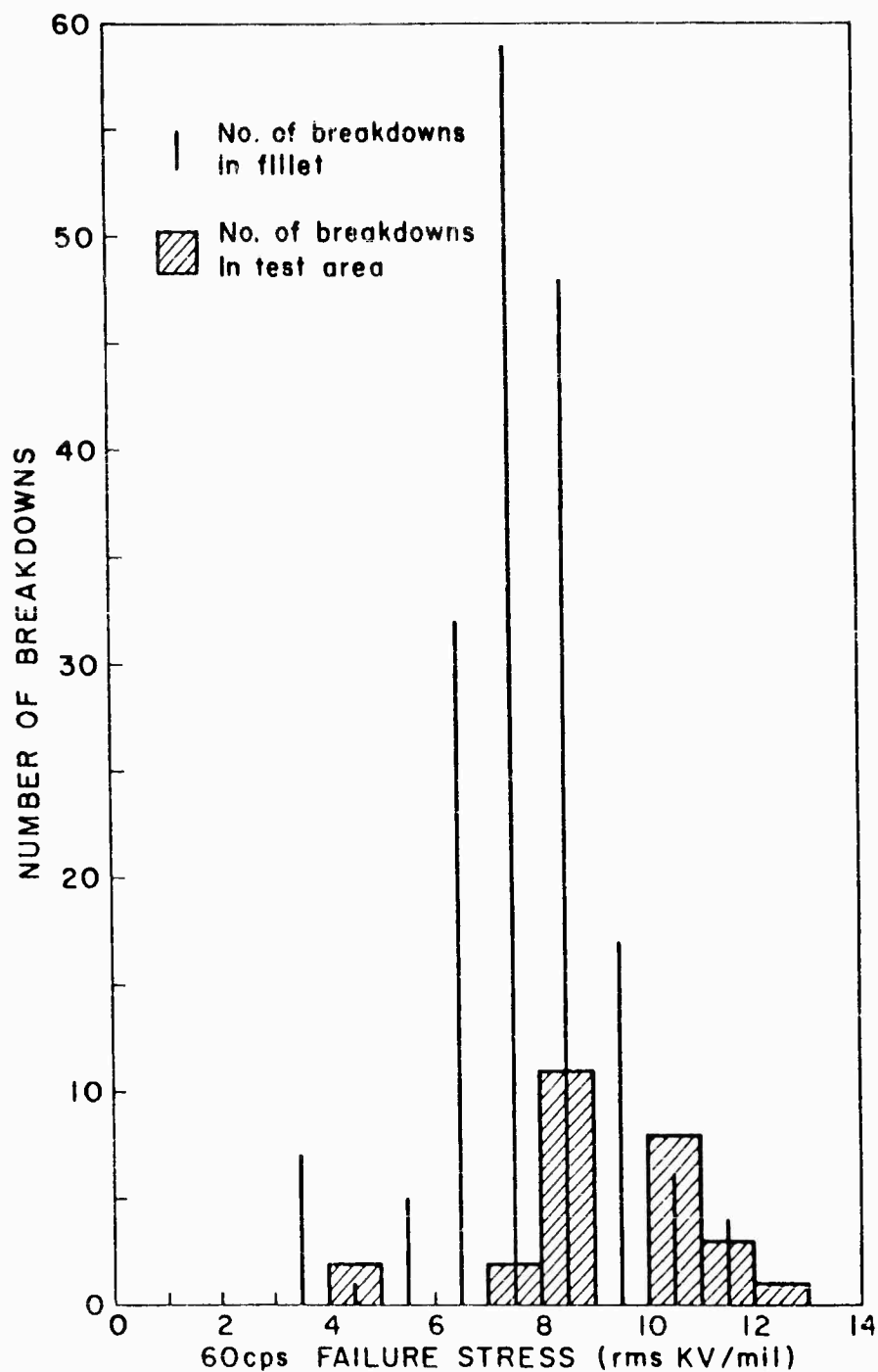


Figure 21. Summary of 60 cps breakdown tests on 0.5 mil Mylar 130-100A using composite specimen of Figure 19.

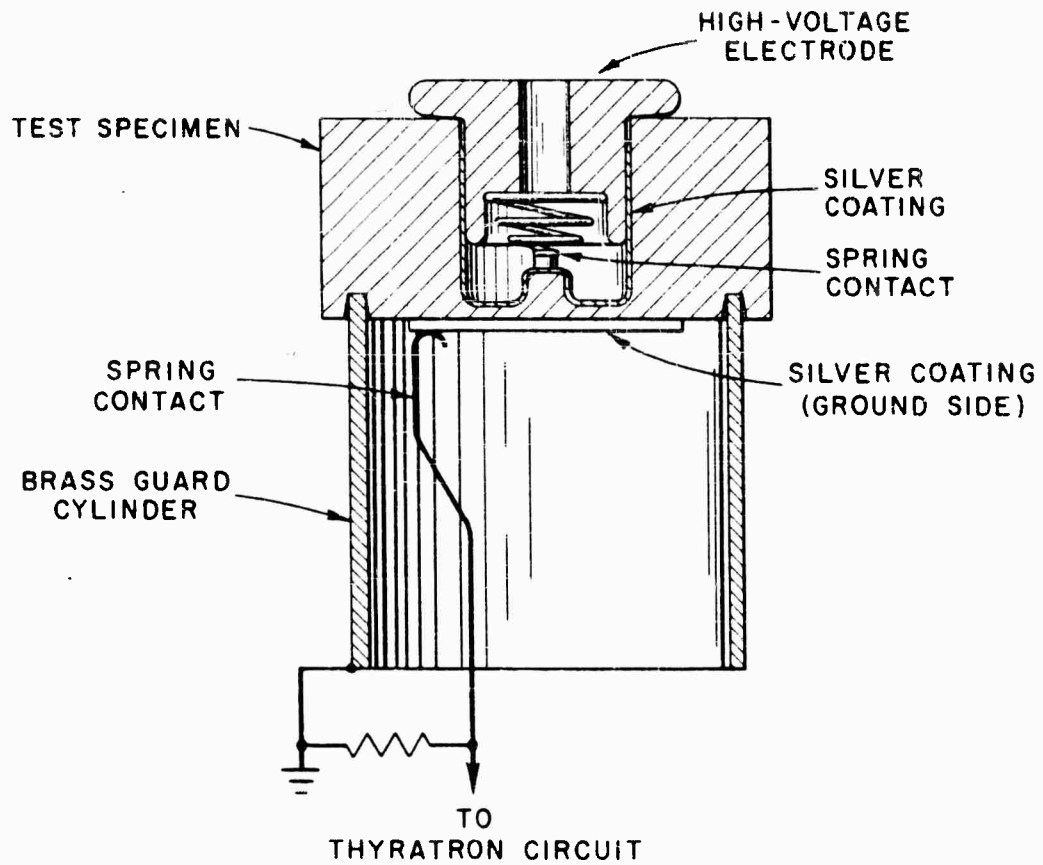


Figure 22. Electric strength specimen with recessed electrode in machined cavity.

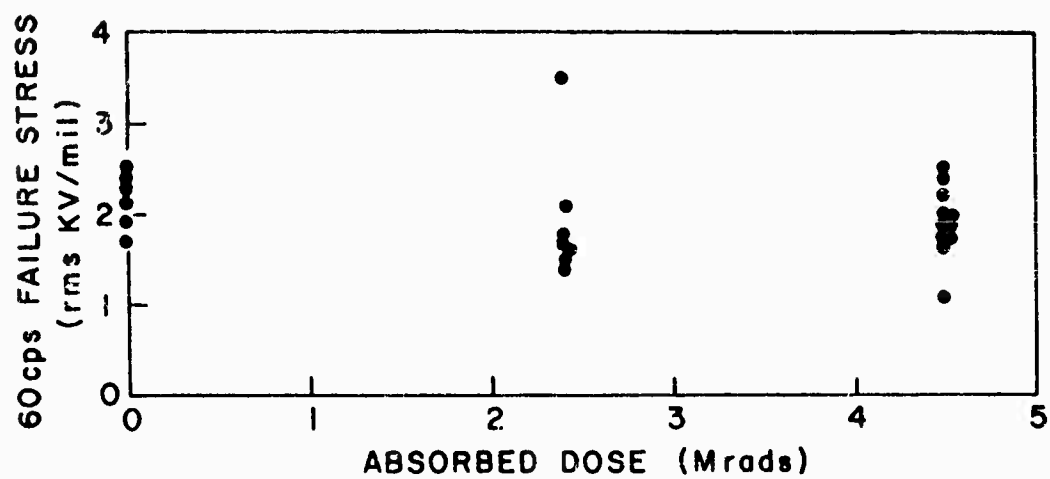


Figure 23. Effect of x-ray irradiation in vacuum on the 60 cps electric strength of PE.

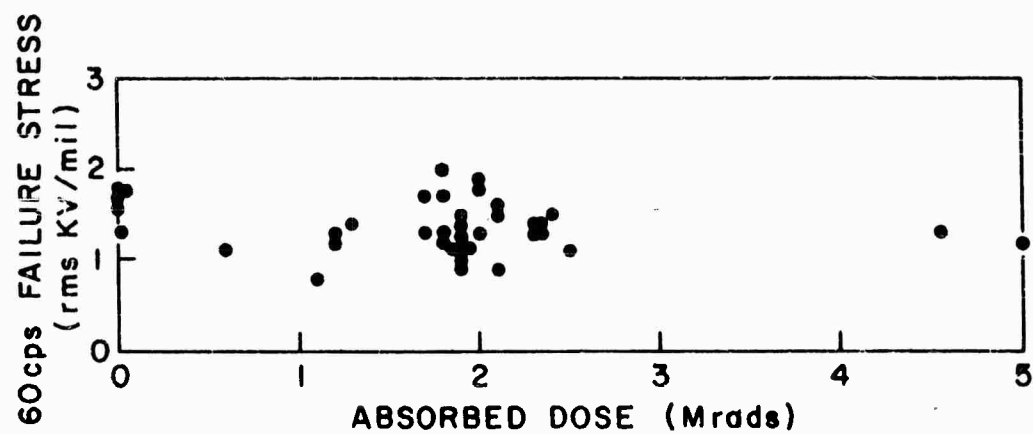


Figure 24. Effect of x-ray irradiation in vacuum on the 60 cps electric strength of TFE-6.

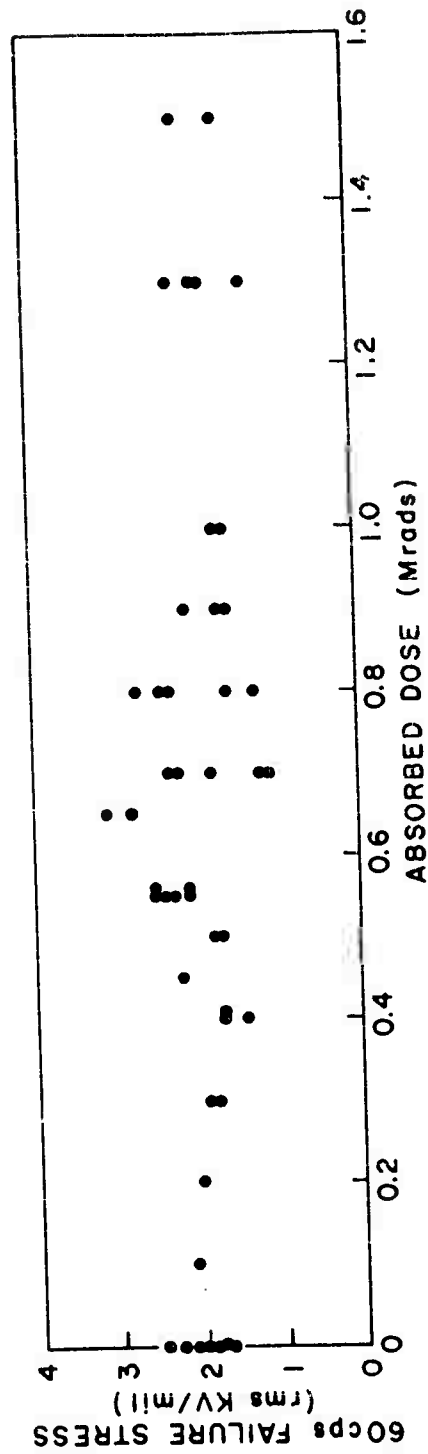


Figure 25. Effect of x-ray irradiation in vacuum on the 60 cps electric strength of TFE-7.



Figure 26. Effect of x-ray irradiation in vacuum on the 60 cps electric strength of FEP-100.

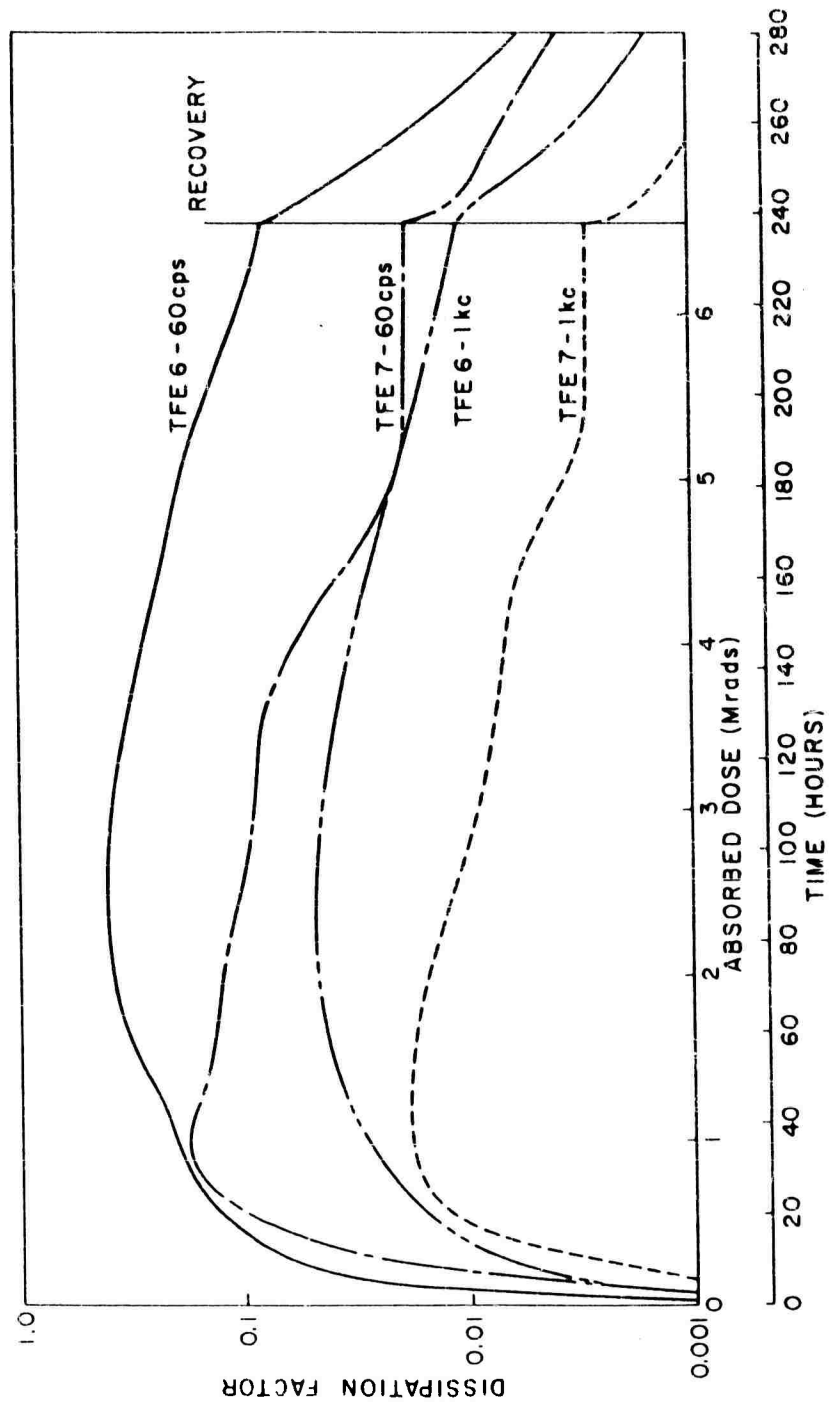


Figure 27. Effect of x-ray irradiation in vacuum on the dissipation factor of TFE-6 and TFE-7.

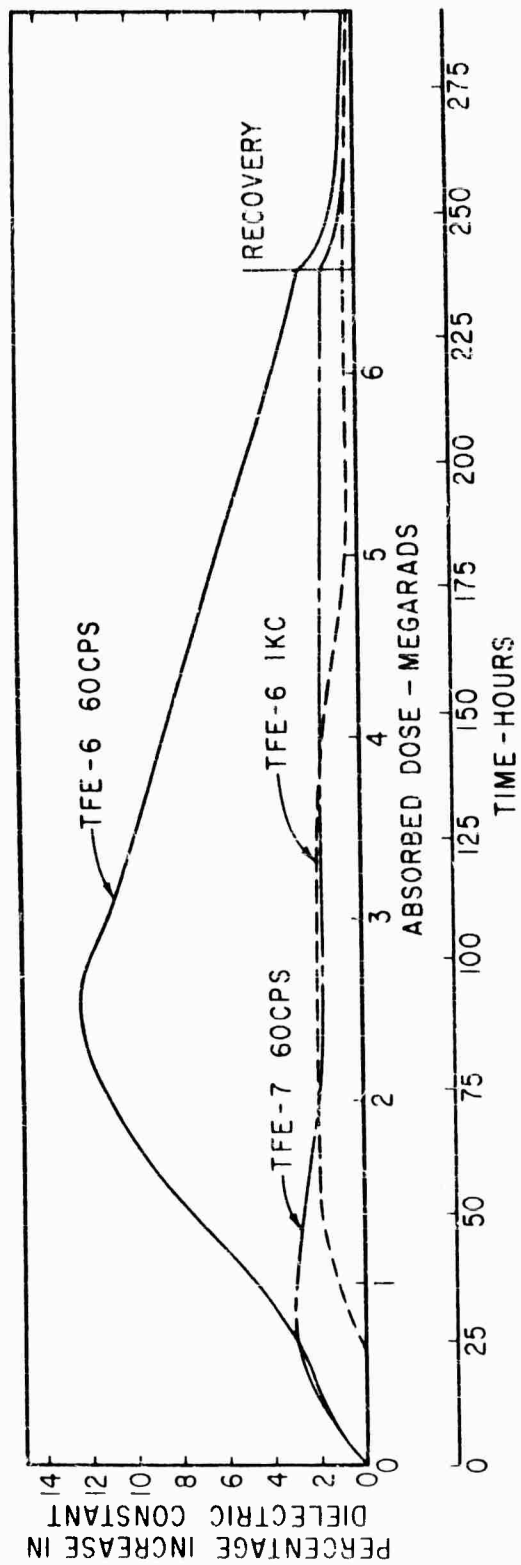


Figure 28. Effect of x-ray irradiation in vacuum on the dielectric constant of TFE-6 and TFE-7.

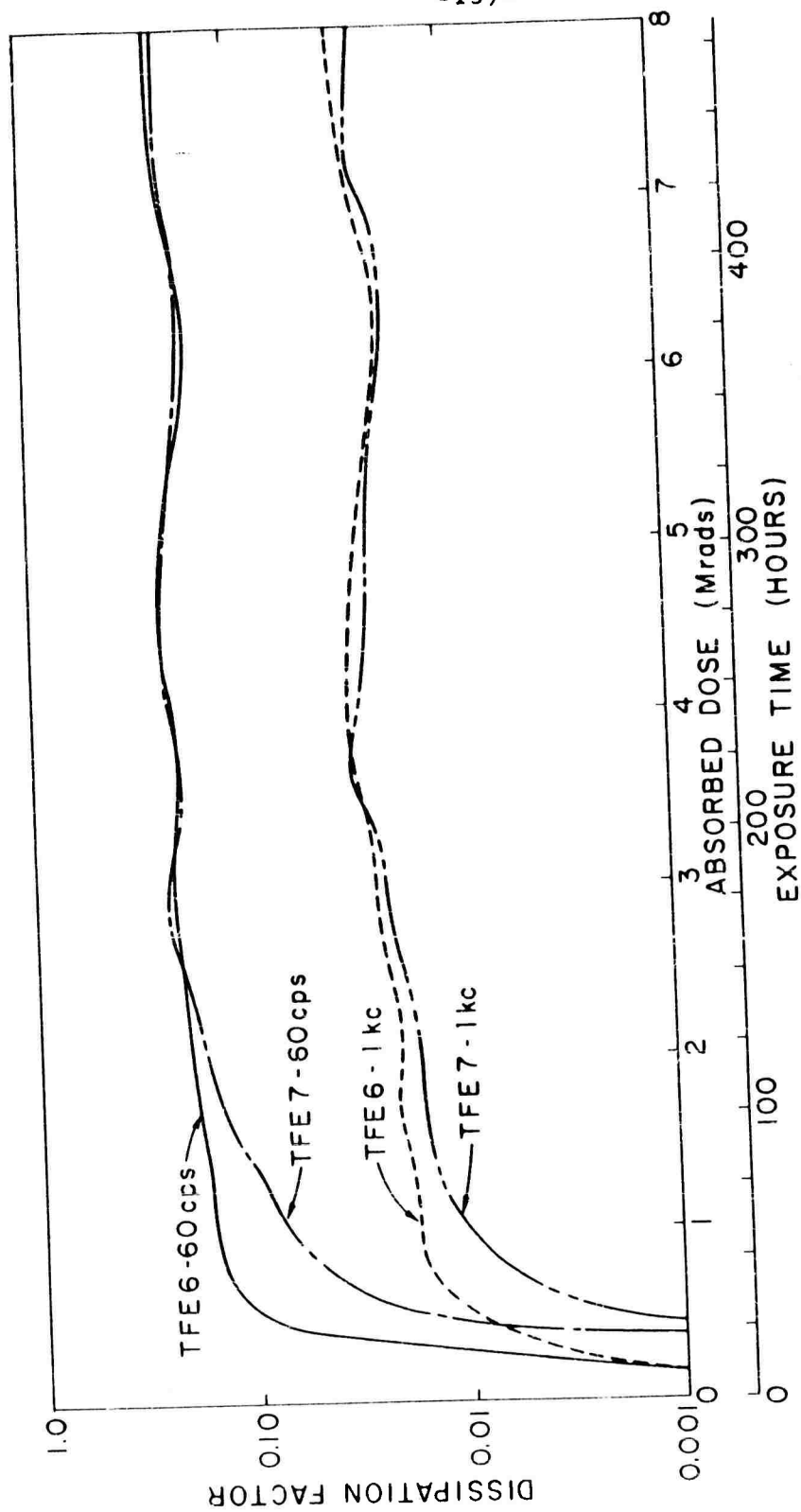


Figure 29. Effect of x-ray irradiation in air on the dissipation factor of TFE-6 and TFE-7.

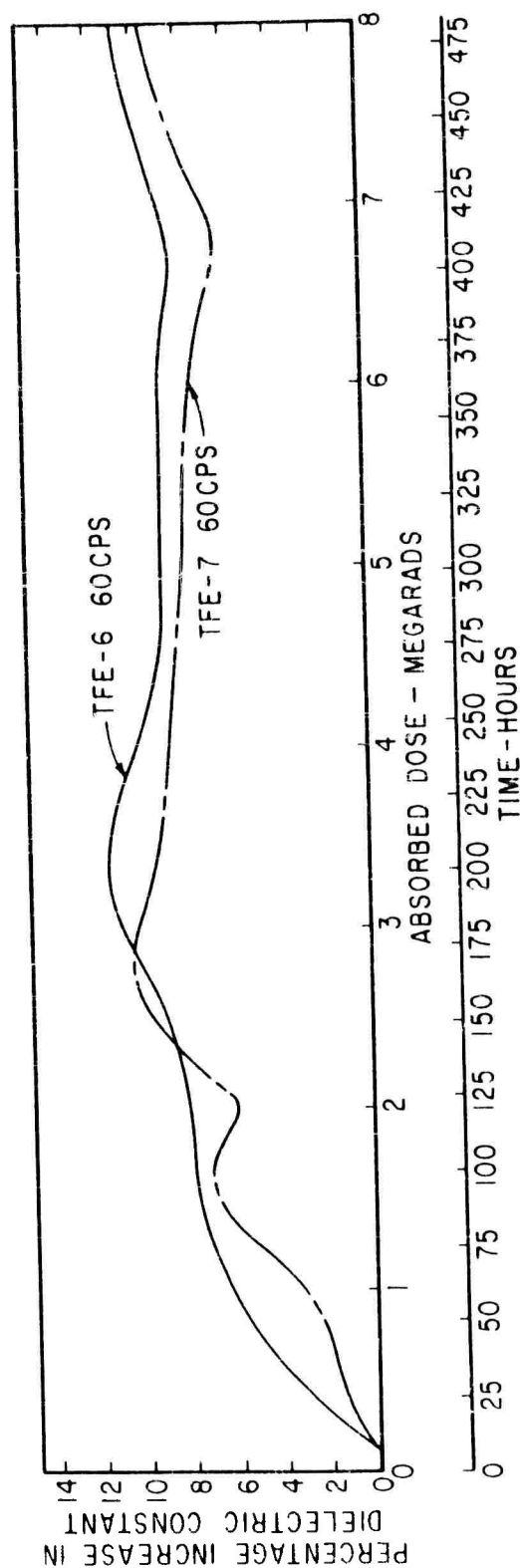


Figure 30. Effect of x-ray irradiation in air on the dielectric constant of TFE-6 and TFE-7.

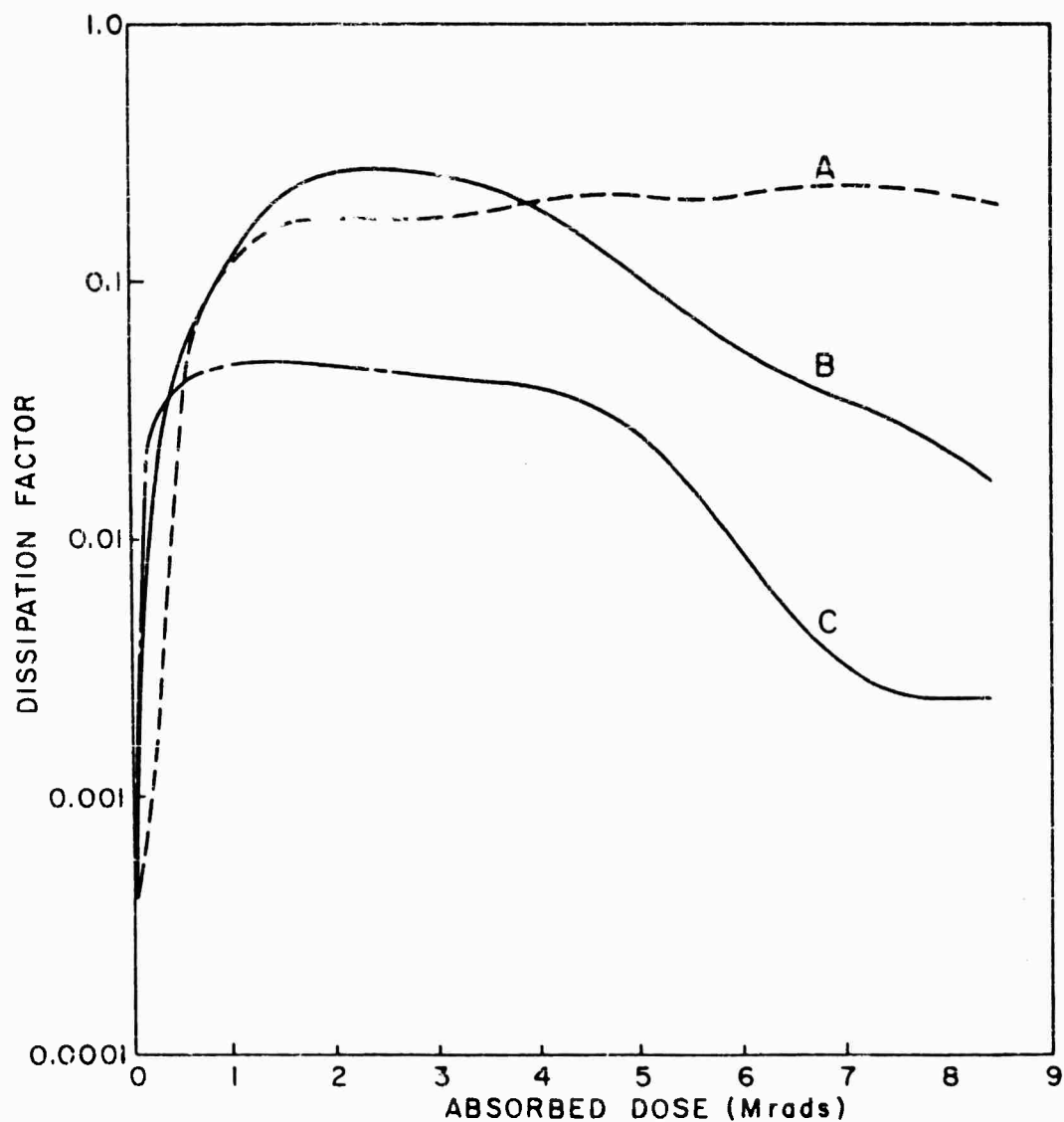


Figure 31. Effect of x-ray irradiation on TFE-6. Curve A - irradiated in air; Curve B - irradiated in vacuum; Curve C - irradiated in vacuum after previous dose of 8.5 megarads, followed by 10 months recovery in air.

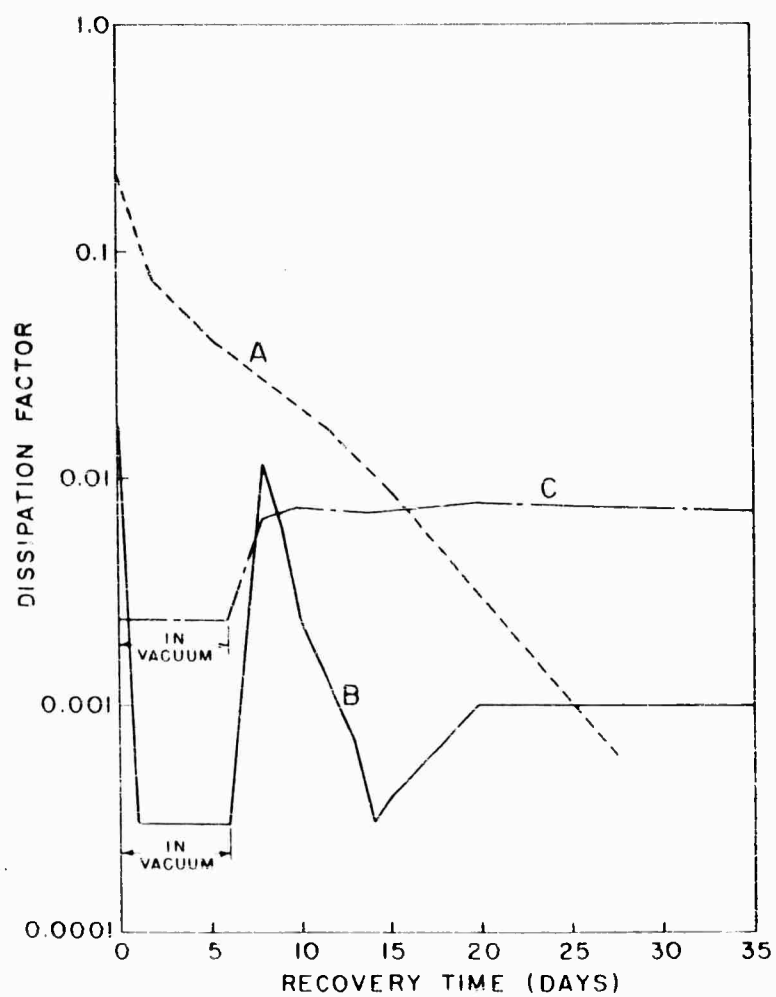


Figure 32. Recovery characteristics of TFE-6 specimens after x-ray irradiation as shown in Figure 31.

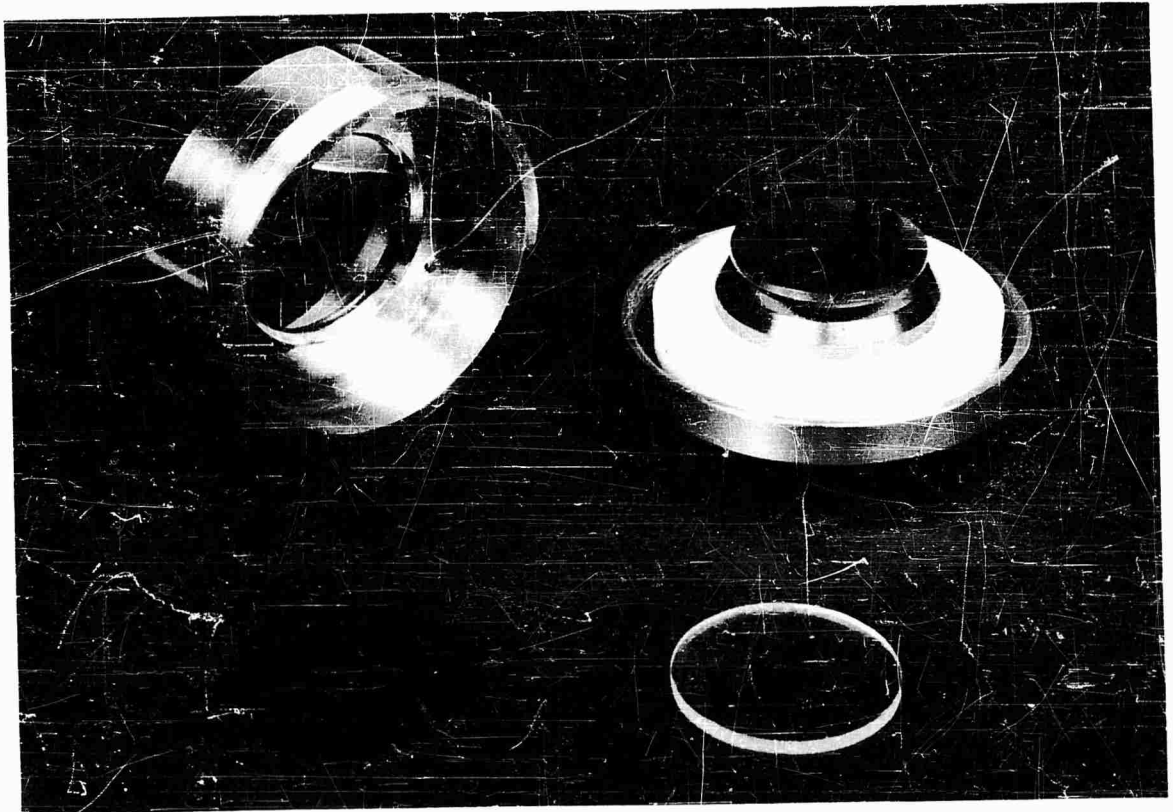


Figure 33. Loss-specimen holder with transparent high-voltage electrode.

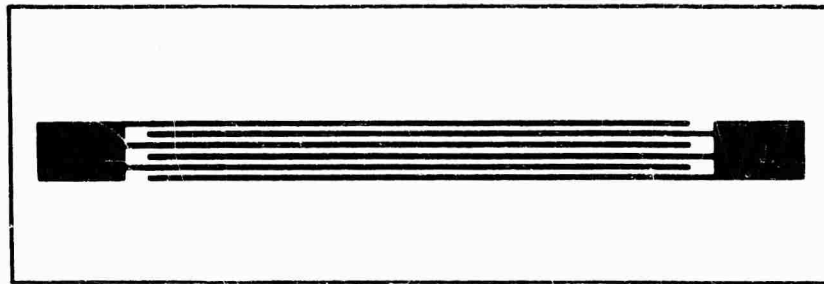


Figure 34. Printed wiring board insulation resistance specimen.

DISTRIBUTION LIST

<u>No. of Copies</u>	<u>Destination</u>
1	OASD (R&E), Rm 3E1065, ATTN: Technical Library, The Pentagon, Washington 25, D.C.
1	Chief of Research and Development, OCS, Department of the Army, Washington 25, D.C.
1	Chief Signal Officer, ATTN: SIGRD, Department of the Army, Washington 25, D.C.
1	Director, U.S. Naval Research Laboratory, ATTN: Code 2027, Washington 25, D.C.
1	Commander, Aeronautical Systems Division, ATTN: ASAPRL, Wright-Patterson Air Force Base, Ohio
1	Commander, Air Force Cambridge Research Laboratories, ATTN: CRO L.G. Hanscom Field, Bedford, Massachusetts
1	Commander, Air Force Command and Control Development Division ATTN: CRZC, L.G. Hanscom Field, Bedford, Massachusetts
2	Commander, Air Force Command and Control Development Division, ATTN: CCRR & CCSD, L.G. Hanscom Field, Bedford, Massachusetts
1	Commander, Rome Air Development Center, ATTN: RAALD, Griffiss Air Force Base, New York
10	Commander, Armed Services Technical Information Agency, ATTN: TIPCR, Arlington Hall Station, Arlington 12, Virginia
2	Chief, U.S. Army Security Agency, Arlington Hall Station, Arlington 12, Virginia
1	Deputy President, U.S. Army Security Agency Board, Arlington Hall Station, Arlington 12, Virginia
1	Commanding Officer, Diamond Ordnance Fuze Laboratories, ATTN: Library, Room 211, Building 92, Washington 25, D.C.
1	Commanding Officer, U.S. Army Signal Equipment Support Agency, ATTN: SIGMS-ADJ, Fort Monmouth, New Jersey
3	U.S. Continental Army Command Liaison Office, U.S. Army Signal Research & Development Laboratory, Fort Monmouth, New Jersey
1	Corps of Engineers Liaison Office, U.S. Army Signal Research & Development Laboratory, Fort Monmouth, New Jersey
1	AFSC Liaison Office, Naval Air R&D Activities Command, Johnsville, Pennsylvania
1	Marine Corps Liaison Office, U.S. Army Signal Research & Development Laboratory, Fort Monmouth, New Jersey
1	Commanding Officer, U.S. Army Signal Research & Development Laboratory, ATTN: Director of Engineering, Fort Monmouth, New Jersey
1	Commanding Officer, U.S. Army Signal Research & Development Laboratory, ATTN: Technical Documents Center, Fort Monmouth, New Jersey
1	Commanding Officer, U.S. Army Signal Research & Development Laboratory, ATTN: MF&R Unit #1, Fort Monmouth, New Jersey
3	Commanding Officer, U.S. Army Signal Research & Development Laboratory, ATTN: Technical Information Division, Fort Monmouth, New Jersey (FOR RETRANSMITTAL TO ACCREDITED BRITISH AND CANADIAN GOVERNMENT REPRESENTATIVES)
1	Mr. Joseph C. Reed, Plastics Department, E.I. du Pont de Nemours & Co., Inc., Wilmington, Delaware
1	Mr. H.J. Gildred, Minnesota Mining and Manufacturing Company, 5698 Rising Sun Avenue, Philadelphia 20, Pennsylvania
1	Mr. J.G. Theodore, Brush Beryllium Company, 4301 Perkins Avenue, Cleveland 3, Ohio
1	Mr. J.D. Kelly, William Brand-Rex Division, American Euka Corporation, 31 Sudbury Road, Concord, Massachusetts
1	Mr. F.H. Hamilton, Formica Corporation, 4614 Spring Grove Avenue, Cincinnati 32, Ohio
1	Dr. Carl J. Heffelfinger, Film Department, E.I. du Pont de Nemours & Co., Inc., Circleville, Ohio
1	Mr. W.E. Bech, George C. Marshall Space Flight Center, National Aeronautics & Space Administration, Huntsville, Alabama
1	General Electric Company, P.O. Box 459, Utica, New York, ATTN: Dr. Robert S. Shane
1	Lockheed Aircraft Corporation, Missiles & Space Division, Sunnyvale, California, ATTN: Dr. Francis J. Clauss (D/53-35)
1	Commanding Officer, Army Advent Management Agency, Fort Monmouth, New Jersey
1	National Aeronautics & Space Agency, 1520 H. Street, N.W., Washington 25, D.C., ATTN: O.R. Lloyd, Information Director

<u>No. of Copies</u>	<u>Destination</u>
1	West Coast Office, USASRDL, 75 South Grand Avenue, Pasadena, California, ATTN: Mr. F.M. Hall
1	Plastics Technical Evaluation Center, Picatinny Arsenal, Dover, New Jersey, ATTN: H.E. Pebly, Jr., Director
1	Commanding Officer, Quartermaster Research & Engineering Center, Natick, Massachusetts, ATTN: QMREL-PRCH
14	Commanding Officer, U.S. Army Signal Research & Development Laboratory, Fort Monmouth, New Jersey, ATTN: SIGRA/SL-PEE (E.G. Linden)
1	Mr. R. T. Jeffrey, Contract Administration, Electron Tubes Division, Radio Corporation of America, Harrison, New Jersey
1	Mr. C.E. Jahnke, Bendix Systems Division, The Bendix Corporation, 3300 Plymouth Road, Ann Arbor, Michigan
1	Mr. Aaron Fisher, Code 623, National Aeronautics & Space Administration, Goddard Space Flight Center, Greenbelt, Maryland

<p>AD- Div. 14, 25</p> <p>Dielectrics Lab., Johns Hopkins U., Baltimore, Md. DIELECTRICS FOR SATELLITES AND SPACE VEHICLES, by L.J. Frisco. Final Report, 1 Mar 1959 - 28 Feb 1962, 144 p. incl. 34 illus., 37 tables, 34 refs. (Contract DA-36-039-SC-78321) Unclassified Report</p> <p>Descriptors: Dielectrics; Electrical Properties; Solids; Ceramic Materials; Plastic Materials; Space Environmental Conditions; Ultraviolet Radiation; X-rays; Vacuum Equipment.</p> <p>Results of a study of the effects of simulated space environment on the electrical properties of solid insulating materials are reported. Equip- ment and techniques are described for the measurement of loss prop- erties, flashover strength and electric strength during x-ray and ultra- violet irradiation at pressures in the 10-6 Torr range. Twenty-one organic and inorganic materials are included in the investigation.</p> <p>High-vacuum sparkover (uniform field) and flashover measurements at d-c and 60 cps show that electrode surface roughness is the con- trolling factor; that the dielectric properties of the material do not influence flashover voltage; and that x-ray and ultraviolet radiation have no effect on flashover voltage. At 2 and 18 Mc high current densities at electrode edges or high losses in the solid material com- promise flashover strength.</p> <p>(over)</p> <p>UNCLASSIFIED</p> <p>I. L.J. Frisco II. U.S. Army Signal Research and Development Laboratory, Ft. Monmouth, N.J. III. Contract DA-36-039-SC-78321</p>	<p>UNCLASSIFIED</p> <p>I. L.J. Frisco II. U.S. Army Signal Research and Development Laboratory, Ft. Monmouth, N.J. III. Contract DA-36-039-SC-78321</p> <p>AD- Div. 14, 25</p> <p>Dielectrics Lab., Johns Hopkins U., Baltimore, Md. DIELECTRICS FOR SATELLITES AND SPACE VEHICLES, by L.J. Frisco. Final Report, 1 Mar 1959 - 28 Feb 1962, 144 p. incl. 34 illus., 37 tables, 34 refs. (Contract DA-36-039-SC-78321) Unclassified Report</p> <p>Descriptors: Dielectrics; Electrical Properties; Solids; Ceramic Materials; Plastic Materials; Space Environmental Conditions; Ultraviolet Radiation; X-rays; Vacuum Equipment.</p> <p>Results of a study of the effects of simulated space environment on the electrical properties of solid insulating materials are reported. Equip- ment and techniques are described for the measurement of loss prop- erties, flashover strength and electric strength during x-ray and ultra- violet irradiation at pressures in the 10-6 Torr range. Twenty-one organic and inorganic materials are included in the investigation.</p> <p>High-vacuum sparkover (uniform field) and flashover measurements at d-c and 60 cps show that electrode surface roughness is the con- trolling factor; that the dielectric properties of the material do not influence flashover voltage; and that x-ray and ultraviolet radiation have no effect on flashover voltage. At 2 and 18 Mc high current densities at electrode edges or high losses in the solid material com- promise flashover strength.</p> <p>(over)</p> <p>UNCLASSIFIED</p> <p>I. L.J. Frisco II. U.S. Army Signal Research and Development Laboratory, Ft. Monmouth, N.J. III. Contract DA-36-039-SC-78321</p>
<p>UNCLASSIFIED</p> <p>AD- Div. 14, 25</p> <p>Dielectrics Lab., Johns Hopkins U., Baltimore, Md. DIELECTRICS FOR SATELLITES AND SPACE VEHICLES, by L.J. Frisco. Final Report, 1 Mar 1959 - 28 Feb 1962, 144 p. incl. 34 illus., 37 tables, 34 refs. (Contract DA-36-039-SC-78321) Unclassified Report</p> <p>Descriptors: Dielectrics; Electrical Properties; Solids; Ceramic Materials; Plastic Materials; Space Environmental Conditions; Ultraviolet Radiation; X-rays; Vacuum Equipment.</p> <p>Results of a study of the effects of simulated space environment on the electrical properties of solid insulating materials are reported. Equip- ment and techniques are described for the measurement of loss prop- erties, flashover strength and electric strength during x-ray and ultra- violet irradiation at pressures in the 10-6 Torr range. Twenty-one organic and inorganic materials are included in the investigation.</p> <p>High-vacuum sparkover (uniform field) and flashover measurements at d-c and 60 cps show that electrode surface roughness is the con- trolling factor; that the dielectric properties of the material do not influence flashover voltage; and that x-ray and ultraviolet radiation have no effect on flashover voltage. At 2 and 18 Mc high current densities at electrode edges or high losses in the solid material com- promise flashover strength.</p> <p>(over)</p> <p>UNCLASSIFIED</p> <p>I. L.J. Frisco II. U.S. Army Signal Research and Development Laboratory, Ft. Monmouth, N.J. III. Contract DA-36-039-SC-78321</p>	<p>UNCLASSIFIED</p> <p>AD- Div. 14, 25</p> <p>Dielectrics Lab., Johns Hopkins U., Baltimore, Md. DIELECTRICS FOR SATELLITES AND SPACE VEHICLES, by L.J. Frisco. Final Report, 1 Mar 1959 - 28 Feb 1962, 144 p. incl. 34 illus., 37 tables, 34 refs. (Contract DA-36-039-SC-78321) Unclassified Report</p> <p>Descriptors: Dielectrics; Electrical Properties; Solids; Ceramic Materials; Plastic Materials; Space Environmental Conditions; Ultraviolet Radiation; X-rays; Vacuum Equipment.</p> <p>Results of a study of the effects of simulated space environment on the electrical properties of solid insulating materials are reported. Equip- ment and techniques are described for the measurement of loss prop- erties, flashover strength and electric strength during x-ray and ultra- violet irradiation at pressures in the 10-6 Torr range. Twenty-one organic and inorganic materials are included in the investigation.</p> <p>High-vacuum sparkover (uniform field) and flashover measurements at d-c and 60 cps show that electrode surface roughness is the con- trolling factor; that the dielectric properties of the material do not influence flashover voltage; and that x-ray and ultraviolet radiation have no effect on flashover voltage. At 2 and 18 Mc high current densities at electrode edges or high losses in the solid material com- promise flashover strength.</p> <p>(over)</p> <p>UNCLASSIFIED</p> <p>I. L.J. Frisco II. U.S. Army Signal Research and Development Laboratory, Ft. Monmouth, N.J. III. Contract DA-36-039-SC-78321</p>

UNCLASSIFIED

Electric strengths of low-loss polymers are not affected by x-ray irradiation in high-vacuum. High-frequency electric strength is compromised by unfavorable thermal conditions in high-vacuum.

X-ray induced a-c losses are exhibited by several materials during and after irradiation. Transient effects during irradiation cause induced 60 cps dissipation factors as high as 0.40 in some tetrafluoroethylene polymers. Detailed exposure and recovery data show the effects of oxygen and absorbed dose.

X-ray induced d-c polarization, absorption and conduction currents are exhibited by most materials. In some cases, recovery is not complete after several months.

Instantaneous and short-time effects of ultraviolet radiation on a-c loss properties are not large enough to be of practical importance. The d-c behavior is dominated by photoelectric effects.

Materials that are subject to moisture absorption exhibit improved electrical properties after short periods in high-vacuum.

Studies are being continued under Contract DA-36-039-SC-89147.

UNCLASSIFIED

UNCLASSIFIED

Electric strengths of low-loss polymers are not affected by x-ray irradiation in high-vacuum. High-frequency electric strength is compromised by unfavorable thermal conditions in high-vacuum.

X-ray induced a-c losses are exhibited by several materials during and after irradiation. Transient effects during irradiation cause induced 60 cps dissipation factors as high as 0.40 in some tetrafluoroethylene polymers. Detailed exposure and recovery data show the effects of oxygen and absorbed dose.

X-ray induced d-c polarization, absorption and conduction currents are exhibited by most materials. In some cases, recovery is not complete after several months.

Instantaneous and short-time effects of ultraviolet radiation on a-c loss properties are not large enough to be of practical importance. The d-c behavior is dominated by photoelectric effects.

Materials that are subject to moisture absorption exhibit improved electrical properties after short periods in high-vacuum.

Studies are being continued under Contract DA-36-039-SC-89147.

UNCLASSIFIED

UNCLASSIFIED

Electric strengths of low-loss polymers are not affected by x-ray irradiation in high-vacuum. High-frequency electric strength is compromised by unfavorable thermal conditions in high-vacuum.

X-ray induced a-c losses are exhibited by several materials during and after irradiation. Transient effects during irradiation cause induced 60 cps dissipation factors as high as 0.40 in some tetrafluoroethylene polymers. Detailed exposure and recovery data show the effects of oxygen and absorbed dose.

X-ray induced d-c polarization, absorption and conduction currents are exhibited by most materials. In some cases, recovery is not complete after several months.

Instantaneous and short-time effects of ultraviolet radiation on a-c loss properties are not large enough to be of practical importance. The d-c behavior is dominated by photoelectric effects.

Materials that are subject to moisture absorption exhibit improved electrical properties after short periods in high-vacuum.

Studies are being continued under Contract DA-36-039-SC-89147.

UNCLASSIFIED

UNCLASSIFIED

Electric strengths of low-loss polymers are not affected by x-ray irradiation in high-vacuum. High-frequency electric strength is compromised by unfavorable thermal conditions in high-vacuum.

X-ray induced a-c losses are exhibited by several materials during and after irradiation. Transient effects during irradiation cause induced 60 cps dissipation factors as high as 0.40 in some tetrafluoroethylene polymers. Detailed exposure and recovery data show the effects of oxygen and absorbed dose.

X-ray induced d-c polarization, absorption and conduction currents are exhibited by most materials. In some cases, recovery is not complete after several months.

Instantaneous and short-time effects of ultraviolet radiation on a-c loss properties are not large enough to be of practical importance. The d-c behavior is dominated by photoelectric effects.

Materials that are subject to moisture absorption exhibit improved electrical properties after short periods in high-vacuum.

Studies are being continued under Contract DA-36-039-SC-89147.

UNCLASSIFIED

<p>AD- Div. 14. 25</p> <p>Dielectrics Lab., Johns Hopkins U., Baltimore, Md. DIELECTRICS FOR SATELLITES AND SPACE VEHICLES. by L. J. Frisco. Final Report, 1 Mar 1959 - 28 Feb 1962. 144 p. incl. 34 illus., 37 tables. 34 refs. Unclassified Report (Contract DA-36-039-SC-78321)</p> <p>Descriptors: Dielectrics; Electrical Properties; Solids; Ceramic Materials; Plastic Materials. Space Environmental Conditions*. Ultraviolet Radiation*; X-rays; Vacuum Equipment*.</p> <p>Results of a study of the effects of simulated space environment on the electrical properties of solid insulating materials are reported. Equip- ment and techniques are described for the measurement of loss prop- erties, flashover strength and electric strength during x-ray and ultra- violet irradiation at pressures in the 10-6 Torr range. Twenty-one organic and inorganic materials are included in the investigation.</p> <p>High-vacuum sparkover (uniform field) and flashover measurements at d-c and 60 cps show that electrode surface roughness is the con- trolling factor; that the dielectric properties of the material do not influence flashover voltage; and that x-ray and ultraviolet radiation have no effect on flashover voltage. At 2 and 18 Mc high current densities at electrode edges or high losses in the solid material com- promise flashover strength.</p> <p>(over)</p> <p>UNCLASSIFIED</p>	<p>UNCLASSIFIED</p> <p>I. L. J. Frisco II. U. S. Army Signal Research and Development Laboratory, Ft. Monmouth, N. J. III. Contract DA-36-039-SC-78321</p>
<p>AD- Div. 14. 25</p> <p>Dielectrics Lab., Johns Hopkins U., Baltimore, Md. DIELECTRICS FOR SATELLITES AND SPACE VEHICLES. by L. J. Frisco. Final Report, 1 Mar 1959 - 28 Feb 1962. 144 p. incl. 34 illus., 37 tables. 34 refs. Unclassified Report (Contract DA-36-039-SC-78321)</p> <p>Descriptors: Dielectrics; Electrical Properties; Solids; Ceramic Materials; Plastic Materials. Space Environmental Conditions*. Ultraviolet Radiation*; X-rays; Vacuum Equipment*.</p> <p>Results of a study of the effects of simulated space environment on the electrical properties of solid insulating materials are reported. Equip- ment and techniques are described for the measurement of loss prop- erties, flashover strength and electric strength during x-ray and ultra- violet irradiation at pressures in the 10-6 Torr range. Twenty-one organic and inorganic materials are included in the investigation.</p> <p>High-vacuum sparkover (uniform field) and flashover measurements at d-c and 60 cps show that electrode surface roughness is the con- trolling factor; that the dielectric properties of the material do not influence flashover voltage; and that x-ray and ultraviolet radiation have no effect on flashover voltage. At 2 and 18 Mc high current densities at electrode edges or high losses in the solid material com- promise flashover strength.</p> <p>(over)</p> <p>UNCLASSIFIED</p>	<p>UNCLASSIFIED</p> <p>I. L. J. Frisco II. U. S. Army Signal Research and Development Laboratory, Ft. Monmouth, N. J. III. Contract DA-36-039-SC-78321</p>

UNCLASSIFIED

Electric strengths of low-loss polymers are not affected by x-ray irradiation in high-vacuum. High-frequency electric strength is compromised by unfavorable thermal conditions in high-vacuum.

X-ray induced a-c losses are exhibited by several materials during and after irradiation. Transient effects during irradiation cause induced 60 cps dissipation factors as high as 0.40 in some tetrafluoroethylene polymers. Detailed exposure and recovery data show the effects of oxygen and absorbed dose.

X-ray induced d-c polarization, absorption and conduction currents are exhibited by most materials. In some cases, recovery is not complete after several months.

Instantaneous and short-time effects of ultraviolet radiation on a-c loss properties are not large enough to be of practical importance. The d-c behavior is dominated by photoelectric effects.

Materials that are subject to moisture absorption exhibit improved electrical properties after short periods in high-vacuum.

Studies are being continued under Contract DA-36-039-SC-89147.

UNCLASSIFIED

UNCLASSIFIED

Electric strengths of low-loss polymers are not affected by x-ray irradiation in high-vacuum. High-frequency electric strength is compromised by unfavorable thermal conditions in high-vacuum.

X-ray induced a-c losses are exhibited by several materials during and after irradiation. Transient effects during irradiation cause induced 60 cps dissipation factors as high as 0.40 in some tetrafluoroethylene polymers. Detailed exposure and recovery data show the effects of oxygen and absorbed dose.

X-ray induced d-c polarization, absorption and conduction currents are exhibited by most materials. In some cases, recovery is not complete after several months.

Instantaneous and short-time effects of ultraviolet radiation on a-c loss properties are not large enough to be of practical importance. The d-c behavior is dominated by photoelectric effects.

Materials that are subject to moisture absorption exhibit improved electrical properties after short periods in high-vacuum.

Studies are being continued under Contract DA-36-039-SC-89147.

UNCLASSIFIED

UNCLASSIFIED

Electric strengths of low-loss polymers are not affected by x-ray irradiation in high-vacuum. High-frequency electric strength is compromised by unfavorable thermal conditions in high-vacuum.

X-ray induced a-c losses are exhibited by several materials during and after irradiation. Transient effects during irradiation cause induced 60 cps dissipation factors as high as 0.40 in some tetrafluoroethylene polymers. Detailed exposure and recovery data show the effects of oxygen and absorbed dose.

X-ray induced d-c polarization, absorption and conduction currents are exhibited by most materials. In some cases, recovery is not complete after several months.

Instantaneous and short-time effects of ultraviolet radiation on a-c loss properties are not large enough to be of practical importance. The d-c behavior is dominated by photoelectric effects.

Materials that are subject to moisture absorption exhibit improved electrical properties after short periods in high-vacuum.

Studies are being continued under Contract DA-36-039-SC-89147.

UNCLASSIFIED

UNCLASSIFIED

Electric strengths of low-loss polymers are not affected by x-ray irradiation in high-vacuum. High-frequency electric strength is compromised by unfavorable thermal conditions in high-vacuum.

X-ray induced a-c losses are exhibited by several materials during and after irradiation. Transient effects during irradiation cause induced 60 cps dissipation factors as high as 0.40 in some tetrafluoroethylene polymers. Detailed exposure and recovery data show the effects of oxygen and absorbed dose.

X-ray induced d-c polarization, absorption and conduction currents are exhibited by most materials. In some cases, recovery is not complete after several months.

Instantaneous and short-time effects of ultraviolet radiation on a-c loss properties are not large enough to be of practical importance. The d-c behavior is dominated by photoelectric effects.

Materials that are subject to moisture absorption exhibit improved electrical properties after short periods in high-vacuum.

Studies are being continued under Contract DA-36-039-SC-89147.

UNCLASSIFIED